PEPTIDE TOXIN BIOENGINEERING: EXPLORING THE POTENTIAL OF CYCLIZED CONOTOXINS AS ORAL DRUGS, FLUORESCENT PROBES AND PHYLA – SELECTIVE PESTICIDES

A DISSERTATION SUMBITTED TO THE GRADUATE DIVISON OF THE UNIVERSITY OF HAWAIʻI AT MĀNOA IN PARTIAL FULFILLMENT OF THE REQUIREMENTS FOR THE DEGREE OF

DOCTOR OF PHILOSOPHY

IN

MOLECULAR BIOSCIENCES AND BIOENGINEERING

DECEMBER 2015

By

PARASHAR THAPA

Dissertation Committee:

Jon-Paul Bingham, Chairperson
Harry Ako
Yong Soo Kim
Gernot Presting
Maria Stewart

Keywords: Peptides, Conotoxins, Native Chemical Ligation, Cyclization, Trifluoromethanesulfonic Acid, Huwentoxin and Bioengineering

Dedication

The following dissertation is dedicated to the influential people in my life who have always been there to guide, support, and encourage me. I would like to thank my parents for providing me with every opportunity a child could dream for. My parents have made countless sacrifices so that I could pursue my academic dreams, for that I am forever grateful. I would like to thank my sister for showing me unwavering love and continued support. I would like to thank my grandparents for their unconditional love, care and concern. I have been blessed to have an extended family that cares for me. To all my uncles, aunties, cousins and friends thank you for supporting me despite all my shortcomings. Special mention must go to my Aunty Saroj for opening her heart and her home for me. I would not have reached this point in my academic career without her continued love and support. She has made many personal sacrifices so that I could pursue my education for that I am forever grateful. I must also thank my Aunty Bindu for her love and generosity. She has always kept me in her thoughts and wished for my well being, thank you very much. Special thanks to Sumil for all the support and wonderful memories. I would like to thank all my teachers and professors for sharing their knowledge with me.

Acknowledgement

I would like to express my gratitude to everyone who has assisted me throughout my academic journey. Firstly, I would like to thank my advisor Dr. Jon-Paul Bingham for giving me an opportunity to work in his lab. I would also like to thank him for providing me with invaluable guidance that has helped me grow professionally and personally. Additionally, I would like to acknowledge the support provided by USDA NIFA (# 2011-37610-31182) (J-PB), USDA HATCH (HAW00595-R) (J-PB) to Dr. Bingham. I would like to thank my committee members Dr. Maria Stewart, Dr. Gernot Presting, Dr. Yong Soo Kim and Dr. Harry Ako for their advice and guidance. Additionally, I would like to thank my committee members for generously dedicating their time despite their busy schedules. I would like to thank Dr. Abby Collier for generously dedicating her time and knowledge throughout my graduate studies.

My time in the Bingham lab has been memorable and enjoyable, for that I need to thank my advisor and my lab mates. My fellow lab mates have been terrific and I will always cherish your friendship. Special mention must go to Braddah Cliff, Zanimal, Joycelyn, Zach, Zeb, Do, Nolan, Chino San, Peter, Mike, Chris, Ray-Gazu, Princess, Jeff, Ted and Vinny. If I get co-workers like you in my next endeavor, I will have lucked out. I would like to thank the Department of Molecular Biology and Bioengineering and the Department of Biology for providing me with TA positions that has allowed me to complete my graduate education.

List of Publications

Materials in this dissertation have been adapted from the following published and non-published (In Preparation) manuscripts.

Published Papers:

1. Thapa, P., *et al.*, *Native chemical ligation: a boon to peptide chemistry.* Molecules, 2014. **19**(9): p. 14461-83.
2. Parashar Thapa, M.J.E., Chino Cabalteja, Jon-Paul Bingham, *The Emergence of Cyclic Peptides: The potential of Bioengineered Peptide Drugs.* International Journal of Peptide Research and Therapeutics, 2014.
3. Thapa, P., *et al*., *Conotoxins and their regulatory considerations.* Regul Toxicol Pharmacol, 2014. **70**(1): p. 197-202.
4. Kapono, C.A†., Thapa, P†, *et al.*, *Conotoxin truncation as a post-translational modification to increase the pharmacological diversity within the milked venom of Conus magus.* Toxicon, 2013. **70**: p. 170-8.

† Contributed equally to this work

5. Bergeron, Z.L., *et al.*, *A 'conovenomic' analysis of the milked venom from the mollusk-hunting cone snail Conus textile--the pharmacological importance of post-translational modifications.* Peptides, 2013. **49**: p. 145-58.

Papers in Preparation:

1. Trifluoromethanesulfonic acid - An alternative cleavage strategy in the generation thioester containing peptide fragments for Native Chemical Ligation.
   Parashar Thapa[1†], Chino C. Cabalteja[1], Edwin E. Philips III, Steven Peigneur, Jan Tytgat and Jon-Paul Bingham[1†*],

† Contributed equally to this work

2. Conovenomic and pharmacological assignment of 4/6 α-conotoxin VIl, and its synthetic isomeric variants, from the vermivorous *Conus virgo*.
   Chino C. Cabalteja[†1], Parashar Thapa[†1], David W. Sandall[†2], Joycelyn B. Chun[1], Margaret R. Baker[1] Shaun Kiyabu[1], Paul A. O'Donnell[2], Ken Gayler[2], Bruce G. Livett[2] and Jon-Paul Bingham[1†*],

† Contributed equally to this work

Abstract

Studies into *N*- to *C*-terminal cyclic peptide backbone structures have provided for the lateral transition of important principles and strategies that clearly resonate within the world of bioactive peptides and peptide toxins. The ability to transform peptide biologics into stable and orally active constituents represents a major pharmacological achievement. This progression has been forthcoming and is potentially intensified by the diminishing expectations of current small organic molecule pipelines.

For our studies we have decided to use conotoxins as the model natural product for cyclization. Conotoxins are disulfide rich neurotoxins found in the venoms of marine cone snails. These neuropeptides have a high number of post-translational modifications (PTMs), which manifest itself in phyla specificity and receptor selectivity. Conotoxins are typically about 10-40 amino acids in length, but exhibit many secondary motifs such as α-helices and β-sheets that are normally found in larger proteins. Their high level of selectivity, potency and structural integrity make them prime candidates for oral drug models, drug scaffolds and bio-conjugation tools. Venom derived peptides from marine cone snails, conotoxins, have demonstrated unique pharmacological targeting properties that have been pivotal in advancing medical research. The awareness of their true toxic origins and potent pharmacological nature is emphasized by their 'select agent' classification by the US Centers for Disease Control and Prevention.

In order to cyclize these natural peptides, we will adapt the Native Chemical Ligation (NCL) strategy. Current techniques use Hydrogen fluoride (HF) to create the thioester, which can ultimately be used for native chemical ligation/cyclization. The use of HF is not recommended due to its highly hazardous and toxic nature. Furthermore, since HF requires special apparatus and hood space its application is limited only to a few privileged laboratories. This research aimed at replacing HF with Trifluoromethanesulfonic acid (TFMSA) without compromising with the yield of the reaction. In order to optimize the reaction conditions to achieve target concentration various variables such as time, acid concentration, and different orthogonal protection group scavengers will be examined. By replacing HF with TFMSA, which is less toxic

and uses conventional lab ware, we aim to make the technique of thioester ligation/cyclization safer and accessible. Here we use a 33 amino acid (αα) test peptide, Huwentoxin-I (HwTx-I) as a candidate to test this novel protocol. Structurally HwTx-I has 6 individual Cysteines (Cys) and an X—Cys-Cys—X sequence mid-region, which makes it an ideal candidate for thioester ligation.

Once we have established a protocol for cyclization/ligation, this novel protocol will be used to synthesize the cyclic conopeptide. After synthesis we will conduct stability and bioactivity assay on the cyclic peptide to assess the impact of cyclization on bioactivity and stability. Cyclized conotoxins display increased structural stability and resistance to enzymatic degradation and may be used to create orally active conotoxin therapeutics. In all, the works presented in this dissertation display a progression in conotoxin bioengineering to improve their pharmacological properties so they may be developed as therapeutics, biopesticides or bioconjugation tools.

Table of Contents

List of Figures

List of Tables

List of Abbreviations

4MOBzl	4-MethylOBenzyl
Acm	Acetamidomethyl
AEP	Asparaginyl Endopetidase
BLA	Biologic License Approval
BOC	tert-Butyloxycarbonyl
Ca^{2+}	Calcium
CDC	Centers for Disease Control and Prevention
CID	Collision-Induced Dissociation
C-Terminus	Carboxy Terminus
Da	Dalton
DCM	Dichloromethane
DI	Deionized
DIEA	*N*,*N*-Diisopropylethylamine
DMF	Dimethylformamide
DMSO	Dimethyl sulfoxide
DNA	Deoxyribonucleic Acid
DTT	Dithiothreitol
DV	Duct Venom
EDT	1,2-Ethanedithiol
EM	*N*-Ethyl-Maleimide
ESI-MS	Electrospray Ionization Mass Spectrometry
FDA	US Food and Drug Administration
Fmoc	9-Fluorenylmethyloxycarbonyl
G	Generation
GC	Gas Chromatography
GdnHCl	Guanidium hydrochloride
GMP	Good Manufacturing Practices
HBTU	2-(1H-benzotriazol-1-yl)-1,1,3,3,-tetramethyluronium hexafluorophosphate
HCTU	2-(6-Chloro-1-H-benzotriazole-1-yl)-1,1,3,3-tetramethylaminium hexafluorophosphate
HF	Hydrogen fluoride
HFA	Hexafluoroacetone
HFBA	Heptaflurobutyric acid
HPLC	High Performance Liquid Chromatography
HSS	HEPES-salt solution
HwTx	Huwentoxin
I_2	Iodine
IC_{50}	Inhibitory Concentration
IND	Investigational New Drug Application
IPA	Ion Pairing Agent
IRB	Institutional Review Board
IT	Intrathecal
IV	Intravenous

KCN	Potassium cyanide
Kd	Dissociation Constant
K_v	Voltage Gated Potassium Channel
LC/MS	Liquid Chromatography interfaced Mass Spectrometry
LD_{50}	Lethal $Dose_{50}$
Mabs	Monoclonal Antibodies
MALDI-TOF	Matrix Assisted Laser Desorption/Ionization Time of Flight
MBHA	4-(Methyl) benzhydrylamine
MH^+	Observed Alkylated Monoisotopic molecular mass
min.	Minutes
mL	Milliliter
MPAA	4-Mercaptophenylacetic acid
MS	Mass Spectrometry
MTBE	tert-Butyl methyl ether
MV	Milked Venom
N	Natural
nAChRs	Nicotinic Acetylcholine Receptors
Na_V	Voltage Gated Sodium Channel
NCE	New Chemical Entity
NCL	Native Chemical Ligation
NDA	New Drug Application
NH_4OAc	Ammonium acetate
NMDA	N-Methyl D-aspartate
NMP	*N*-Methylpyrrolidone
NMR	Nuclear Magnetic Resonance
NTA	Ni-nitrilotriacetic acid
N-terminus	Amino Terminus
NV	Ninhydrin Value
N-VGCC	N-Type Voltage Gated Calcium Channel
OBzl	OBenzyl
PBS	Phosphate Buffered Saline
Pbf	2,2,4,6,7-Pentamethyldihydrobenzofuran- 5-sulfonyl
PDA	Photo Diode Array
PDI	Protein Disulfide Isomerase
PEG	Polyethylene glycol
PM	*N*-Phenylmaleimide
PTM	Post-Transnationally Modified
PSD	Post-Source Decay
RoA	Route of Administration
RP	Revere Phase
R_t	Retention time
S	Synthetic
Sol. A	Solvent A (0.1% v/v Trifluoroacetic acid aqueous)

Sol. A’	Solvent A’ (0.1% v/v Formic acid aqueous)
Sol. B	Solvent B (90% v/v Acetonitrile in 0.8% v/v Trifluoroacetic acid aqueous)
Sol. B’	Solvent B’ (90% v/v Acetonitrile in 0.8% v/v Formic acid aqueous)
SOM	Small Organic Molecule
SPPS	Solid Phase Peptide Synthesis
S_N2	Substitution Nucleophilic Bimolecular
SV	Substitution Value
TAMRA	Tetramethylrhodamine
TCEP	Tris (2-carboxyethyl) phosphine
TFA	Triflouroacetic acid
TFMSA	Trifluoromethylsulfonic Acid
Thz	1,3-Thiazolidine-4-carboxo
Trt	Trityl
UPLC	Ultra Performance Liquid Chromatography
USDA	United States Department of Agriculture
UV	Ultraviolet
Xan	Xanthyl
Z [2-Cl]-OSu	N-(2-Chlorobenzyloxycarbonyloxy) succinimide

Chapter 1: Literature Review, Objective and Hypotheses

1.1 Literature Review

1.1.1 Brief Introduction to Small Organic Molecule Drugs:

Small organic molecules (SOMs) have been largely recognized as the mainstay of the pharmaceutical industry. However with the latest advancement in proteomics and genomics, biologics have been making progressive footholds in the pharmaceutical business. Numerous ancient civilizations have documented records of using mineral and plant extract for therapeutic purposes. The practice of extracting botanics for potential medicinal purposes is known to be common act across societies and centuries [1]. Aspirin, the highly successful antipyretic pain reliever marketed by Bayer® had annual sales of $916 million US in 2013 [2]. This highly successful drug was extracted from the bark of the willow tree [3]. In its natural state salicylic acid cannot be used in humans because its acidic nature causes irritation to mucous membrane. However in 1893 Felix Hoffman a chemist at Bayer® produced acetylsalicylic acid by adding acetyl group to salicylic acid [4]. This new SOM was marketed by Bayer as Aspirin and is a blockbuster drug in today's pharmaceutical market. SOMs have been highly successful in the therapeutic market. Their success can be attributed to ease of synthesis, desirable pharmacokinetic properties, and a proven track record that continues to demand investment in research and development.

1.1.2 The Need for New Biologic Therapeutics:

Despite their success, SOMs face multitude of challenges. SOMs are losing prominence due to the lack of new leads, the rising cost of their development, and competition from affordable generics. This in-turn has spiraled the pharmaceutical industry down a path of production of so called ‘‘Me too’’ drugs [5]. ‘‘Me too’’ drugs are chemical analogs of patented original new chemical entities (NCEs) which are released prior to patent expiration. Viagra® (Pfizer), Cialis® (Eli Lilly) and Levitra®/Vivanza® (Bayer Pharmaceuticals, GlaxoSmithKline, and Schering-Plough) are common examples of some of the “Me too” drugs available in the market. “Me too” drugs have been successful in providing consumers with more choices but the fascination of pharmaceutical industry towards these drugs has also invited new challenges. With an increase in budget allocation towards the development of “Me too” drugs less research funding is directed towards finding NCEs. The profit obtained from ‘‘Me too’’ drugs allows businesses to provide funding for research and development of NCEs. However, these are potentially viewed as inefficient funding mechanisms for the discovery of much needed new therapeutics. This may account for the more recent strengthening of collaborative ‘‘fast-track discovery’’ ties between academic and industrial institutions in an attempt to supplement the apparent developmental deficiencies of NCEs. Other major problems such as lack of good methodologies to accurately predict novel drug designs, inability to eliminate off-target effects, and the high probability of failure in clinical trials have all contributed to greatly reducing the number of NCEs entering the supply chain for future drugs. In an attempt to remedy the current deficiencies of NCEs, and continue feeding new molecules into the drug-lead pipeline, increased attention has been drawn to biologics as a source for new therapies. The recent trend in pharmaceutical industry indicates there has been a paradigm shift within the business and efforts are being made to develop biologics as potential new therapeutics [6].

1.1.3 Emergence of Biologic Therapeutics:

Some of the most successful biologics include monoclonal antibodies or Mabs such as the cancer fighting Trastuzumab (Herceptin®; Genentech), and Cetuximab (Erbitux®; Bristol-Myers Squibb and Eli Lilly and Company), as well as Mabs for rheumatoid arthritis such as Atlizumab/Tocilizumab (Actemra®; Hoffmann–La Roche and Chugai). In recent years the selective nature of Mabs has been highly critical in its success. Their recent success has led to an increase in the number of new biologic license approvals (BLAs) issued by the US Food and Drug Administration (FDA). In 2011-12 Mabs accounted for 5 out of 14 (35 %) new BLAs and approximately 9 % of all therapeutics. A decade ago, Mabs only accounted for approximately 3.5 % of the drug market and 16 % of BLAs [7]. Initially, the development of antibody-based therapeutics was a considerable challenge but the efforts of scientists such as Frederick Sanger and Pehr Edman (Peptide Sequencing) [8, 9], Bruce Merrifield (Peptide Synthesis) [10], John Fenn and Koichi Tanaka (Mass Spectrometry) [11, 12], Paul Berg (Recombinant Synthesis) [13] and Gregory Winter (Human Antibodies) [14] among others has allowed antibody based therapeutics to become a viable option in the therapeutic market. In addition to antibodies pegylated proteins are another class of biologics that have been gaining significance as drugs in recent times. Some of the commercially available therapeutics in this category are Pegasys® and PegIntron® to treat Hepatitis C, Pegloticase® to treat Gout, Neulasta® for the treatment of Neutropenia, and Somavert® to treat Acromegaly.

1.1.4 Impact of Proteomics and Genomics on Biologics:

With the recent advances made in proteomics and genomics, biologics have slowly started making inroads into the therapeutic market. Advanced proteomic techniques such as Mass Spectrometry (MS), High Performance Liquid Chromatography (HPLC) and Nuclear Magnetic Resonance (NMR) have enabled researchers to make rapid strides in the field of protein science. MS provides information on protein sequence and post-translational modifications (PTMs); HPLC allows separation and visualization of biologics; NMR is an invaluable tool in structure elucidation. All these tools in combination have enabled researchers to find and validate biologic therapeutic leads [15, 16].

The Human Genome Project completed in 2001 through public and private cooperation has greatly helped in the advancement of biologics [17]. Information generated through this initiative allows researchers and pharmaceutical companies to identify molecular drug targets that can be modified or deleted through targeted gene therapy. Genomic advances might enable pharmaceutical companies to identify potential population groups that might respond adversely to certain families of drug leads due to polymorphism in their metabolic enzymes. This will not only reduce the failure rate for potential biologics entering clinical trials but might also contribute to the development of better predictive models to accurately identify drug targets. Advances made in genomics and proteomics have allowed therapy to enter the realm of personalized medicine and biologics such as antibody drug conjugates and peptide therapies are primed to make a significant contribution in this field [1, 18].

1.1.5 Biologic Based Therapeutics: Overcoming the Hurdle of Oral Bioavailability

In recent years there has been a significant push towards creating bioengineered synthetic peptides that can be used in a clinical setting. This synthetic integration bridges the gap between the pharmacodynamic/pharmacokinetic advantages of SOMs over biologics. Such an approach may ultimately provide an opportunity to target diseases that SOMs have failed to treat. Examples of bioengineering practices include *N*- to *C*-terminal backbone cyclization and peptide stapling [19, 20]. These modifications enhance desirable pharmacokinetic characteristics such as absorption and stability. Peptide stapling enhances absorption by adding a lipophilic linker and cyclization increases stability by eliminating free *N*- and *C*-termini.

With a few exceptions all peptide and protein based therapies are administered intravenously, subcutaneously or intramuscularly. These routes of administration are more invasive, inconvenient and less desirable than the oral intake of drugs [21]. Clinically, oral intake of drugs remains the desired route of administration among healthcare professionals. Oral administration of peptide-based therapeutics remains a challenge due to the low bioavailability of peptides/protein taken orally [21].

Low bioavailability of orally taken peptide therapeutics can be attributed to the presence of digestive enzymes in the intestinal lumen [22, 23] and inability of peptides to permeate through the membranes owing to its size and polarity [21, 24]. Yet peptide based therapeutics remain highly attractive because they are derived from natural products and their metabolism results in amino acids that can be incorporated in the body's natural metabolic processes.

The gastrointestinal tract contains a plethora of peptidases, with exopeptidases and endopeptidases working in tandem to metabolize the dietary protein, and will account for peptide drug circulatory decay and clearance. Small molecules utilize concentration dependent simple diffusion using trans-cellular and paracellular pathways to diffuse across the gut [25, 26]. These pathways are generally not suitable for peptides due to their size and polarity.

Peptides offer great potential as therapeutic agents because of their target selectivity and activity in nanomolar to picomolar range [27]. However, this high potency of biologics can also be a challenge in drug development by causing biological leads to fall outside of their desired therapeutic range. Consideration of *in vivo* interactions and circulatory bioavailability then becomes paramount in their assessment. In this case refinement can be addressed by reverse bioengineering, in which simple amino acid substitutions influence their pharmacokinetic properties [28]. Naturally, such ventures require an in-depth understanding of their individual structure activity relationships–a task commonly addressed in the initial research phase of drug discovery [29].

1.1.6 Cyclic Peptides: The Potential for Orally Active Biologic Therapeutics

Eliminating the charges on the *N*- and *C*-termini through cyclization can improve stability and membrane permeability. Cyclization in nature affords protection against exopeptidases and endopeptidases that have evolved as protective measure against foreign material. Bockus *et al.* [30] have categorized naturally occurring and synthetically produced cyclic peptides into 4 categories based on their physical properties and biological activity [30]. Characteristics of these molecules involve the following: (i) highly charged poly cationic or poly anionic molecules that function as antimicrobial agents by disrupting the microbial cell membrane; (ii) non-polar cyclic compounds which possess non-polar amino acids in majority thereby producing a lipophilic backbone, allowing for greater passive diffusion across membranes; (iii) amphiphilic cyclic compounds that possess a mixed polarity and; (iv) cyclic compounds which are stabilized by disulfide bonds. Within these four categories there are three additional subgroups: (i) homodetic cyclic compounds that have head to tail cyclization between their *N*-termini and *C*-termini; (ii) cyclic compounds with heterodetic linkage which possess a linkage between side chains or between a single side chain and one of their termini, and (iii) cyclic compounds which consists of a mixture of homodetic and heterodetic linkages (Figure 1 and Table 1). Each type of linkage strategy offers different advantages and susceptibilities, with the homodetic group offering the best natural-like encompassment with fully compatible degradation.

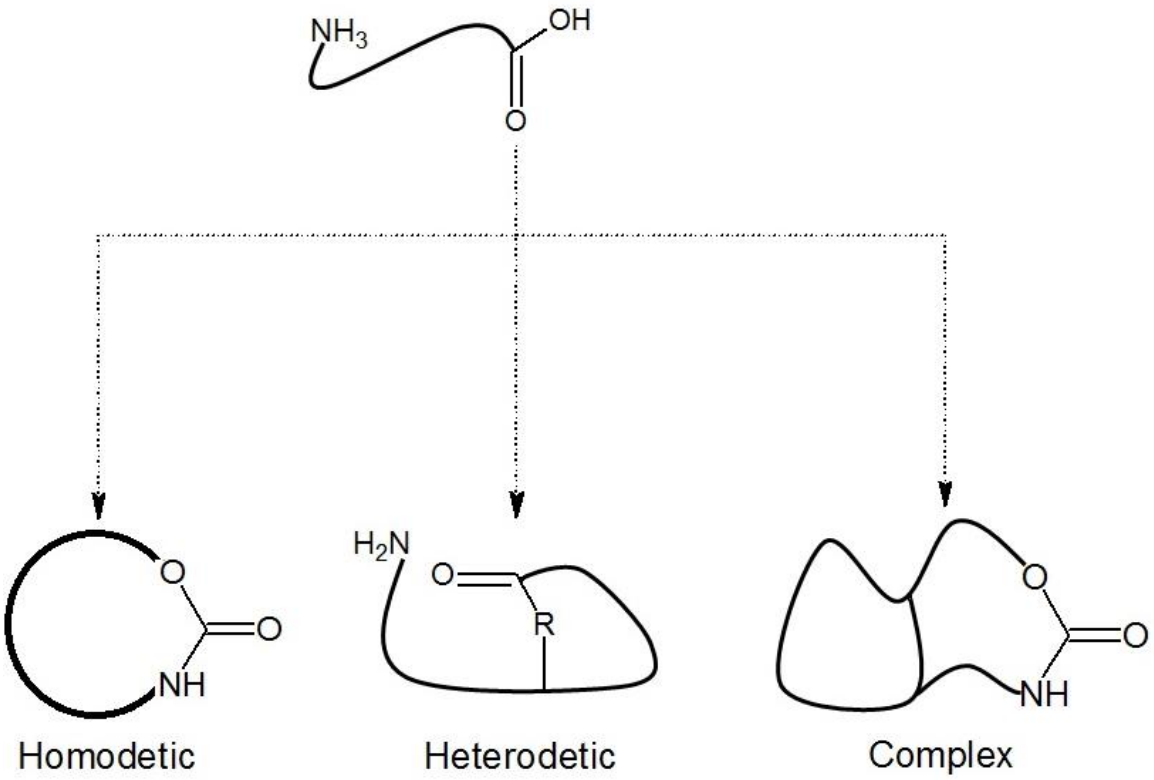

Figure 1: Subgroups within cyclic peptides as adapted from Bockus *et al* [30]. The natural products used in this research have multiple disulfide bonds and were chemically engineered to have a head to tail cyclized structure therefore they belong to the complex category.

Table 1: Examples of different cyclic peptides and their potential applications. Naturally occurring and chemically synthesized cyclic peptides can be divided into 3 categories (Homodetic, Heterodetic and Complex)

Name	Type	Source	Sequence	Type of Cyclization	Potential application	Reference
Kalata B1	N	*Oldenlandia affinis*	GLPVCGETCVGGTCNT PGCTCSWPVCTRN	*N*- to *C*- backbone (Complex)	Anti HIV activity, insecticidal activity	[31, 32]
Cyclic Vc 1.1	S	*Conus victoriae*	GCCSDPRCNYDHPEIC GGAAGG	*N*- to *C*- backbone (Complex)	Treatment of neuropathic pain	[19]
Bactenecin	S	Bovine neutrophils	RLCRIVVIRVCR	Heterodetic	Antimicrobial	[33]
MCoTI-II	N	*Momordica cochinchinensis*	GGVCPKILKKCRRDSD CPGACICRGNGYCGSG SD	*N*- to *C*- backbone (Complex)	Drug Delivery	[34, 35]
SFTI-I	N	*Helianthus annus*	GRCTKSIPPICFPD	*N*- to *C*- backbone (Complex)	Drug Delivery	[34, 36]
Lactocyclicin Q	N	*Lactococcus sp. QU 12*	LIDHLGAPRWAVDTILG AIAVGNLASWVLALVPG PGWAVKAGLATAAAIVK HQGKAAAAAW	*N*- to *C*- backbone (Homodetic)	Bacteriocin	[37]
Alpha Amantinin	N	*Amanita phalloides*	IWGIGCNP	*N*- to *C*- backbone (Complex)	Inhibitor of RNA polymerase II and III	[38]
RTD-1	N	*Macaca mulatta*	RCICTRGFCRCLCRRG VC	*N*- to *C*- backbone (Complex)	Antimicrobial	[39, 40]

N = Natural, S = Synthetic

Several methods currently exist for the production of cyclic peptides including: (a) solid phase peptide synthesis (SPPS) in combination with intramolecular native chemical ligation (NCL); (b) recombinant production through the use of a removable intein; (c) cyclization through enzyme catalysis, and; (d) the production of a stapled domain using a hydrocarbon linker. Each method contains its own specific advantages and disadvantages regarding the ability to obtain high throughput production, compatibility with specific amino acid sequences, and overall cost of production.

SPPS in combination with NCL is one of the most common methods of producing synthetic cyclic peptides due to the ease of the stepwise synthesis and straightforward application of NCL [19]. This method allows for partial automation due to the wide range of peptide synthesizers currently available, providing for a higher throughput production, and it allows for the incorporation of non-native or post-transnationally modified amino acid equivalents that would be difficult to incorporate in peptides that are produced recombinantly, as they generally rely on standard ribosomal processes. The major limitation of this technology is the requirement of a free cysteine residue for ligation. However “ligation-desulfurization” techniques have been developed that allow for the ligation at an Alanine, Valine, and Phenylalanine [41]. Examples of cyclic peptides synthesized by SPPS and NCL include Cyclic MrIA [42], Cyclic Vc 1.1 [43] and synthetic versions of members of the cyclotide family such as Kalata B1 [44].

Intein mediated synthesis is a recombinant expression technique that utilizes multiple internally excised protein sequences sometimes referred to as a “protein exons” to perform NCL *in vitro* without the interference of synthetic chemistry [45]. Cyclization through enzyme catalysis can be used in combination with SPPS to produce cyclic peptides [46]. This technique requires the use of partial synthetic and *in vitro* processes.

Macrocyclizaton is another technique employed by chemists to produce cyclic molecules [47]. Traditional methodologies such as lactomization and lactonization [48, 49], as well as newer techniques such as Ring Closing Metathesis (RCM) and “click” chemistry cycloadditions, have been used in producing macrocycles [47]. Macrocyclization has been known to improve peptide drug qualities by reducing polarity, by restricting peptide confirmation, and by increasing peptide stability by providing resistance to proteolysis [50, 51]. Different geometries of macrocycles such as (head to

tail, side chain to side chain, head to side chain) have been successfully designed [52]. Macrocyclization has been successful in designing therapeutics that target proteases, protein-protein interactions, and G-protein coupled receptors.

Finally, peptide stapling, a form of domain or peptide stabilization, performs many similar functions and contains its own advantages in comparison to *N*- to *C*-terminal backbone cyclization, these include: (i) increased lipophilicity for better absorption, and; (ii) membrane permeability and domain stabilization for retention of activity. However, this approach is limited for the further use of proteins as biochemical tools or markers due to a rarity of potential conjugation sites in native sequences [20].

1.1.7 Diversity of Ribosomally Synthesized Circular Proteins Found in Nature:

Circular proteins with their *N*-terminus and *C*-terminus linked in a peptide bond are found in bacteria, fungi, plants and animals. Initially these circular proteins were thought to be small (12 amino acids) and non-ribosomally synthesized [53]. However, today we know that these circular proteins can be synthesized ribosomally and can range in size from 6 to 80 amino acids. Naturally occurring cyclic molecules are incredibly stable and function as defense agents in host organism [54].

Bacteriocins are circular proteins produced by gram-positive bacteria. Generally ranging from approximately 35 to 70 amino acids, bacteriocins possess antimicrobial properties against a broad range of pathogenic microbes. The antimicrobial property of bacteriocins arises from their ability to disrupt cell membrane [34, 55, 56]. Host bacteria are immune to bacteriocins because they possess immunity proteins, which in conjugation with secretory ABC system help maintain bacteriocins at low cytoplasmic levels. Bacteriocins are rich in hydrophobic residues and unlike circular proteins of higher organisms lack disulfide bonds [57-60].

Until recently it was believed that all circular proteins in fungi were synthesized non-ribosomally. Cyclosporine the commonly used immunosuppressant is a non-ribosomal circular protein found in fungi [61]. However with the discovery of sequences corresponding to toxic cyclic compounds in the genome of *Amanita bisporigera*, a

mushroom that perception had to be modified [56]. Ribosomally synthesized circular proteins in fungi can be divided into two categories. The first category is amantoxins, which are RNA polymerase II inhibiting octapeptides, and the second category is phallocidins, which are F-actin stabilizing heptapeptide [34].

Mammals express antimicrobial proteins called defensins as part of their innate immune system. α- and β-defensins are disulfide rich linear peptides of 30 to 45 amino acids in length. However the more recently discovered θ-defensins are smaller in size and are characterized by head to tail backbone cyclization [34, 62]. The prototypic θ-defensin, Rhesus θ-defensin -1 (RTD-1) is 18 amino acids in length and has 3 disulfide bonds. Initially discovered for its antimicrobial properties, this circular molecule was later found to have protection against HIV-1 infection [63, 64]. Defensins are expressed in several Old world monkeys and orangutan but not in New World monkeys and humans. Humans have pseudogenes for θ-defensins but due to a mutation that introduces an immature stop codon in signal region the mRNA is not translated. However when the protein product corresponding to the pseudogenes was chemically synthesized the peptide possessed antimicrobial properties [65].

Cyclotides are circular plant proteins found in plants and form the largest family of circular proteins with nearly 250 sequences reported to date. Cyclotides are disulfide rich compounds naturally occurring in plants. They generally have about 30 amino acids and are found in range of plant families including *Rubiaceae* (coffee) and *Violaceae* (violet), *Fabaceae* (legume), *Solanaceae* (nightshade) and *Cucurbitaceae* (cucurbit). Cyclotides fall into two major subfamilies, the bracelet family that contains two-thirds of cyclotides, and the mobius family that contains the remaining one-third. There is a third subfamily called trypsin inhibitor family comprising of eight members [66-68]. Cyclotides are characterized by head to tail cyclization and contain six-conserved cysteine residues arranged in a knotted topology. The cyclic cystine knot morphology provides cyclotides with exceptional stability thereby making them prime candidates for grafting studies and as templates for drug design. These cyclic molecules have shown a vast array of activities ranging from antimicrobial, cytotoxic and anti-HIV. In nature cyclotides function as host defense agents and possess potent insecticidal activity [69, 70].

1.1.8 Conotoxin Bioengineering:

Conotoxins are disulfide rich neurotoxins found in the venom of marine conesnails. Conotoxins are typically about 10-40 amino acids in length, but exhibit many motifs such as α-helices and β-sheets that are normally found in larger proteins. These structural features are stabilized by disulfide bonds generated from the abundance of cysteine moieties in its primary structure [71]. Interestingly, these cysteine residues are found in predictable locations within a conotoxin's sequence, giving rise to loops of known amino acid lengths, which influence their bioactivity. Conotoxins can contain anywhere from one to five disulfide bonds which typically produce intramolecular connections [72]. However, conotoxins are also capable of forming intermolecular disulfide bridges as seen with Conotoxin Vt3.1 [73]. These dimeric conotoxins are worth investigating for unique receptor specificity and or augmented pharmacokinetic properties.

Conotoxins have been bioengineered to improve their stability, selectivity and affinity. According to Bingham *et al.* [74] conotoxin bioengineering can be divided to 6 generations. The first generation (G1) of bioengineering involves changes made to the primary sequence of conopeptides. In this phase changes were made to the primary sequence by adding or deleting amino acids (αα). All changes made during G1 involved the usage of native amino acids. During second generation (G2) of bioengineering changes were made by the introduction of unnatural amino acid-like analogues either by covalent chemical derivatization, or by strategic substitution(s). During the third phase (G3) of bioengineering modification were made by covalent addition of larger functional biomolecule(s) into the parent sequence. The fourth generation (G4) of conopeptide bioengineering involved *N*- to *C*-terminal cyclization of conopeptide to generate a peptide with no free terminus. Fifth generation (G5) bioengineering involved *N*- to *C*-terminal backbone cyclization as in G4 but in this case the cyclized molecule also had modifications from G1 to G3 incorporated into it. The sixth generation (G6) of bioengineering involved the creation of conopeptides that resembled organic molecules

in structure. These peptides were highly condensed and only contained the essential portion required for bioactivity [71].

Bioactivity of conotoxins is dependent on the peptide's ability to bind to multiple sites on the target receptor [75]. Efficient receptor-ligand interaction is contingent upon strong non-covalent interaction between amino acids of the receptor and the amino acids of peptide-toxin. Disrupting these interactions by mutating the peptide sequence can lead to loss of toxin bioactivity and can help in elucidating receptor physiology. Work done during G1 bioengineering phase has revealed essential amino acids required for bioactivity and laid the foundation for the next step in bioengineering. Luo *et al.* [76] demonstrated that substitution of only one amino acid could have profound impact on peptide activity. By replacing [Ala]-10 to [Leu]-10 in α-Conotoxin PnIA [A10L] they were able to shift of specificity from α3β2 to α7 nicotinic acetylcholine receptor (nAChR) subtypes. In addition to the change in receptor selectivity, this change of one amino acid also resulted in increased binding efficiency. The superior binding affinity of the mutated peptide can be attributed to the increased hydrophobic interaction between Leu of [A10L] of α-Conotoxin PnIA and a hydrophobic macro-site within the α7 receptor.

Work has also been done to determine the impact of peptide backbone truncation on peptide activity. Since peptide structure is directly related to peptide function a minimum number of amino acids is required to maintain a stable 3-dimensional structure. Backbone reduction experiment conducted on α-Conotoxin PnIA, one of the most potent and selective conopeptides for the α7 isoform subtype of the nAChR (IC_{50} of 12.6 nM), typifies the correlation of loop size and structure to biological function. The parent conopeptide 4/7 α-Conotoxin PnIA [A10L] has 7 amino acids between the 3rd and 4th Cysteine residues and an IC_{50} of 55 ± 9 nM for α7 nAChR. Gradual removal of 1 amino acid Tyr15 (4/6), 2 amino acids Asp14 (4/5) and 3 amino acids Pro13 (4/4) did not significantly impact the activity of the peptide (IC_{50} 79–207 nM). However, a removal of a 4th amino acid 4/3 [A10L] α-Conotoxin PnIA greatly decreased the activity (IC_{50} > 1000 nM). NMR studies conducted on parent peptide and its deletion variants revealed that removal of 1,2 and 3 amino acid maintained the α helix structure but the removal of 4th amino acid caused the α helix to collapse which lead to a loss in activity [77].

Another form of bioengineering is the creation of chimeras with peptide fragments from two different conotoxins/conopeptides joined together. By joining fragments from different peptides researchers can create a new molecule with enhanced binding affinity and selectivity. Sato *et al.* [78] combined the *N*-terminal half of ω-Conotoxin MVIIA, an N-type voltage gated calcium channel (N-VGCC) blocker, with the *C*-terminal portion of ω-Conotoxin MVIIC, a P/Q-type VGCC selective blocker to create a chimeric peptide that had higher affinity for P/Q-type VGCC. Chimeras of conopeptides and epitopes have been produced to create a molecule that possesses the structural stability of conopeptides and immunogenicity of epitopes. Drakopoulou *et al.* [79] and Mezo *et al.* [80] used α-Conotoxin GI as a 'host' peptide and inserted the core peptide epitopes from glycoprotein D (Asp-Pro-Val-Gly), and mucin1 glycoprotein (Pro-Asp-Thr-Arg) of the herpes simplex virus into the conopeptide. The chimeric molecule possessed the immunogenicity towards the epitope and contained the structural stability resulting from the disulfide bonds of conopeptide.

Another important form of conotoxin bioengineering is the modification of disulfide bonds for enhanced stability and bioactivity. The abundance of disulfide bonds within conopeptides makes them prime candidates for modification. Selective disulfide bond technology using Acetamidomethyl (Acm) is commonly used to chemically generate isomers not seen in nature. Additionally, oxidative conditions with different chaotrophic agents can be employed to generate various non-native isomers. By generating non-native isomers researchers aim to synthesize molecules with enhanced stability and bioactivity which are not produced naturally [81-83]. Researchers have also undertaken disulfide bond replacement technology in which the disulfide bond has been replaced to create a conopeptide analog that is more stable than its natural counterpart. Cysteine residues have been replaced with selenocystenine and disulfide bonds have been replaced with dicarba bonds to synthetically produce an analog that is more stable [84, 85]. In addition to these modifications other modifications commonly seen in conotoxins are replacement of amino acids with non-natural amino acids and radio labeling of amino acids.

1.1.9 Bioconjugation of Conotoxins Through Fluorophore Attachment:

Conotoxins offer high degree of selectivity and potency therefore they make ideal candidates for receptor probe development. A radiolabelled molecule presents issues regarding their synthesis, laboratory use, detection and disposal. Antibody based visualization tools are unable to visualize “live” cells and cross membranes. Since majority of the visualization tools have limitations a conopeptide based visualization platform would be able to complement current technologies [74].

Conotoxins are currently known to be of great benefit for use as molecular probes due to their ability to selectively interact with receptor subtypes. A prominent example of this is ω-Conotoxin MVIIA, which has been cited as a probe in over 2000 scientific publications [86]. The bioconjugation of visually traceable media such as biotin and fluorophores is fostering the potential for activity and structural investigation. Many examples depicting the usefulness of conotoxins as biological probes exist in literature and include receptor subtypes in calcium channels, potassium channels, sodium channels, 5-HT3 receptors, NMDA receptors and more [71]. Cohen *et al.* [87] attached a fluorophore to ω-Conotoxin GVIA by modifying the lysine residue at the 24th position by using tetramethylrhodamine (TAMRA) succinimidyl ester. The retention of bioactivity in this modified peptide was confirmed through radio ligand binding studies that showed similar Kd for native and fluorophore conjugated peptide (Kd 10–20 nM vs. native 0.6 nM). Durand *et al.* [88] used Conantokin G, a 17 αα, 5 γ-carboxyl glutamic acid (Gla) residue stabilized peptide that targets *N*-methyl-D-aspartate (NMDA) receptor as a template for fluorescent incorporation They used BODIPY Succinimidyl ester to covalently attach the fluorophore to the *N*-terminus. BODIPY-Conantokin G was then employed to label NMDA receptors in living neurons derived from the visual cortex of embryonic rats. The fluorescent bioconjugated Conantokin G tetramethylrhodamine (C-6906) is commercially available from Molecular probes/Invitrogen (www.invitrogen.com).

The lysine residue in conotoxins can be modified to a lysine azide and this functionality can be used for fluorophore attachment using Staudinger ligation. In the absence of a lysine residue any other residue with minimal contribution towards bioactivity as determined by 'Alanine–Walk' can be substituted for lysine azide and used for fluorophore addition. In case of multiple lysine residues, the lysine residue with the least contribution towards bioactivity can be modified.

Developed by Saxon and Bertozzi [89], the Staudinger ligation is a modification of the original Stuadinger reaction (Figure 2). The original reaction does not covalently attach the molecule after hydrolysis but the Staudinger ligation "ligates" or covalently attaches two molecules together. The mild conditions, sponteneity, and sensitivity make this chemoselective reaction highly attractive for use in live animals and physiologic conditions.

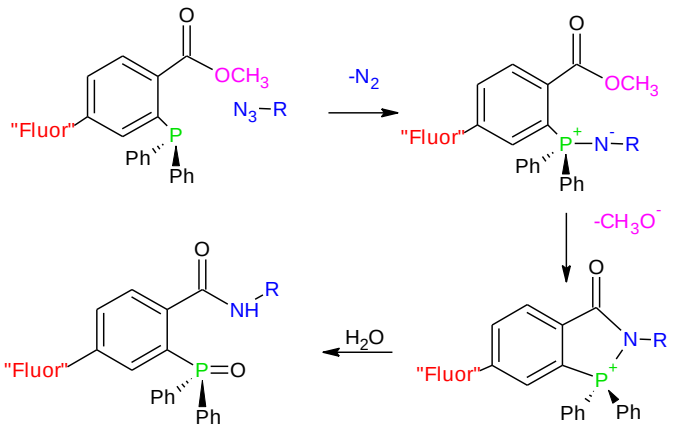

Figure 2: The Staudinger Ligation [86]. The phosphane is presented to the azide-containing molecule in water and the reaction proceeds spontaneously to ultimately form a stable amide bond conjugation. The above reaction can be used to produce imaging agents by conjugating an ion channel selective conotoxin to a fluorophore.

1.1.10 Therapeutics from Conotoxins:

An important feature of conotoxins is their nature to exhibit a high amount of biological activity. Since peptides in the milked venoms of *Conus* are highly processed and ready for prey envenomation these peptides offer phyla selectivity and high level of potency. *Conus* milked venom peptides thus represents a large natural library which if effectively mined might produce a new therapy for pain management, Alzheimer's, epilepsy or Parkinson's. To date, ω-Conotoxin MVIIA is the only FDA approved conotoxin for use as a therapeutic and is known for being extremely potent, displaying bioactivity in the low nanomolar range (7.6 nM IC_{50}) [90, 91]. However, this type of activity is not unique to this single peptide, as many conotoxins appear to be exceedingly potent. Examples of nanomolar potency among conotoxins include but are not limited to: the μ-Conotoxin MrVIA (IC_{50} = 345 nM) [92, 93] and the α-Conotoxin MIC (K_i = 248.7 nM).

ω-Conotoxin MVIIA, otherwise known as Ziconotide, has undergone extensive clinical testing [94]. Pharmacokinetics on Intravenous (IV) and Intrathecal (IT) injections of this peptide has been established. Classical distribution, metabolism, and excretion studies were undertaken before Ziconotide was entered into clinical trial. Ziconotide is the first non-opioid IT treatment for the management of chronic refractory pain and is known by its brand name Prialt®. The therapeutic is designed to be delivered intrathecally and should not be administered via any other Route of Administration (RoA). Prialt® is meant to be delivered only under the supervision of a physician using a programmable implanted variable-rate micro infusion device or an external micro infusion device and catheter. Prialt® is available as 1mL, 2mL or 5 mL vials (100 mcg/mL) and each vial is intended for single use. It should be stored at 2 to 8 ^{o}C and protected from light. Patients with existing psychotic conditions should not be treated with Prialt® as severe psychotic symptoms and neurological impairment may occur during treatment with Prialt®. Regular monitoring for cognitive impairment, hallucinations and mood swings should be undertaken during the treatment regimen [91]. Several publications describing the safety and efficacy of Prialt® have been published and can be studied for more comprehensive information.

The success of Prialt has led several biotechnology companies to search for the next therapeutic drug from conesnail venom. Several conotoxins like ω-Conotoxin CVID (AM336, Leconotide; Relevare Pharmaceuticals), Conantokin- G (CGX 1007; Cognetix), Contulakin-G (CGX 1160; Cognetix), and Xen2174 (structural analog of χ-Conotoxin MrIA; Xenome Pharmaceuticals), ACV1 (α-Conotoxin Vc1.1, Metabolic Pharmaceuticals) have reached various stages of clinical trial testing but so far Ziconotide is the only FDA approved therapeutic developed from conotoxin [95]. Kineta®, a Seattle based Biotech Company announced in January 2013 that it had acquired the developmental rights to α-Conotoxin RgIA (U2902) from the University of Utah research foundation. α-Conotoxin RgIA was isolated by the team of Dr. Olivera and found to selectively block α9α10 nAChRs [96, 97]. Kineta® intends to develop α-Conotoxin RgIA as a non-narcotic treatment for severe pain. Currently α-Conotoxin RgIA is in preclinical stage of development and Kineta® states that early results have been promising.

Even though majority of the conopeptides entering clinical trials have failed to develop as therapeutics all is not lost with these failed peptides. Viagra® one of the most marketable drugs in recent times was initially developed as a medication for hypertension (high blood pressure) and angina pectoris (a symptom of ischemic heart disease) [98]. During Phase I clinical trial it was discovered that the drug had little effect on angina but caused penile erection [99, 100]. The information gathered during Phase I clinical trial allowed Pfizer to redevelop sildenafil as a medication for erectile dysfunction and market it as Viagra®. These conopeptides that have failed during the clinical trial have undoubtedly garnered valuable information. This data might enable the pharmaceutical companies to reevaluate these potential drugs or have better understanding when developing the next conopeptide as therapeutic.

1.2 Overall Objective

The objective of this research is to explore the potential of conopeptides, which are disulfide rich neuropeptides found in the venom of conesnails as orally available drugs, biodegradable pesticides, and fluorescent probes. Conesnails are slow moving gastropods therefore they rely on conopeptides for prey incapacitation and capture. Since conesnails prey on faster moving organisms, their envenomation strategy must be quick and efficient [73, 101, 102]. Conesnails impale their prey in a harpoon like fashion using a hollow disposable tooth known as radula. The radula is attached to the venom duct and serves as a hypodermic needle that the snails use to inject venom into its prey [103-105]. These marine gastropods are able to paralyze their prey because conopeptides are highly selective towards various receptors and show a high level of potency. Even though these peptides may be as small as 10 amino acids they possess secondary structures such as alpha helices and beta sheets, which are commonly associated with larger peptides and proteins. As demonstrated by Jin *et al.* [77] the secondary structures in conopeptides are important in determining the bioactivity. Through their experiment Jin *et al.* [74] showed that a truncated peptide would possess bioactivity if the truncated sequence is able to maintain its secondary structure. Conopeptides are highly posttranslationally modified and these PTMs contribute towards venom diversity and phyla selectivity [103, 106-108]. Our interest in conopeptide development is greatly enhanced and aided by our location in Hawaii.

The waters of Hawaii are home for many unique conesnails. In the past extracting conesnail venom was an inefficient procedure, which required the animal to be sacrificed. Our lab has developed a sustainable method in which the venoms can be extracted without dissection. Using our method, the conesnails are raised and periodically milked for multiple venom collections. In our milking procedure a fish is first presented in front of the snail and the conesnail is then coaxed into firing its radula into the tail of the fish. The power generated during this envenomation process allows the radula to pierce the tail of the fish and pass into the strategically placed collection tube, where venom is ejected and collected.

In order to achieve our goal of developing stable drugs, biopesticides, and fluorescent probes from conopeptides, the first step is to choose the natural conopeptide that we want to explore further. We have thus far analyzed conopeptides from *Conus magus*, *Conus textile,* and *Conus virgo* before deciding on which conopeptide was the best candidate to bioengineer. After deciding on the appropriate conopeptide we devised a protocol to chemically synthesize and cyclize the newly engineered peptide. In their natural state conopeptides contain a free amino terminus and a free carboxy terminus. The presence of the free termini decreases the stability of peptides as it makes them susceptible to degradation from endopeptidases and exopeptidases. In order to overcome this hurdle, we planned to bioengineer cyclic peptides in which the amino and carboxy terminus are connected in a stable covalent bond. Through cyclization we planned to eliminate the free termini and thereby improve the stability of the peptides by decreasing their affinity for proteases. In our quest to develop a new protocol we used HwTx-I, a 33 amino acid peptide from *Ornithoctonus huwena* as a model peptide for this experiment. Once we had established a protocol for ligation, this novel protocol was used for cyclization. After synthesis we conducted preliminary stability and bioactivity assays on the cyclic peptides to assess the impact of cyclization on bioactivity and stability.

1.3 Objectives and Hypotheses

<u>Objective 1:</u> To investigate the implications of Post Translational Modifications (PTMs) on the selectivity of the conotoxins in an effort to change their activity and selectivity.

<u>Hypothesis for Objective 1:</u> Chemically synthesized conotoxin peptides having or lacking Post Translational Modifications (*N*-terminal truncation, Hydroxylation, Carboxylation), will have altered activity and receptor selectivity.

<u>Activities undertaken in objective 1:</u>

a) Use Solid Phase Peptide Synthesis (SPPS) to chemically synthesize α-Conotoxin MI [GRCCHPACGKNYSC-NH_2], α-Conotoxin MIC [CCHPACGKNYSC-NH_2], and α-Conotoxin MI-Des-[Gly]^1 [RCCHPACGKNYSC-NH_2]. α-MIC and α-MI-Des-[Gly]^1 are the *N*-terminal truncated version of α-MI.

b) Use SPPS to synthesize α-Conotoxin VIl [DC^{2}C^{3}SNOPC^{8}AHNNODC^{15}-NH_2, O = *4-trans* hydroxyproline (Hyp)], and α-Conotoxin Vi 1.1 [DC^{2}C^{3}SNPPC^{8}AHNNPDC^{15}-NH_2]. Vi 1.1 is the non-PTM version of VIl and lacks hydroxyprolines on residues 6 and 15.

c) Use SPPS to synthesize α-Conotoxin TxIC [ROQCCSHOACNVDHPγIC-NH_2; γ = γ-carboxyglutamic acid (Gla), O = *4-trans* hydroxyproline (Hyp)] and its non-PTM versions that lack hydroxyproline and γ-carboxyglutamic acid.

d) Purify synthesized peptides using manual preparative RP-HPLC.

e) Quantify isolated peptides by amino acid analysis and use these as peptide standards to determine LD_{50}.

f) Use the data to demonstrate intra-phyla specificity within worms, mollusks and fish, thus providing evidence to show that greater diversity of peptides results from PTM.

<u>Objective 2:</u> To replace hazardous Hydrogen Fluoride (HF) with milder Trifluoromethanesulfonic acid (TFMSA) in generating a *C*-terminal thioester, which is essential to conducting Native Chemical Ligation.

<u>Hypothesis for Objective 2:</u> Changing the volume of TFMSA and the incubation time in ice and room temperature will allow us to replace HF with TFMSA without compromising with the efficiency of the reaction.

<u>Activities undertaken in objective 2:</u>

a) Synthesis of 'Home-Made' thioester support resin for Solid Phase Peptide Synthesis (SPPS).
b) Use SPPS (Boc-chemistry) to produce the *N*-terminal fragment of Huwentoxin-I (HwTx-I) [ACKGVFDACTPGKNEC-THIOESTER], containing the thioester functionality.
c) Vary the kinetics and thermodynamics of the resin reaction to optimize the production of the *N*-terminal peptide with thioester functionality at the *C*-terminus.

<u>Objective 3:</u> Use Huwentoxin (HwTx-I) as an example to show the viability of our novel TFMSA cleavage technology in producing thioester containing fragment, which will be utilized in Native Chemical Ligation to produce bioactive peptide.

<u>Hypothesis for Objective 3:</u> We hypothesize that the use of TFMSA cleavage in conjugation with thioester ligation strategy can be used to generate a single linear peptide fragment by joining two peptide fragments. The fragment made through ligation is expected to have activity similar to the native peptide.

<u>Activities undertaken in objective 3:</u>

a) Generate the *N*-terminal peptide [ACKGVFDACTPGKNEC-THIOESTER] with a thioester at the *C*-terminus using Boc chemistry.
b) Synthesize the *C*-terminal peptide [CPNRVCSDKHKWCKWKL] using Fmoc chemistry.
c) Ligate the *N*-terminal fragment with the *C*-terminal fragment in a native peptide bond to produce ligated reduced HwTx-I [ACKGVFDACTPGKNEC CPNRVCSDKHKWCKWKL].
d) Compare the oxidized peptide produced through thioester ligation with the native peptide.

<u>Objective 4:</u> Utilize the novel thioester technology to synthesize cyclic α-Conotoxin Tx2005, which is the cyclized non-PTM version of α-Conotoxin TxIC (This objective is the culmination of skills acquired from the previous objectives).

<u>Hypothesis for Objective 4:</u> The novel TFMSA cleavage protocol can be used to generate the thioester moiety and this fragment will have the ability to undergo intramolecular thioester ligation to form a cyclic peptide.

<u>Activities undertaken in objective 4:</u>

a) Choose the conotoxin to cyclize and determine the approximate linker length using structural modeling. (As per Objective 1)
b) Synthesize the cyclic peptide on “Home-made” thioester resin. (As per Objective 2)
c) Cleave the peptide using the novel thioester protocol. (As per Objective 2)
d) Cyclize the linear peptide to produce a cyclic peptide. (As per Objective 3)
e) Oxidize the cyclic peptide so that it retains its three dimensional structure. (As per Objective 1)

Objective 5: **Determine the Pharmacodynamics of Cyclic Tx2005.**

Hypothesis for objective 5: **Since cyclization maintains the native conformation and disulfide bond connectivity. The receptor selectivity and activity (inhibition) of the cyclic peptide should be similar to the native linear peptide.**

Activities undertaken in objective 5:

a) Test the activity of linear and cyclic peptides on various isoforms of neuronal and muscular nAChR.
b) Test the activity of linear and cyclic peptides on various ion channels (sodium, potassium and calcium).

Objective 6: **Examination of bio-stability of Cyclic Tx2005, and Linear Tx2005.**

Hypothesis for objective 6: **Cyclic Tx2005 and Linear Tx2005 should have different stability profiles. The cyclic peptide should be more stable to enzymatic degradation than the linear peptide because the cyclic peptide has the two termini linked in a stable covalent bond.**

Activities undertaken in Objective 6:

a) Conduct stability assay on Linear Tx2005, Cyclic Tx2005 and Linear Tx2005 with linker using trypsin, pancreatin and carboxypeptidase.

Chapter 2: Conotoxins, Post Translational Modifications and Phyla Selectivity

This part of the study was undertaken to explore **Objective 1: To investigate the implications of Post Translational Modifications (PTMs) on the selectivity of the conotoxins in an effort to change their activity and selectivity.**

2.1 Introduction

The venom of *Conus* sea snails has evolved as an efficient means of prey incapacitation and as an effective defense mechanism [102]. The deadly effects of this cocktail are a direct result of Conotoxins, small disulfide-rich peptides that are potent antagonists of a range neuronal receptors and ion channels including nicotinic acetylcholine receptors (nAChRs), voltage-sensitive sodium and calcium channels, *N*-methyl D-aspartate (NMDA) receptors, and more. These bioactive peptides express selectivity towards their target receptors and are even able to discriminate between receptor subtypes, as demonstrated with α-Conotoxin ImI. α-Conotoxin ImI has an Inhibitory Concentration (IC_{50}) of 40.8 nM in the human acetylcholine receptor subtype α3β2 and an IC_{50} greater than 10 μM in the receptor subtype α1β1δε [109]. These properties are being utilized to design receptor-modulating ligands with potential therapeutic, bio-pesticide and ion channel visualization applications.

One of the most important and well-known aspects of conotoxins is their ability to selectively target ion channel subtypes [103]. This dynamic receptor-ligand interaction can be utilized to understand subtle differences in the normal physiology of various ion channel subtypes. As such, conotoxins are viewed as valuable resources for phyla selective receptor probes. Phyla selectivity is commonly seen amongst individual conotoxins, representing their native predatory preferences [101]. Many peptides isolated from a piscivorous cone snail such as *Conus magus*, will only display activity in receptor subtypes related to higher order organisms, whereas molluscivorous cone snails tend to produce conotoxins, which target mollusk receptor subtypes [110]. This type of selectivity can be greatly utilized in terms of creating safe and effective

pesticides. Potential pesticides produced from the venoms of molluscivorous cone snails may provide compounds that could be naturally degraded by microorganisms without producing harmful byproducts or causing environmental damage [111].

κ-Conotoxin PVIIA and δ-Conotoxin PVIA isolated from *Conus purpurascens* are conotoxins present in the same venom profile but exhibit two distinct mechanisms of action [112]. These peptides were categorically determined to be part of two individual "cabals" or modes of attack: κ-Conotoxin PVIIA on the lightning strike cabal, and δ-Conotoxin PVIA on the motor cabal. κ-Conotoxin PVIIA inhibits the Shaker potassium channel $K_v2.4$ and δ-Conotoxin PVIA delays the inactivation of sodium channels, allowing for a reinforced strategy of prey paralysis and capture, a synergistic technique akin to what modern drug companies are only now attempting to mimic. These techniques are often seen in *Conus* venoms and occasionally appear to be perplexing and contradictory. This is especially true when considering conotoxins from the motor cabal that inhibit sodium channel conductance and conotoxins from the lighting strike cabal that inhibit sodium channel inactivation. These two seemingly contradictory mechanisms are only beneficial if the afflicting conotoxins are highly selective for receptor subtypes acting in different areas of the cone snail's prey [103,105,112].

Post-translational modifications (PTMs) diversify the number of peptide toxins that can be made from the same genomic sequence [15, 113]. Considerable research has focused on elucidating the function of PTMs on conotoxin/conopeptide receptor selectivity and specificity [108, 114]. Studies in which PTMs such as γ-carboxyglutamic acid from Conantokin G (Conotoxin GV) and sulfated tyrosine in α-Conotoxin AnIb were eliminated have resulted in a significant decrease of bioactivity [115-117]. However, studies on the synthetic peptide α-Conotoxin Vc1.1 have revealed the converse. Clark *et al.* [19] observed that the non-PTM α-Conotoxin Vc1.1 was more effective at blocking α3α5β2 nAChR (94% inhibition at 7.2 ± 0.2 mM) compared to its PTM analog α-Conotoxin VcIa, [P6O]-Vc1.1, which failed to inhibit ACh-evoked currents [118]. This reveals considerable potential in the examination of non-PTM peptide variants as novel bioactive peptide templates.

Additionally, the impact of disulfide bond connectivity on structure activity relationships (SARs) has been explored since the majority of conotoxins contain

multiple disulfide bonds [74]. The selective production of disulfide bond isomers has now created additional novel unnatural conotoxin scaffolds that may possess differential pharmacological selectivity [119, 120]. In α-conotoxins with four cysteines, three isomers can be theoretically formed: (i) globular, (ii) ribbon and (iii) beaded. Chemical synthesis of the non-native ribbon structure, via selective disulfide bond formation, results in differential selectivity when compared to its native globular counterpart. This is observed with the ribbon form of α-Conotoxin AuIB at the α3β4 neuronal nicotinic acetylcholine receptor (nAChR; 1:1 α3:β4 ratio), with an IC_{50} of 0.77 μM compared to an IC_{50} of 2.48 μM for the globular form [42, 119, 120]. More recently, Khoo et al. [121] reported that two non-native μ-conotoxin isomers retained biological activity to the $Na_V1.2$ voltage-gated sodium channel. These findings highlight unique SARs that newly bioengineered conotoxins share with their receptor targets, thereby increasing their potential as novel drug templates [122].

2.2 Material and Methods

2.2.1 *Conus magus* Housing, Milking and Venom Extraction:

Nine specimens of *C. magus* were collected from Night Island, Far North Queensland, Australia (13°11′3″S 143°34′25″E). Specimens were fed weekly, using juvenile *Carassius auratus* (goldfish; weight 1 to 2 grams) and 'milked' of venom for a period of 12 months [123]. Individual MV volumes were measured, acidified with 0.1% v/v aqueous Trifluoroacetic acid (TFA/aq.; 50 µL) and stored at -20^{o}C to inhibit any enzymatic activity and/or degradation. For longer-term storage samples were Speed-Vac dried.

2.2.2 Conotoxin Reduction:

MV was Speed-Vac dried and re-suspended in 100 mM Tris(2-carboxyethyl)phosphine (TCEP; Pierce Chemicals) in 25 mM NH_4OAc, pH 4.5. To aid reduction, samples were heated at 60^{o}C for 15 min., and then RP-HPLC/UV purified.

2.2.3 Thiol Alkylation and *N*-terminal Edman Degradation:

TCEP reduced RP-HPLC purified peptides were dissolved in 25 mM NH_4OAc (90–150 µL), pH 4.5, and alkylated by adding 100 mM *N*-phenylmaleimide (Fluka, Switzerland) in isopropanol. Typically 20–40 fold excess w/w of the alkylating agent were used. Alkylation was allowed to proceed at 50°C for 15 min., prior to RP-HPLC/UV re-purification. Non-alkylated and *N*-phenylmaleimide alkylated peptides were applied to Polybrene-treated glass fiber support filters for automated *N*-terminal (Edman) degradation on a gas-phase sequencer (Model 470A; Applied Biosystems, Foster City, CA, USA). Phenylthiohydantoin (PTH) derivatives of 4-*trans*-Hydroxyproline (Hyp) and *N*-phenylmaleimide-alkylated cysteine were added into the amino acid standard mix to aid identification and sequence assignment.

2.2.4 Synthesis of α-MI, α-MI Des-Gly, and α-M1280:

2.2.4.1 Swelling of Pre-Loaded Resin:

Rink amide resin was measured for a 0.5 mmol scale synthesis and poured into a reaction vessel. Around 10-20 mL of Dimethylformamide (DMF) was added to the reaction vessel and allowed to shake for 30 minutes. The DMF was drained and 20 mL of DMF with 347 µL of Diisopropylethylamine (DIEA) was added to the reaction vessel. Basic DIEA was added to increase the pH of the reaction mixture thereby increasing the activity of the resin. The resin was allowed to swell overnight.

2.2.4.2 Deprotecting the *N*-terminus of the Rink Amide Resin:

The resin was flow washed with ample amount of DMF. Approximately 5 mL solution of 50 % v/v piperidine in DMF was added to the reaction vessel and shaken for 1 minute. The solution was drained and the piperidine shake was repeated. Piperidine wash ensures that the resin has a free amino group to which the incoming orthogonally protected amino acid can be added. Remnants of piperidine and Fmoc were flow washed from the reaction vessel using approximately 100 mL of DMF.

2.2.4.3 Activation of Fmoc Amino Acid:

The desired amino acid of choice was measured to a 2 mmol scale and placed in a scintillation vessel. In a separate scintillation vessel 2 mmol of 2-(1H-benzotriazol-1-yl)-1,1,3,3,-tetramethyluronium hexafluorophosphate (HBTU) or 2-(6-chloro-1-H-benzotriazole-1-yl)-1,1,3,3-tetramethylaminium hexafluorophosphate (HCTU) was weighed. HBTU/HCTU was dissolved in 4 mL of DMF and the solution was transferred to the scintillation vial containing amino acid. The scintillation vessel was vortexed to ensure that the amino acid and coupling reagents are fully dissolved. Once dissolution happens 347 µL of DIEA was added to the reaction vessel to quench the protons generated during amino acid activation. The amino acid and activating reagents were measured in 4-fold access to the 0.5 mmol resin.

2.2.4.4 Coupling of the Amino acid:

The activated amino acid at 2 mmol scale was added to the reaction vessel containing 0.5 mmol resin and allowed to couple for 20 minutes. Since the amino acid is in 4-fold access to the potential binding sites on the resin the reaction is expected to reach theoretical completion. The reaction is considered complete when the % coupling as determined by ninhydrin test exceeds 99.5 %.

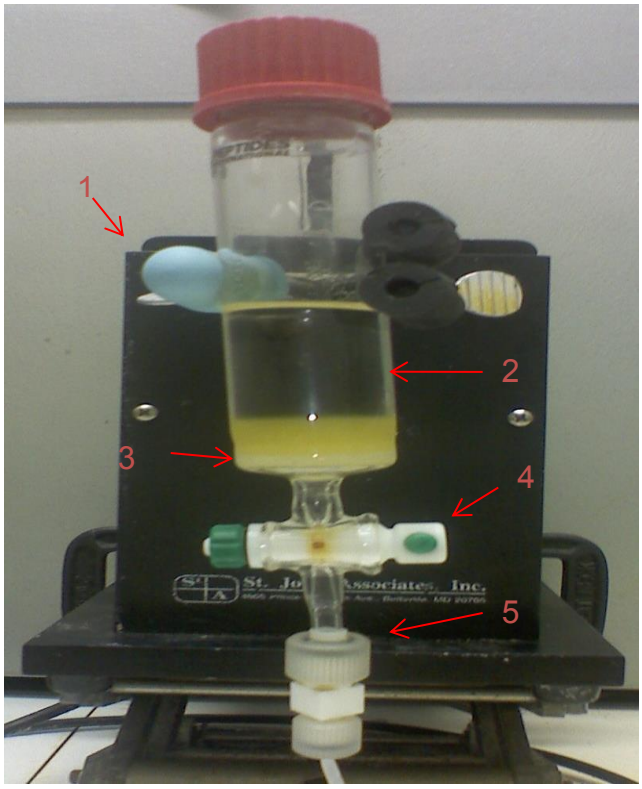

Figure 3: A standard setup for SPPS. 1) Mechanical shaker for mixing of reagents and resin, 2) Reaction chamber with solvent (clear liquid) and resin bound peptide (yellow layer), 3) The glass filter section that retains the resin during a flow wash while allowing the solvent to pass through, 4) Stop-cock which allows for manual regulation of flow rate, and 5) Vacuum tube that is connected to a waste receptacle which provides the suction for draining of solvent.

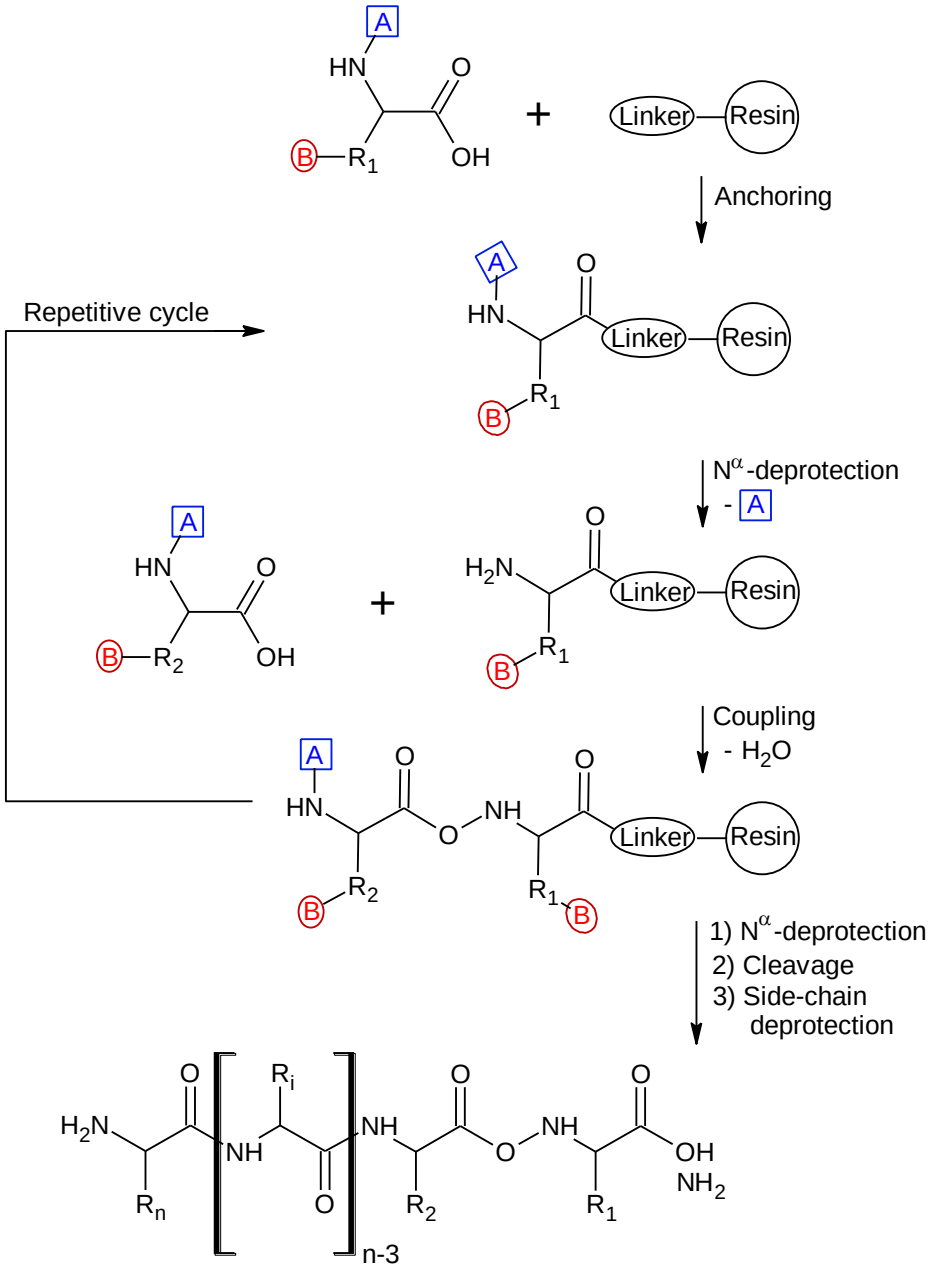

Figure 4: Mechanism of SPPS for peptide synthesis. An N^{α}-protected amino acid is covalently bonded to the insoluble and inert solid support. The N^{α}-protecting group (A) is selectively removed. The next N^{α} and orthogonally (B)-protected amino acid is coupled. The deprotection/coupling steps are repeated in a sequential manner until the primary sequence is synthesized from the *C*-terminus to the *N*-terminus. Cleavage frees the peptide from the resin and allows for further processing.

2.2.5 Ninhydrin Analysis:

2.2.5.1 Procedure:

Ninhydrin analysis was undertaken to determine if the coupling % of amino acid is satisfactory and the next amino acid in the primary sequence can be added to the growing peptide chain. 2 to 5 mg of the peptide resin was removed from the reaction vessel and flow washed with 50 % v/v DCM in Methanol on a filter thimble under vacuum until the peptide resin is dry. The resin was transferred to a tared tube and the mass was recorded. To the test tube containing the peptide and an empty control tube the following reagents were added: 2 drops of Reagent 1 (76 % w/w phenol in ethanol), 4 drops of Reagent 2 (0.2 mM potassium cyanide KCN in pyridine), and 2 drops of Reagent 3 (0.28 M ninhydrin in ethanol). Both the tubes were covered with Parafilm® and placed in a sand bath, regulated at 95º C for 5 minutes. After removal from the sand bath, 3 mLs of 60 % ethanol in water (v/v) was added to each test tube and centrifuged for 30 seconds. The supernatant was collected and absorbance of the resin sample was read against the control blank at 570 nm and recorded [124].

2.2.5.2 Calculation:

The % coupling can be determined by using the following equation

$$\%\ Coupling = 1 - \left(\frac{NV}{SV}\right) * 100$$

The NV stands for Ninhyndrin Value and gives us an estimate for the NH_2 group that did not bind to the amino acid in the coupling step. NV can be calculated using the following equation. The variables required for NV calculation were obtained from the procedure mentioned above.

$$NV = \frac{(absorbance_{570})(200)}{resin\ mass\ (mg)}$$

The SV stands for Substitution value and provides the theoretical mole value of the total peptide. SV was calculated using the equation below.

New SV = (previous SV)/ [1 + (previous SV x AA MW)]

The previous SV for the first amino acid was determined through the Resin loading value, which was provided by the manufacture. This value indicates the number of [moles/g or mmole/mg) of resin. While calculating the amino acid molecular weight we must consider that all amino acids have a protection group at the *N*-terminus and some amino acids also have a side chain protection group.

Inputting the observed data into % coupling equation provides us with the % coupling. If this value is more than or equal to 99.5 % the next amino acid is coupled to the growing peptide chain. A score of below 99.5 % indicates that the coupling has not reached the desired level of completion and is considered to be incomplete, hence must be improved upon. In this scenario one option is to add a small aliquot (100 µL to 200 µL) of DIEA and allow the coupling to go for additional 30 minutes. Another option is a re-coupling of more activated amino acid following a DMF wash of reaction vessel to wash out the reagents and unreacted amino acids.

2.2.6 *N*-Capping:

If a sequence of hydrophobic or sterically hindered amino acids is encountered during SPPS some or all of the amino acids couplings may not reach 99.5 %. Free NH_2 functions cause a deletion product when the new amino acid is coupled to the growing peptide chain. The deletion product is permanent and leads to side products that reduce the final yield of target peptide and cause problems during peptide purification. One way to stop this from happening is by capping the free NH_2 and preventing that functionality from taking any further part in synthesis. End Capping increases the yield of the final product and by minimizing the byproducts saves time and resources during purification. Firstly, the resin was flow washed with abundant DMF to remove any former unreacted amino acids and reagents from the system. 50 % v/v *N*-methylpyrrolidone (NMP) in DCM was flow washed through the resin twice using ~20 mL each time. While doing this step extreme caution must be undertaken to avoid letting air pass through and dry the resin. The reagent *N*-(2-chlorobenzyloxycarbonyloxy) succinimide (Z [2-Cl]-OSu) was weighed out in a scintillation vial to 0.5 mmol and dissolved in 4 mL of the NMP/DCM solvent previously prepared to activate the Z(2-Cl)-OSu. 347 µL of DIEA was added to the scintillation vial, mixed, and poured into the reaction vessel to react for 5 minutes. The reagents were then removed by two flow washes of approximately 20 mL using the NMP/DCM solvent with care, and then using abundant DMF. All free N^{α}-terminal groups of the peptidyl-resin are now terminated and the next required amino acid could to be coupled to the growing peptide chain.

2.2.7 Cleavage of the Peptide Resin:

Upon completion of the synthesis the peptide must be cleaved from the resin. The Cleavage cocktail for Fmoc synthesis is called Reagent K and has the following composition: 82.5 % v/v TFA, 5 % v/v DI water, 5 % v/v thioanisole, 5 % v/v phenol, and 2.5 % v/v 1,2-ethanedithiol (EDT). TFA is used to release the resin bound peptide. TFA is also used to scavenge Fmoc protective group, tert-Butyl side chain protective groups and trityl side chain protective groups. Phenol is used to scavenge tert-butyl groups and EDT is used to scavenge thiols. Thioanisole is used to mop up trityl protection group and water performs the function of a universal scavenger of side chain protecting groups.

Reagent K was prepared at 20 to 40 mL per gram of the resin and stored in an Erlenmeyer flask containing a stir bar. The weighed amount of resin was carefully transferred to the Erlenmeyer flask and the resin reagent slurry was allowed to stir at room temperature for 150 minutes. After incubation the slurry was vacuum filtered in a glass Buchner funnel over a Whatman® filter (No.4) and the supernatant was collected in a pear flask. The contents in the pear flask were equally transferred to a 50 mL Falcon tubes containing 30 mL of liquid nitrogen chilled tert butyl methyl ether (MTBE). The falcon tubes were balanced and centrifuged at 3500 rpm for 8 minutes. Supernatant was carefully decanted without disturbing the peptide pellet. The peptide pellet was suspended in 30 mL of cold MTBE and the centrifugation and decantation process was repeated twice. After 3 centrifugations with MTBE a final centrifugation without MTBE was done to remove all scavenging agents from the peptide pellet. A 30 mL solution of 5 mLs of acetic acid (25 % v/v) and 25 mL water was placed in each of the falcon tubes to dissolve the peptide pellet. All materials were then pooled into one round-bottom flask. The pear flask was shelled using liquid nitrogen and freeze-dried. The lyophilized peptidic material was removed, massed, and stored in a scintillation vial for future purification.

2.2.8 Oxidation of Peptide Material:

The free cysteines of reduced peptides were folded to disulfide-bonded cystines of oxidized peptide by exposing the peptide to aqueous basic buffer. Oxidation of cysteine was achieved by allowing the peptide to stir in 0.1 M Ammonium bicarbonate buffer at pH 8. Since the free thiol of cysteine has a pH of 8.18 it was expected that a buffer of pH 7.5 or more would be able to oxidize the cysteine over the course of 5 days. To ensure the production of most favorable product the oxidation process was thermodynamically slowed and done at 4^{o}C. Peptide oxidations were done at a concentration of 1mg peptide/10 mL oxidation buffer. The desired amount of peptide was weighed in an Erlenmeyer flask containing a stir bar and the required amount of buffer was gradually poured into the flask. The flask was covered with Parafilm® and allowed to stir at conditions as mentioned above.

2.2.9 Desalting of Peptide:

Dropping the pH of the oxidation buffer to 4 terminates the reaction; this was achieved by gradually adding neat acetic acid to the oxidation solution. Once the required pH was achieved the solution was transferred to a round bottom flask and shelled using liquid nitrogen. The lyophilized material was dissolved in 50 to 100 mL Solvent A and was filtered using 0.42 µm filter. The solution was then loaded to a C_{18} preparative column and the gradient was set at (95 % solvent A, 5 % solvent B). At this gradient salts and other buffer reagents are eluted off the column whereas the peptide material is bound to the column. After the salts were removed as indicated by the absorbance reading the gradient was changed to (20 % solvent A and 80 % solvent B). The peptide was collected in a round bottom flask and the solution was shelled and freeze-dried. The lyophilized peptidic material is stored in -20º C for further purifications.

2.2.10 RP-HPLC Solvent Composition:

RP-HPLC uses a combination of solvents for its mobile phase. The mobile phase is a mixture of aqueous polar solvent and organic non-polar solvent. Water is the most commonly used polar solvent while methanol and acetonitrile are the most common non-polar solvents. Most HPLC systems run both solvents at the same time and they are referred as solvent A (Sol. A) and solvent B (Sol. B). Solvent A is maintained at 100 % polar (aqueous) whereas solvent B is a mixture of 90 % organic and 10 % aqueous. Ion pairing agents (IPA) such as Trifluoroacetic Acid (TFA), Heptaflurobutyric Acid (HFBA), Hexafluoroacetone (HFA), Formic Acid and Hydrochloric Acid are added to the solvents. IPA is used to increase the binding probability of analyte to the stationary phase by increasing the hydrophobic interaction between analyte and non-polar stationary phase. Since the retention time is dependent on the concentration and type of IPA used, choosing the right IPA combination is of paramount importance. HFBA is known to provide the longest retention time while shorter retention time can be achieved by using TFA.

2.2.11 RP-HPLC Gradient:

The initial solvent composition when loading the sample was 95 % Sol. A and 5 % Sol. B. At this combination the mobile phase is polar, which allows the non-polar target molecule (peptide) to bind to the column and causes unwanted polar material, like salts, to elute. Gradually the mobile phase was transitioned to being non-polar at a gradient of 1 % minute^{-1}. At 5-65 minutes, the initial flow conditions (5 % v/v Sol. B in Sol. A) undergoes a 1 % minute^{-1} increase of Sol. B and a decrease of Sol. A at 1 % minute^{-1}. Thus, at 65 minutes the flow conditions are at 65 % v/v Sol. B and 35 % v/v Sol. A. The next 5 minutes experience a 3 % v/v increase of Sol. B and a 3 % v/v decrease of Sol. A, finishing with a 5 minute period at 80 % v/v Sol. B in Sol. A to flush the column. The final 5 minutes reset the flow back to the initial conditions, in which a 15 % v/v increase of Sol. A per minute and 15 % v/v decrease of Sol. B per

minute occurs. When the required solvent composition is reached the target material elutes from the column and is collected accordingly. When dealing with an unknown material it is advisable to run the entire gradient (Table 2). Once you have established the retention time of the desired material you can reduce the run accordingly.

Table 2: Gradient of a typical HPLC run over the course of 80 minutes. Initially the solvent is polar (95 % Solvent A and 5 % Solvent B). During the course of the HPLC run the solvent becomes non-polar by increasing the percentage of Solvent B and decreasing the percentage of Solvent A.

Time (minutes)	Solvent A	Solvent B
0	95 %	5 %
5	95 %	5 %
30	70 %	30 %
65	35 %	65 %
70	20 %	80 %
75	20 %	80 %
80	95 %	5 %

2.2.12 Sample Preparation:

The lyophilized samples were transferred to a scintillation vial and dissolved in large volume of solvent A (90 to 95 %) and small volume of solvent B (5 to 10 %). The peptide solution was sonicated for 10 minutes to ensure the total homogenous solubility of peptide. Post sonication the solution is filtered using 0.45µm filter and is ready to be loaded into the HPLC for fractionation.

2.2.13 Sample Loading:

The filtered sample was manually injected into the injection port in a Waters® 600E/2695 HPLC system and pumped onto the attached column. During injection the solvent gradient is set at baseline conditions (95 % Sol. A and 5 % Sol. B) and the flow rate is dependent on the type of column used (Table 3). This baseline conditions allows salt and other hydrophilic waste to elute while the hydrophobic peptide attaches to the column. The amount of injected material determines the type of column used (Table 3)

Table 3: Flow rate and type of column used in HPLC for a range of injected masses. The type of column used is dependent on the amount of material injected. When a small amount has to be purified a capillary column is used and a large semi-preparatory column is used for large-scale purifications.

Column	Gradient	Flow Rate	Mass Limitation
Large semi-preparatory C_{18}	Large semi-prep method	5 mL/minute	20-100 mg
Semi-preparatory C_{18}	MV method	3 mL/minute	5-20 mg
Analytical C_{18}	Analytical MV method	1 mL/minute	1-5 mg
Capillary C_{18}	LC-MS method	0.1 mL/minute	10-100 µg

2.2.14 Sample Detection:

Samples were visualized by the Waters® PDA 996 and collected with their retention times recorded. Peptides and proteins are detected using their covalent amide bond, which has UV absorption at 214 nm. If the protein or peptide has an aromatic amino acid in its sequence it has UV absorption at 280nm.

2.2.15 Sample Collection:

Samples of large volume (5 to 8 mL) were collected in a scintillation vial and small volume samples (less than 1mL) were collected in an Eppendorf tube. All collected samples were shelled using liquid nitrogen and placed under vacuum on a freeze dryer to lyophilize the peptide. The dried samples were kept in a -20°C freezer for storage and future use.

2.2.16 Mass Spectrometer:

2.2.16.1 Sample Preparation:

The lyophilized sample was reconstituted in (50:50 v/v Solvent A': Solvent B') Mass Spectrometer (MS) buffer (Solvent A': 0.1 % v/v formic acid/*aq* and Solvent B': 90 % v/v MeCN in 0.8 % v/v formic acid). The MS buffer is similar in composition to the HPLC buffer but differs in the type of ion pairing agent. Since TFA has a tendency to promote charge suppression, it is replaced by formic acid in MS buffer.

2.2.16.2 Sample Injection:

10 µL of sample was inserted into an injection port using a Hamilton® syringe that was back-pressured by a solvent pump and partially (2-3 µL) injected onto the system. The solvent pump was set at a flow rate of 50 µL/minute of solvent A/B (50/50 v/v, formic acid). The sample was injected onto a PE Sciex API 3000 LC/MS/MS and monitored with Analyst® Software recording the ionization pattern of the sample.

2.2.17 Determination of Bioactivity:

2.2.17.1 LD_{50} Toxicity Assay:

Concentrations of 30, 20, 15, 12, 10, 8, 6, 2, and 1 nmol/g of conotoxins α-MI, des [Gly][1] α-MI and α-MIC, in 1 mL volumes, were injected intramuscularly by Hamilton micro-liter syringe into 0.3–0.4 gram green swordtail fish (*Xiphophorus helleri*). LD_{50} injections were also carried out on Indian Blue worms (*Perionyx excavates*) and golden apple snails (*Pomacea diffusa*). Dosage and survival times were recorded and plotted in dose as a function of dose/survival time, with an estimated LD_{50} value being determined based on the y-intercept and converted to mg/kg [125]. All dose experiments were performed in triplicate.

2.2.17.2 Nicotinic Acetylcholine Receptor Competitive Radioligand Binding Assay:

2.2.17.2.1 Nicotinic Acetylcholine Receptor Binding Assays:

(i) $\alpha 4\beta 2$* nAChR: Rat brain membranes (60-70 µg of protein; Pel-Freez Biologicals, Rogers, AR, USA) were incubated at 22°C for 90 minutes in 0.5 mL HSS containing 0.5 nM (±)-[^{3}H] epibatidine (56.3 Ci mmoL^{-1}; PerkinElmer, Boston, MA, USA) and different concentrations of conotoxins α-MI, *des* [Gly][1]α-MI, and α-MIC. Non-specific binding was determined using 300 µM (-)-nicotine hydrogen tartrate. (ii) $\alpha 3\beta 4$* nAChR: Membranes derived from pig adrenals (60-70 µg of protein; Pel-Freez Biologicals, Rogers, AR, USA) were incubated at 22°C for 90 minutes in 0.5 mL HSS containing 0.5 nM (±)-[^{3}H] epibatidine and different concentrations of conotoxins α-MI, *des* [Gly][1]α-MI, and α-MIC accordingly. Non-specific binding was determined using 600 µM (-)-nicotine hydrogen tartrate. (iii) Muscle-type nAChR: Membranes (60-70 µg of protein) from *Torpedo californica* electroplax (Aquatic Research Consultants, San

Pedro, CA, USA) were incubated for 90 minutes in 0.5 mL HSS containing 2 nM (±)-[^{3}H]epibatidine and different concentrations of conotoxins α-MI, *des* [Gly]^{1}α-MI, and α-MIC accordingly. Non-specific binding was determined using 600 µM (-)-nicotine hydrogen tartrate. All incubations were terminated by vacuum filtration through Whatman GF/B glass fiber filters, presoaked in 1 % poly(ethylenimine) using a Brandel 48-channel cell harvester. The radioactivity was measured using a liquid scintillation counter (Tri-Carb 2910 TR, PerkinElmer, Shelton, CT, USA). Protein measurements were performed using the Bradford method (Bio-Rad assay kit) and bovine serum albumin, diluted in HSS, as a standard.

2.2.17.2.2 Data Analysis:

Competitive binding data were analyzed using nonlinear regression methods. K_i values were calculated by the Cheng-Prusoff equation, $K_i = LC_{50} / (1 + [S]/ K_d)$, based on the measured LC_{50} values and K_d = 8±0.3 pM for binding of (±)-[^{3}H] epibatidine to $\alpha4\beta2$*, K_d = 50±2.3 pM for binding of (±)-[^{3}H] epibatidine to $\alpha3\beta4$* and K_d = 2±0.3 nM for binding of (±)-[^{3}H]epibatidine to muscle type receptor. The K_d values were obtained from 5 independent experiments performed on the same membrane preparations that were used for the competition assays.

2.2.18 Methods for *Conus textile* Project

Synthesis, cleavage, oxidation and purification of α-Conotoxin TxIC [ROQC^{4}CSHOAC^{10}NVDHPγIC-NH_2; γ = γ-carboxyglutamic acid (Gla), O = *4-trans* hydroxyproline (Hyp)] and a non-PTM amino acid variant of α-Conotoxin TxIC, (i.e. [Pro]^{2,8}[Glu]^{16}α-Conotoxin TxIC [RPQC^{4}CSHPAC^{10}NVDHPEIC-NH_2] was undertaken in a similar fashion to the magus project as described above. The venom analysis and bioactivity section for this part of the project was different and is discussed below.

2.2.18.1 MALDI-TOF MS Venom Analysis:

ZipTip™ or RP-HPLC/UV purified venom fractions in Solvent A (0.1% v/v aq. TFA) were mixed 1:1 with matrix solution (40 g L^{-1} 2,5-dihydroxybenzoic acid (DHB) in 1:1 0.1% v/v aq. TFA: CH_3CN) and 1 μL was spotted on a MTP 384 polished steel target plate (Bruker Daltonics). The spots were dried under a stream of N_2 gas. Mass spectra were acquired on the Ultraflex III (Bruker Daltonics), controlled by the Compass 1.2 SR1 software package (Bruker Daltonics), in positive reflector mode from *m/z* 500 to 5000. Mass spectra were summed (400 to 1200 laser shots) until no further improvement to the signal to noise ratio of peaks was achieved. Peptide II Calibration Mix (Bruker Daltonics) was used for external calibration, with a 5-ppm mass accuracy. Analysis of the spectra was completed using FlexAnalysis v3.0 (Bruker Daltonics).

2.2.18.2 MALDI-TOF/TOF MS Peptide Sequencing and PTM Characterization:

The reduced venom peptide, α-conotoxin TxIC, was desalted via ZipTip™ (C_{18} reversed-phase media, Millipore) or RP-HPLC/UV isolated and spotted onto the target plate with DHB matrix. Tandem mass spectra (MS/MS) were acquired in reflector positive LIFT mode on the UltraflexIII (Bruker Daltonics), externally calibrated with Peptide Calibration Mix II (Bruker Daltonics) with a MS/MS accuracy of 0.04 Da. FlexAnalysis v3.0 (Bruker Daltonics) was used for manual inspection and annotation of the LIFT-spectra. The RapiDeNovo module in BioTools (Bruker Daltonics) was used to make additional assignments to the amino acid sequence.

2.2.18.3 Pharmacology:

2.2.18.3.1 Expression of Voltage-Gated Ion Channels in *Xenopus laevis* Oocytes:

For the expression of nAChR (α1, α3, α4, α5; β2, β4; γ; δ; ε) in *Xenopus* oocytes, the linearized plasmids were transcribed using the T7 or SP6 mMESSAGE-mMACHINE transcription kit (Ambion®, Carlsbad, CA, USA). The harvesting of stage V–VI oocytes from anaesthetized female *Xenopus laevis* frog was previously described Liman *et al.* [126]. Oocytes were injected with 50 nL of cRNA at a concentration of 1 ng/nL using a micro-injector (Drummond Scientific®, Broomall, PA, USA). The oocytes were incubated in a solution containing (in mM): NaCl, 96; KCl, 2; $CaCl_2$, 1.8; $MgCl_2$, 2 and HEPES, 5 (pH 7.4), supplemented with 50 mg/L gentamycin sulfate.

2.2.18.3.2 Electrophysiological Recordings:

Two-electrode voltage-clamp recordings were performed at room temperature (18–22°C) using a Geneclamp 500 amplifier (Molecular Devices®, Downingtown, PA, USA) controlled by a pClamp data acquisition system (Axon Instruments®, Union City, CA, USA). Whole cell currents from oocytes were recorded 1–4 days after injection. Bath solution composition was (in mM): NaCl, 96; KCl, 2; $CaCl_2$, 1.8; $MgCl_2$, 2 and HEPES, 5 (pH 7.4). Voltage and current electrodes were filled with 3 M KCl. Resistances of both electrodes were kept between 0.5–1.5 MΩ. During recordings, the oocytes were voltage-clamped at a holding potential of −70 mV and superfused continuously with ND96 buffer via gravity-fed tubes at 0.1–0.2 mL/minute, with 5 minute incubation times for the bath-applied peptides. Acetylcholine (ACh) was applied via gravity-fed tubes until peak current amplitude was obtained (1–3 sec.), with 1–2 minute washout periods between applications. Data were sampled at 500 Hz and filtered at 200 Hz. Peak current amplitude was measured before and following incubation of the peptide.

To assess the concentration-response relationships, data were fitted with the Hill equation: $y = 100/[1 + (EC_{50}/[\text{toxin}])^{h}]$, where y is the amplitude of the toxin-induced effect, EC_{50} is the toxin concentration at half maximal efficacy, [toxin] is the toxin concentration and h is the Hill coefficient. Comparison of two sample means was made using a paired Student's t test ($p<0.05$). All data are presented as mean ± standard error (S.E.M) of at least 4 independent experiments ($n \geq 4$). All data was analyzed using pClamp Clampfit 10.0 (Molecular Devices®, Downingtown, PA, USA) and Origin 7.5 software (Originlab®, Northampton, MA, USA). Our collaborator Dr. Jan Tytgat (KU Leuven) performed this section.

2.2.18.3.3 Whole Animal Bioassay:

Standardized concentrations of native of α-Conotoxin TxIC (2.5, 5, 10, 20, 40, 80, 160, 320 and 640 pMole/g) and synthetic $[Pro]^{2,8}[Glu]^{16}$α-Conotoxin TxIC (0.16, 0.32, 0.64, 1.28, 2.56, 5.12 and 10.24 nMole/g) in 10 mL volumes (PBS), were injected intramuscularly (IM - foot) into Hawaiian snakehead cowries (*Cypraea caputserpentis*) using a Hamilton 10 µL syringe at a depth of 2 mm. Following injection, animals were placed in glass Petri dishes filled with fresh aerated seawater, where paralysis was determined by the inability of the animal to cling to the substrate. Dosage and paralysis were recorded and plotted according to Reed and Muench [127] and the PD_{50} was extrapolated using GraphPad Prism Software (v5.02). All dose experiments were repeated in triplicate or greater ($n \geq 3$).

2.2.19 Methods for *Conus virgo* Project

The methods for Virgo project were similar to the previously mentioned section of the project. Additional sections for this portion of the project is mentioned below

2.2.19.1 Peptide Synthesis:

α-Conotoxin ViI [$DC^2C^3SNOPC^8AHNNODC^{15}$-$NH_2$] and α-Conotoxin Vi1.1 [$DC^2C^3SNPPC^8AHNNPDC^{15}$-$NH_2$], the non-PTM version of α-Conotoxin ViI, was manually assembled using a 0.5 mMole scale by 9-fluorenylmethoxycarbonyl solid-phase-peptide synthesis (Fmoc SPPS) using a MBHA resin. An additional 0.5 mMole synthesis of Vi1.1-Isomer A and B was undertaken using orthogonally protected Cys (Acm) to direct disulfide bond formation. Cys (Acm) was placed in positions 2 and 15 for Vi1.1-Isomer A and position 3 and 15 in Vi1.1-Isomer B in the above sequence

2.2.19.2 Random Disulfide Bond Formation:

Peptide oxidation was achieved with 15 mg of TCEP reduced C_{18} RP-HPLC/UV purified peptide using 0.1 M NH_4HCO_3 pH 8.7 (5 days stirring at room temp.). Air oxidized material was isolated and re-purified by semi-preparative RP-HPLC/UV, with ESI-MS molecular mass verification

2.2.19.3 Directed Disulfide Bond Formation:

Cleaved orthogonally protected Cys variants of Vi1.1-Isomers A and B were RP-HPLC/UV purified and air oxidized, as described above. Partially oxidized material, as confirmed by ESI-MS, was then subjected to spontaneous thiol deprotection and final disulfide bond formation.

Rapid iodine oxidation was undertaken for directed peptide oxidation by removing the Acm protection group. Approximately 21 mg of Iodine crystals (I_2) was crushed into a fine powder and dissolved in 840 µL of 100 % acetic acid. The solution was vortexed until the solution takes a deep red/brown color, which is an indication that the iodine is well dissolved. In a separate vial 1 to 5 mg of peptide was dissolved in 1 mL-2 mL of 50 % v/v acetic acid. 600 µL of saturated I_2 solution was gradually added drop wise into the peptide solution. After 5 minutes of vortex the reaction was terminated by drop wise (2 µL to 4µL) addition of 1M $Na_2S_2O_3$. Initially the peptide iodine solution is deep brown but once the reaction is quenched the solution becomes clear. After the reaction is quenched, 5 mL to 7 mL of 0.1 % v/v TFA aq. was added. The solution is filtered and loaded onto the HPLC column for purification.

2.2.19.4 Selective Disulfide Reduction and Thiol Alkylation:

For assignment and confirmation of disulfide bond connectivity of randomly oxidized materials, two isomers were monitored individually in-real time by ESI-MS (AB/MDS-Sciex API 3000) in a process of selective TCEP reduction and alkylation as previously described by Bingham *et al.* [114]. Fully reduced mono-alkylated, partially reduced di-alkylated and differentially alkylated target samples, using *N*-Ethyl-Maleimide (EM) and *N*-Phenyl-Maleimide (PM), were C_4 RP-HPLC/UV purified and molecular mass (ESI-MS) assigned prior to post source decay (PSD) fragment analysis by MALDI-TOF/TOF.

2.2.19.5 MALDI TOF/TOF Disulfide Connectivity Assignment:

ZipTip® or RP-HPLC/UV isolated Vi1.1 analyte was analysed using an Ultraflex III MALDI TOF/TOF (Bruker Daltonics), controlled by Compass 1.2 SR1 software package (Bruker Daltonics). Peptides were analysed on a 2,5-dihydroxybenzoic acid (DHB) matrix, using a “dried droplet method” as recommended by Bruker Daltonics. Analyte solution was mixed 1:1 with matrix solution (40 mg/mL DHB in 1:2 MeCN:0.1 % v/v TFA) directly on the target. The spots were dried under N_2 gas. After parent ions

were identified, PSD fragment ion mass analysis was used to assign both partially and fully alkylated sequences. Most analysis was automatically performed with BioTools analysis™ (Bruker Daltonics), with uncommon portions of the peptide analysed manually with mass comparisons. Peptide Calibration Standard II (Bruker Daltonics) was used for external calibration, with a <5-ppm mass accuracy. Analysis of the spectra was done using flex Analysis 3.0 (Bruker Daltonics)

2.2.19.6 Oxidation of Peptides for Structural Studies:

In order to investigate the impact of PTM's on generation of isomers the peptides were oxidized under various buffers as mentioned in Table 4. Peptide oxidations were done at concentration of 1 mg peptide/10 mL buffer. The desired amount of peptide was weighed in an Erlenmeyer flask containing a stir bar and the required amount of buffer was gradually poured into the flask. The flask was covered with Parafilm® and allowed to stir at conditions as mentioned in the Table 4.

Table 4: Various oxidation conditions undertaken to study the impact of PTMs on the generation of structural isomers. α-Conotoxin ViI [$DC^2C^3SNOPC^8AHNNODC^{15}$-$NH_2$] and its non-PTM variant α-Conotoxin Vi1.1 [$DC^2C^3SNPPC^8AHNNPDC^{15}$-$NH_2$] were subjected to the 6 oxidation conditions and analyzed for structural isomers.

Condition #	Oxidation Condition	pH	Temperature ^oC	Duration
1	0.1M ammonium bicarbonate	8	4	120 hours
2	0.33M NH_4OAc/ 0.5M GdnHCl	7.5	4	120 hours
3	0.33M NH_4OAc/ 0.5M GdnHCl/50 % 2-Propanol	7.5	4	120 hours
4	2M urea/0.1 M NaCl/ 0.1M glycine	7.8	4	120 hours
5	2M urea/ 0.1M NaCl/ 0.1M glycine/ 50 % 2-Propanol	7.8	4	120 hours
6	0.1M NH_4HCO_3 /6M urea/ 50 % 2-propanol	7.5	4	120 hours

2.3 Results and Discussion

Firstly, as part of our effort to discover novel peptide therapeutics, we looked at the milked venom profile of captive *Conus magus*. The milked venom from *magus* was examined because Prialt, which is the only FDA approved *Conus* therapeutic, was developed from ω-Conotoxin MVIIA, a 27 amino acid calcium channel inhibitor found in *magus* [90, 91, 94]. Upon analyzing the milked venom through traditional biochemical approaches such as Edman degradation and state of the art ESI-MS we discovered a novel 12 amino acid peptide, which we named α-Conotoxin MIC. This novel peptide is the *N*-terminal truncated variant of α-Conotoxin MI (14 amino acids) and is the smallest reported 3/5 α-Conotoxin to date. Their total chemical synthesis, including the production of the intermediate peptide of 13 amino acids, *des*-[Gly]^{1}α-Conotoxin MI was undertaken (Figure 5, Figure 6 and Figure 7). These three peptides are used to illustrate how, through posttranslational modification, cone snails are able to increase the chemical and pharmacological diversity of their venoms (Table 5). Furthermore, these three peptides also help in elucidating the contribution of the *N*-terminus in bioactivity.

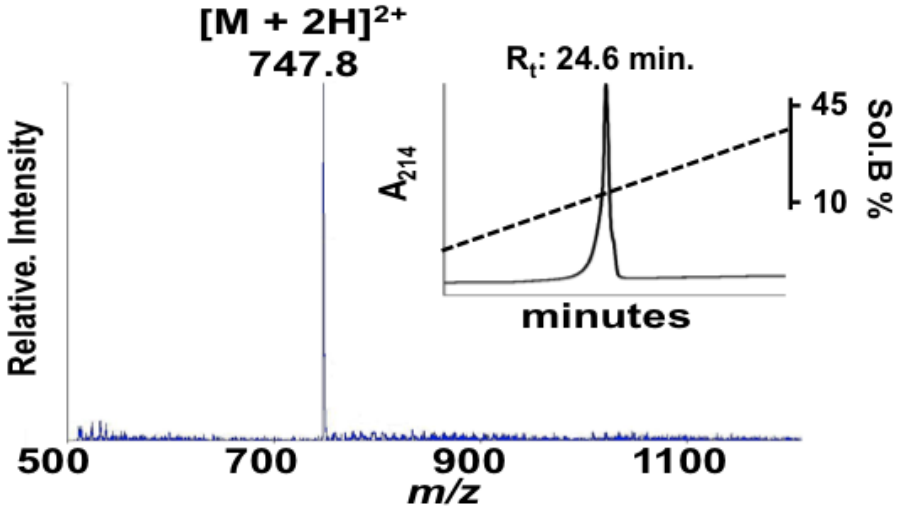

Figure 5: ESI-MS and RP-HPLC Chromatogram of α-Conotoxin MI (GRCCHPACGKNYSC-NH_2). The ESI-MS shows a dominant *m/z of* $[M+2H]^{2+}$ of 747.8. The theoretical calculated mass of α-Conotoxin MIC is $[M+2H]^{2+}$ of 747.5. α-Conotoxin MI eluted at 24.6 minutes when run on a 1 mm C_{18} Phenomenex® narrow bore column using a 1 % minute^{-1} gradient of 90:10 Acetonitrile (MeCN): 0.08 % v/v *aq.* TFA. The chromatograph has a shoulder, which is a characteristic of α-Conotoxin MI.

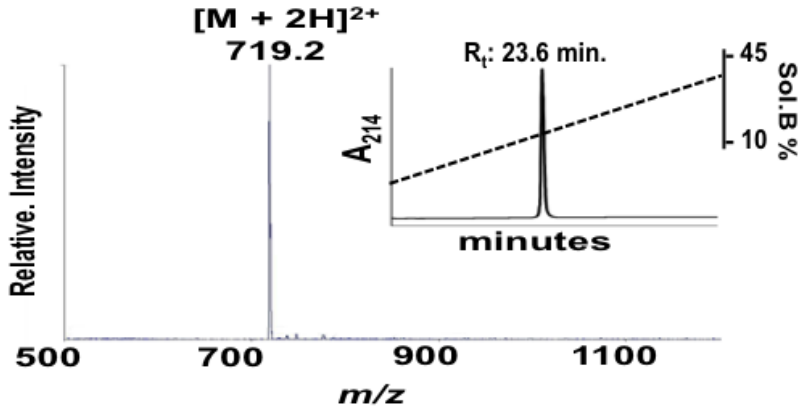

Figure 6: ESI-MS and RP-HPLC Chromatogram of des-[Gly] α-Conotoxin MI (RCCHPACGKNYSC-NH_2), the *N*-terminus truncated synthetic version of α-Conotoxin MI. The ESI-MS shows a dominant *m/z of* $[M+2H]^{2+}$ of 719.2. The theoretical calculated mass of des-[Gly] α-Conotoxin MIC is $[M+2H]^{2+}$ of 719.0 des-[Gly]. α-Conotoxin MIC eluted at 23.1 minutes when run on a 1 mm C_{18} Phenomenex® narrow bore column using a 1 % $minute^{-1}$ gradient of 90:10 Acetonitrile (MeCN): 0.08 % v/v *aq.* TFA.

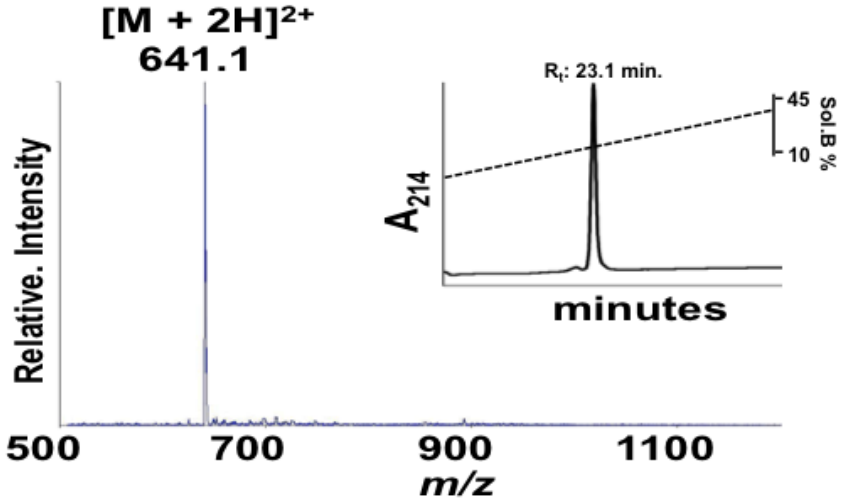

Figure 7: ESI-MS and RP-HPLC Chromatogram of α-Conotoxin MIC (CCHPACGKNYSC-NH_2), the *N*-terminus truncated version of α-Conotoxin MI. The ESI-MS shows a dominant *m/z of* $[M+2H]^{2+}$ of 641.1. The theoretical calculated mass of α-Conotoxin M1280 is $[M+2H]^{2+}$ of 641.0. α-Conotoxin M1280 eluted at 23.1 minutes when run on a 1 mm C_{18} Phenomenex® narrow bore column using a 1% $minute^{-1}$ gradient of 90:10 Acetonitrile (MeCN): 0.08 % v/v *aq.* TFA.

Table 5: Pharmacological activity of α-Conotoxin MI (GRCCHPACGKNYSC-NH_2), its natural *N*-terminus truncated variant α-Conotoxin MIC (CCHPACGKNYSC-NH_2) and synthetic des-[Gly] α-Conotoxin MI (RCCHPACGKNYSC-NH_2).

Conopeptide	Sequence	Pharmacological Activity			
		nAChR Ki $(\alpha1)_2\beta1\gamma\delta$ [nM]‡	LD_{50} (Fish) ($ng.kg^{-1}$)	LD_{50} (Worms) ($ng.kg^{-1}$)	LD_{50} (Snails) ($ng.kg^{-1}$)
α-Conotoxin MI[#]	GR**CC**HPA**C**GKNYS**C***	89.1 ± 9.1	12.2	N/A	N/A
Des [Gly][1] α-Conotoxin MI	R**CC**HPA**C**GKNYS**C***	73.3 ± 5.8	8.2	N/A	N/A
α-Conotoxin MIC[#]	**CC**HPA**C**GKNYS**C***	248.7 ± 10.9	23.7	N/A	N/A

*= *C*-terminal amide; [#] = Observed in MV; [‡] = K_i values represent mean ± S.E.M obtained from 5 experiments; N/A=The injected peptides were only lethal in fish; lethality was not observed with any of the three peptides in worms or snails up to 100 µg/kg.

As seen in Table 5, the competitive ligand binding assay performed on muscle-type nAChR subtypes demonstrated ~3 times greater binding affinity for α-Conotoxin MI (K_i = 89.1±9.1 nM) compared to α-Conotoxin MIC (K_i = 248.7±10.9 nM). Synthetically derived *des*-[Gly]^{1}α-Conotoxin MI displayed similar affinity (K_i = 73.3±5.8 nM) to α-Conotoxin MI. LD_{50} assays were conducted on fish, snails and worms. The injected peptides were only lethal in fish; lethality was not observed with any of the three peptides in worms or snails up to 100 µg/kg. This finding was as expected because *magus* is a piscivorous snail and it was expected to show the highest lethality in fish. The LD_{50} for α-Conotoxin MIC administered intra-muscular (IM) in fish was 23.29 mg.Kg^{-1} (18.5 nmol.g^{-1}). In contrast, the LD_{50} for IM α-Conotoxin MI injections was 12.24 mg.Kg^{-1} (8.2 nmol.g^{-1}). The synthetic *des*-[Gly]^{1}α-Conotoxin MI produced the lowest LD_{50} value (8.2 mg.Kg^{-1}; 5.7 nmol.g^{-1}). The LD_{50} of α-Conotoxin MIC was found to be greater than that of the other two peptides, which is in agreement with the ligand binding data. Comparative sequence analysis indicates that the positively charged arginine residue present within the *N*-terminus of both *des*-[Gly]^{1}α-Conotoxin MI and α-Conotoxin MI could account for this increase. The α-Conotoxin MIC lacks this arginine, which appears to be critical for higher binding affinity. In *C. magus* we observe that *N*-terminal peptide truncation conserves conotoxin isoform selectivity, while affecting its potency. Furthermore, the presence of α-Conotoxins MI and MIC, together with α-Conotoxin MII, maximizes the number of potential options for nAChR inhibition, which raises questions regarding the necessity in saturating a particular target with many different α-conotoxins in a single MV. Further investigation into phylogenetic differences in nAChR isoforms may provide answer to this question. Our results indicate that the *N*-terminal amino acid in α-Conotoxin MI probably play an important role for activity. Truncation of the *N*-terminus affects potency. Since cyclization changes the functionality at the *N*-terminus α-Conotoxin MI might not be the best candidate for cyclization.

In order to expand our understanding of molluscivorous milked venoms, our lab initiated a study to perform a comprehensive investigation into the venomic multiplicity of *Conus textile* using (RP-HPLC) profiling and mass spectral analysis of both duct (DV) and milked venoms (MV) collected from non-captive specimens representing diverse locations throughout the Pacific (Hawaii, American Samoa and Australia) (Figure 8).

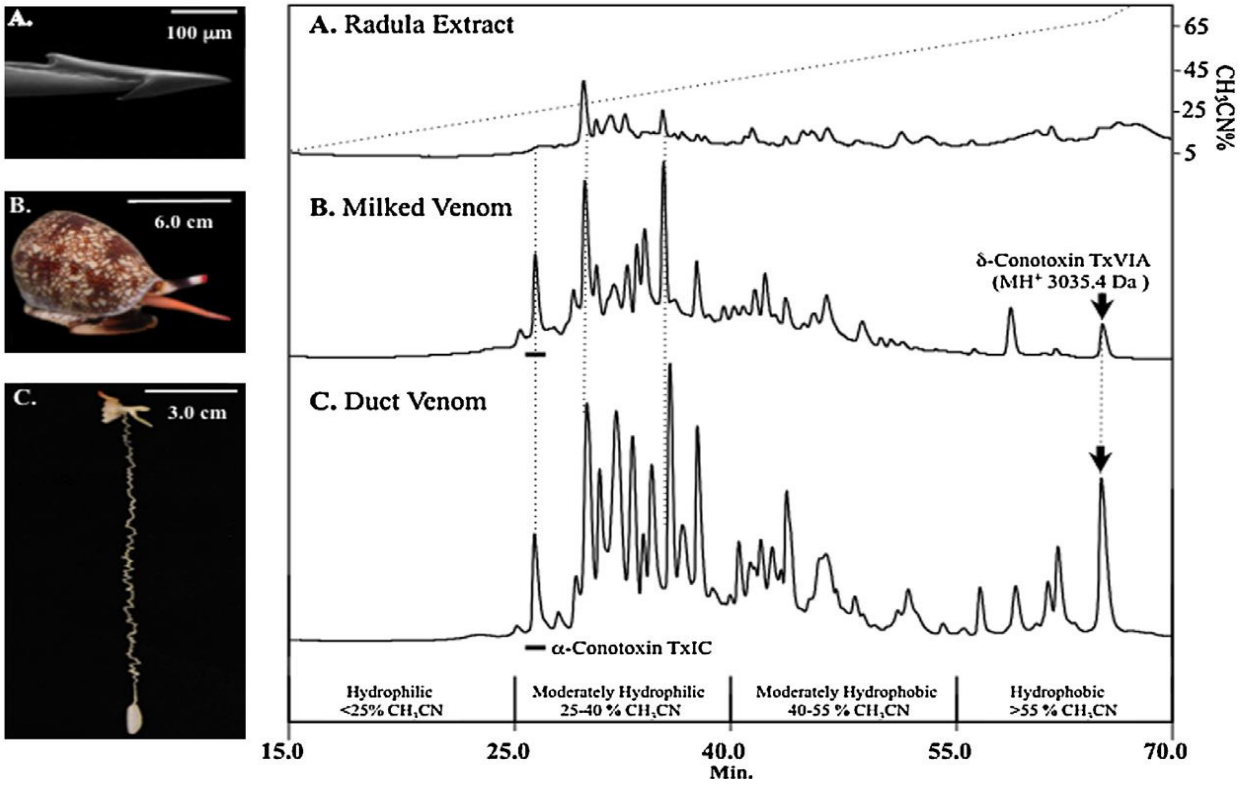

Figure 8: RP-HPLC comparison of venom obtained from (A) Radula Lumen Extract (RE); (B) Milked Venom (MV); and (C) Duct Venom (DV) from a representative specimen of *C. textile*. (A) The RE revealed limited similarity of peptides within the hydrophilic region to those in the hydrophilic regions of MV and DV. Note that α-Conotoxin TxIC (underscore) and δ-Conotoxin TxVIA (arrow) were not detected in the RE. Both (B) MV and (C) DV demonstrated a high level of peptide abundance and continuity. These samples were profiled via MALDI-TOF MS. Our goal was to isolate and characterize α-Conotoxin TxIC from the venom profile.

This widely distributed tropical species is one of the best-studied molluscivorous cone snail venoms, with countless molecular constituents including 77 fully characterized conopeptides. The comparison of geographically diverse venom profiles led to the identification of a previously uncharacterized peptide, α-Conotoxin TxIC. Differentiating α-Conotoxin TxIC from other α-conotoxins is its' high degree of post-translational modification (44 % of the residues in this 17 amino acid peptide are post-translationally modified). This includes the incorporation of γ-carboxyglutamic acid, two moieties of *4-trans* hydroxyproline, two disulfide bond linkages, and *C*-terminal amidation (Figure 9).

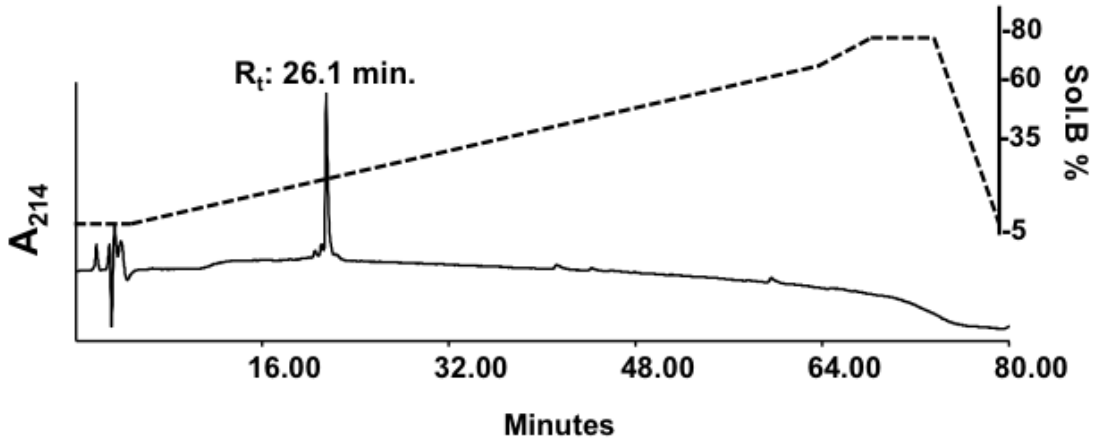

Figure 9: RP-HPLC chromatogram for α-Conotoxin TxIC [ROQCCSHOACNVDHPγIC-NH$_2$; γ = γ-carboxyglutamic acid (Gla), O = *4-trans* hydroxyproline (Hyp)]. α-Conotoxin TxIC was isolated from the whole venom profile of *Conus textile* (Figure 6). α-Conotoxin TxIC eluted at 26.1 minutes when run on a 1 mm C_{18} Phenomenex® narrow bore column using a 1 % minute^{-1} gradient of 90:10 Acetonitrile (MeCN): 0.08 % v/v *aq.* TFA.

In order to demonstrate how the PTM amino acids act as determining factors for selective targeting of the nicotinic acetylcholine receptor (nAChR), a well-documented therapeutic target for the treatment of chronic neuropathic pain, we synthesized the two synthetic non-PTM variants of α-Conotoxin TxIC, [[Pro]^{2,8}[Glu]^{16}α-Conotoxin TxIC (Tx 2005) and [Glu]^{16} α-Conotoxin TxIC (Tx 2037)] (Figure 10 and Figure 11).

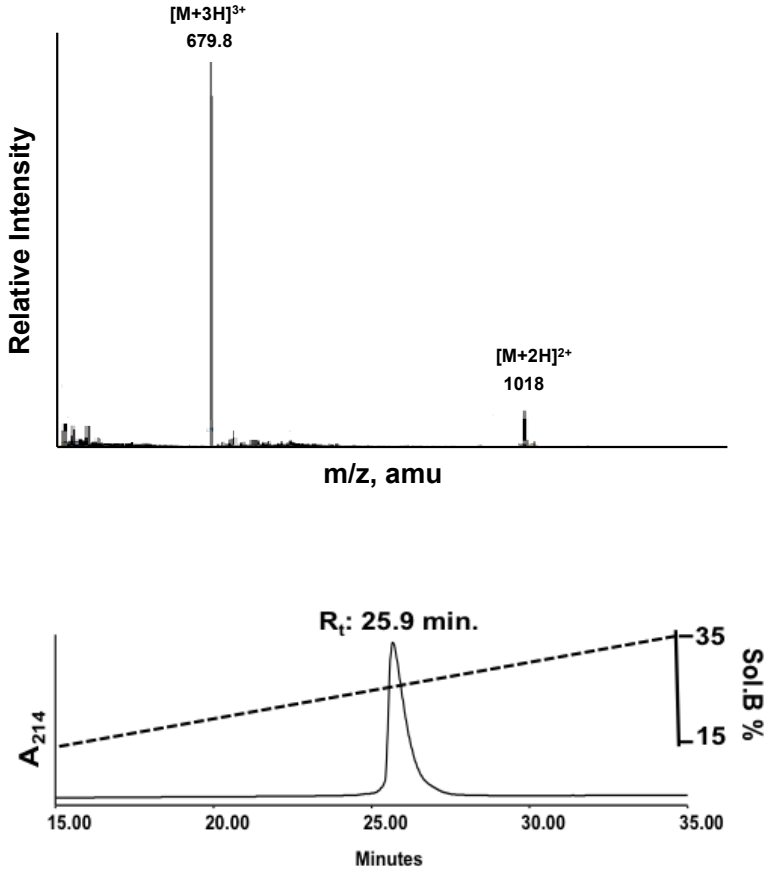

Figure 10: ESI-MS (Top) and RP-HPLC Chromatogram (Bottom) of α-Conotoxin Tx2037 [ROQCCSHOACNVDHPEIC-NH$_2$; O = *4-trans* hydroxyproline (Hyp)]. α-Conotoxin Tx2037 is a synthetic variant of α-Conotoxin TxIC, which has a PTM on both proline residue and a regular glutamic acid instead of γ-carboxyglutamic acid. The ESI-MS shows a dominant *m/z* of $[M+3H]^{3+}$ of 679.8 and a minor *m/z* of $[M+2H]^{2+}$ of 1018.0. The theoretical calculated mass of α-Conotoxin Tx2037 is $[M+3H]^{3+}$ of 680.0 and $[M+2H]^{2+}$ of 1019.5. α-Conotoxin Tx2037 eluted at 24.8 minutes when run on a 1 mm C_{18} Phenomenex® narrow bore column using a 1 % minute^{-1} gradient of 90:10 Acetonitrile (MeCN): 0.08 % v/v *aq.* TFA.

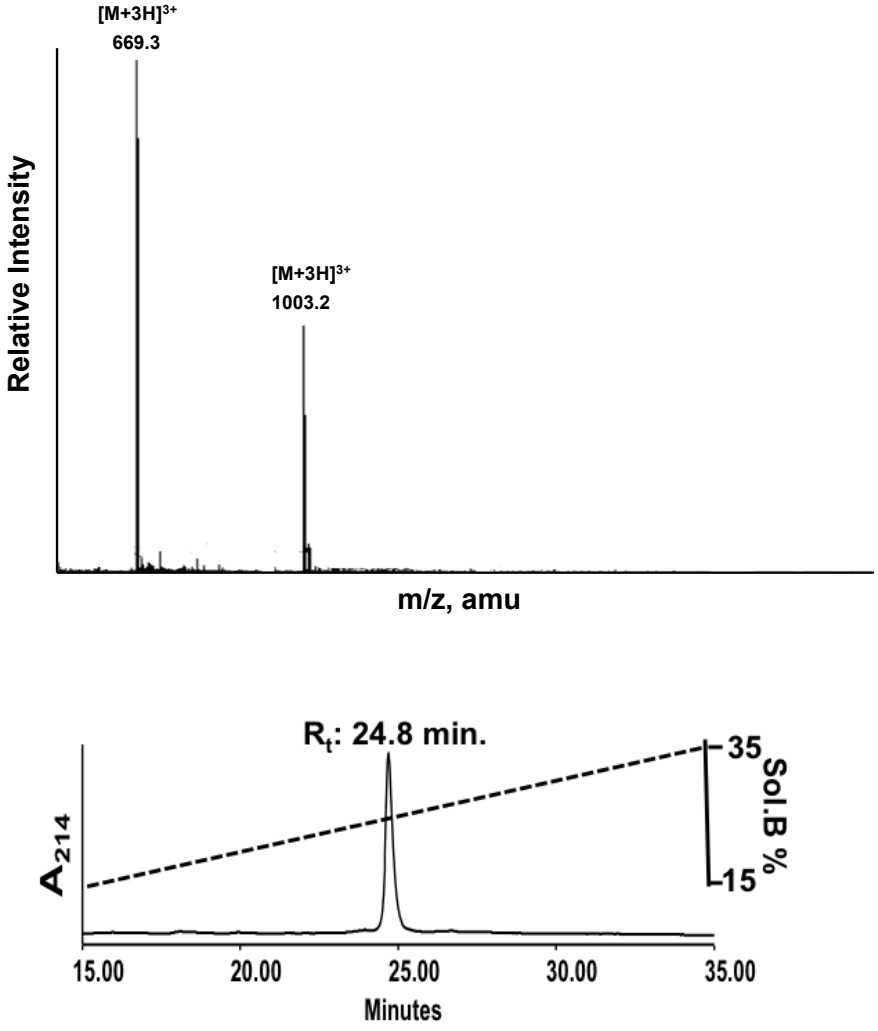

Figure 11: ESI-MS (Top) and RP-HPLC Chromatogram (Bottom) of α-Conotoxin Tx2005 [RPQCCSHPACNVDHPEIC-NH_2]. α-Conotoxin Tx2005 is a synthetic variant of α-Conotoxin TxIC, which has no PTMs. The ESI-MS shows a dominant *m/z of* $[M+3H]^{3+}$ of 669.3 and a minor $[M+2H]^{2+}$ of 1003.2. The theoretical calculated mass of α-Conotoxin Tx2037 is $[M+3H]^{3+}$ of 669.3 and $[M+2H]^{2+}$ of 1003.5. α-Conotoxin Tx2005 eluted at 24.8 minutes when run on a 1 mm C_{18} Phenomenex® narrow bore column using a 1 % $minute^{-1}$ gradient of 90:10 Acetonitrile (MeCN): 0.08 % v/v *aq.* TFA.

Our collaborator (Dr. Jan Tytgat, KU Leuven) examined the bioactivity of α-Conotoxin TxIC and its two synthetic non PTM variants [[Pro]^{2,8}[Glu]^{16}α-Conotoxin TxIC (Tx 2005) and [Glu]^{16} α-Conotoxin TxIC (Tx 20337)] (Figure 12 and Table 6).

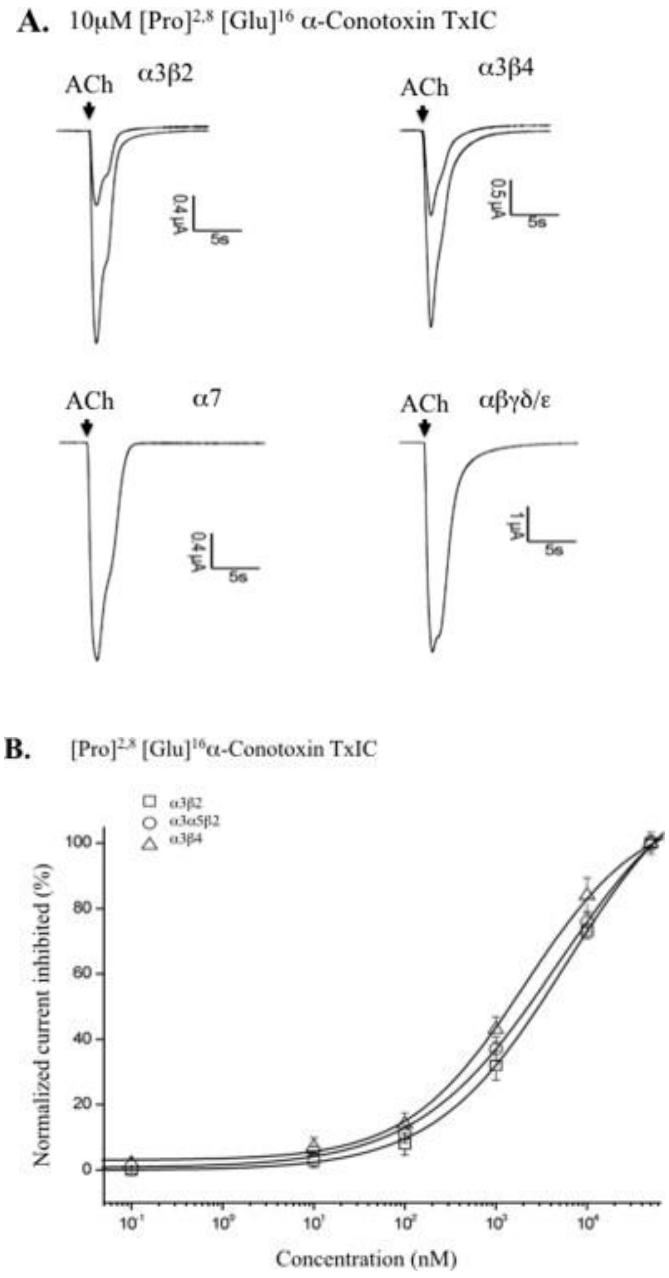

Figure 12: A) Inhibition of nAChR subtypes by α-Conotoxin Tx2005 at 10 μM. B) Resulting dose dependent inhibition of nAChR subtypes by α-Conotoxin Tx2005. α-Conotoxin Tx2005 showed 96 % inhibition at the α3β2 nAChR subtype, 91 % inhibition at the α3α5β2 nAChR subtype and 77 % inhibition at the α3β4 nAChR subtype.

Table 6: The pharmacological activity of native α-Conotoxin TxIC, synthetic α-Conotoxin Tx2005 and synthetic α-Conotoxin Tx2037. The native α-Conotoxin TxIC showed no activity at the human nAChR subtypes but was able to elicit a paralytic response when injected into a snail. The synthetic α-Conotoxin Tx2005, which has no PTMs was not able to elicit a paralytic response in snails but was able to inhibit human nAChR subtypes.

Peptide	nAChR subtype [a]	IC_{50} [b]	M.I. %	PD_{50} [c]
α-Conotoxin TxIC	α3β2, α3α5β2, α3β4	100	<5	34.2
	α4β4, α7, α2β2, αβγε	50	0	
α-Conotoxin Tx2005	α3β2	5.4±0.5	96	3600
	α3α5β2	4.9±0.8	91	
	α3β4	2.1±0.2	77	
	α4β4, α7, α2β2, αβγε	≥100	<10	
α-Conotoxin Tx2037	NA	NA	NA	NA

[a] Human variants.

[b] Half-maximal inhibitory concentration (human in μM).

[c] Paralytic dose (mollusk in nMol g^{-1}).

M.I. = Maximum Inhibition. NA= the assay on nAChR subtype is pending, but the initial screening showed activity on an inward rectifying Na^{+}channel.

As demonstrated in Table 6, native α-Conotoxin TxIC (≤100 μM) had minimal inhibitory action on human nicotinic acetylcholine receptor (nAChR) subunit combinations α4β2 (brain), α4β4* (neuronal), α7* (neuronal), αβγδ (muscle), αβγε* (muscle) or the human peripheral nAChR subtypes α3β2*, α3β2α5* and α3β4*. Biological activity was observed with $[Pro]^{2,8}[Glu]^{16}$α-Conotoxin TxIC, the synthetic non-PTM form. This analogue inhibited the human nAChR subtypes (α3β2*, α3α5β2* and α3β4*), with the α3β4* isoform demonstrating the highest sensitivity (IC_{50} 2.1±0.2 μM) and exhibiting a 77 % maximum inhibition. While the isoform α3β2* demonstrated the highest level of inhibition (96 %) with an IC_{50} of 5.4±0.5 μM (Table 6). No significant inhibition was observed at the remaining isoform targets (α4β2*, α4β4*, α7*, αβγδ*, αβγε*) at concentrations up to 100 μM (Table 6). A whole animal bioassay using the native α-Conotoxin TxIC demonstrated a dose-dependency in its ability to produce animal paralysis (Figure 12). α-Conotoxin TxIC produced total paralysis at 640 pMol g^{-1} (n=14); this dose did not cause lethality in test animals. A PD_{50} of 34.2 pMol g^{-1}(34.2 nMol Kg^{-1}; whole snail weight) was determined for the native toxin (Table 5). The synthetic non-PTM analogue of α-Conotoxin TxIC (Tx2005) demonstrated an inability to cause paralysis at same PD_{50} concentration (n=15). Total paralysis was achieved with 10.24 nMol g^{-1} (n=7), this being ~16x than the paralytic dose for native TxIC. A similar dose-dependent trend was observed for Tx2005 (Figure 12), with the maximal dose used not causing animal lethality. A PD_{50} of 3.6 nMol g^{-1} (3.6 nMol Kg^{-1}; whole snail weight) was calculated (Table 6), this PD_{50} concentration being ~100x more than observed with the native PTM toxin.

While remaining biologically active in the whole animal bioassay, native α-Conotoxin TxIC is inactive when tested human nAChR channel isoforms (Table 6). The synthetic unmodified α-Conotoxin TxIC (i.e. $[Pro]^{2,8}[Glu]^{16}$α-Conotoxin TxIC), however remains active at the nAChR and is isoform selective (Table 6). These features highlight the importance of PTMs in the selective targeting of α-conotoxins. This is further illustrated at a phylogenic level with the observed switching in potency in invertebrate models, which represent the native prey target.

The phyla-selectivity and reduced potency of the native α-Conotoxin TxIC towards human nAChR isoforms demonstrates an underlying differentiation between

receptor selectivity and pharmacodynamic properties in ion channels from different phyla. An area reiterated by the PTM of the nAChR in the Egyptian mongoose (*Herpestes ichneumon*) that provides a level of resistance to α-bungarotoxin [128]. Here genomic and proteomic investigation into invertebrate nAChR isoforms, as well as other receptors (e.g. N-type ($Ca_V2.2$) calcium channels and $GABA_B$), may provide insight into the determinants for pharmacological potency and phyla selective characteristics commonly observed in *Conus*. Such information will provide insights into toxin target specificity enhancement through peptide bioengineering and the potential manipulation/incorporation of PTMs.

Considerable research has focused on the disulfide bond connectivity of conotoxins and its impact on pharmacological selectivity. The majority of conotoxins contain 1-5 disulfide bonds [105, 129]. The relationship between their connectivity and pharmacological selectivity has been recognized for some time. As an example, disulfide bond contortion can produce peptide isomers representing 'globular' and 'ribbon' structures. Synthesis of the non-native ribbon structure, via selective formation of disulfide bonds, results in differential selectivity and inhibitory mechanisms, when compared to its native 'globular' form. This has been observed with the α-Conotoxin AuIB, as presented in its non-native 'ribbon' form at the α3β4 neuronal nicotinic acetylcholine receptor. More recently, Khoo *et al.* [121] reported that two non-native μ-conotoxin isomers retained biological activity to the $Na_V1.2$ voltage-gated sodium channel [121]. These findings highlight a unique and rare structure-activity relationship that synthetic conotoxins share with their receptor targets, thereby increasing their bioengineering potential for drug design. Since the bioactivity of conotoxins is directly dependent on its structure we conducted a study to investigate the generation of non-native isomers of conotoxins through the elimination of PTMs or by using various oxidation conditions with differing chaotrophic agents (Table 4). Through chemical oxidation we can generate various non-native peaks whereby expanding the repertoire of conotoxin scaffolds that can be used for bioengineering pharmaceuticals or receptor-specific probes.

α-Conotoxin VIl is a 15 amino acid peptide present in the venom of *Conus virgo*, a vermivorous cone snail distributed throughout the Indo-Pacific region and Australia. The peptide exhibits a 4/6-cysteine framework and contains two hydroxyprolines residues located at positions 6 and 13 in its sequence. We have chemically synthesized α-Conotoxin VIl (Figure 13) and its non-PTM variant α-Conotoxin Vi1.1 (Figure 14) to study the impact of hydroxyproline and oxidation conditions on generation of native and non-native isomers.

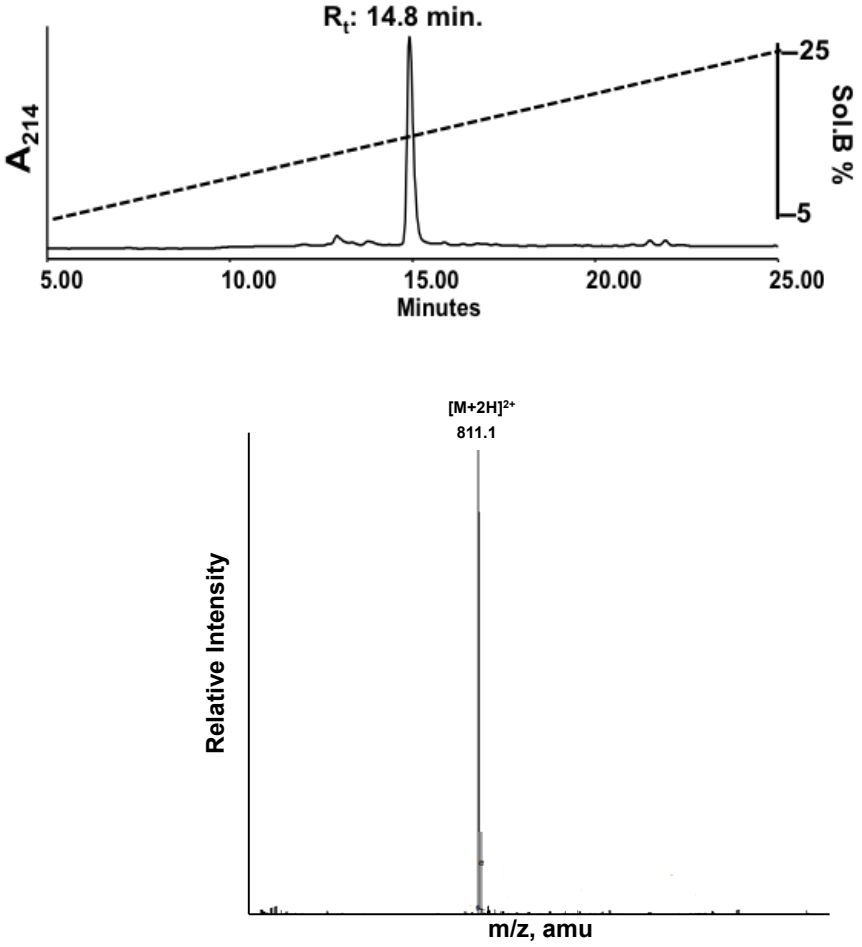

Figure 13: RP-HPLC chromatogram (top) and ESI-MS (bottom) of reduced α-Conotoxin VIl [DC^{2}C^{3}SNOPC^{8}AHNNODC^{15}-NH$_2$; O = *4-trans* hydroxyproline (Hyp)]. α-Conotoxin VIl is the starting material for the various oxidation conditions used to study the relation between PTMs and structural isomers. The ESI-MS shows a dominant *m/z of* [M+2H]$^{2+}$ of 811.1. The theoretical calculated mass of α-Conotoxin VIl is [M+2H]$^{2+}$ of 812.0. α-Conotoxin VIl eluted at 14.8 minutes when run on a 4.6 mm C_{18} Phenomenex® analytical column using a 1 % minute^{-1} gradient of 90:10 Acetonitrile (MeCN): 0.08 % v/v *aq.* TFA.

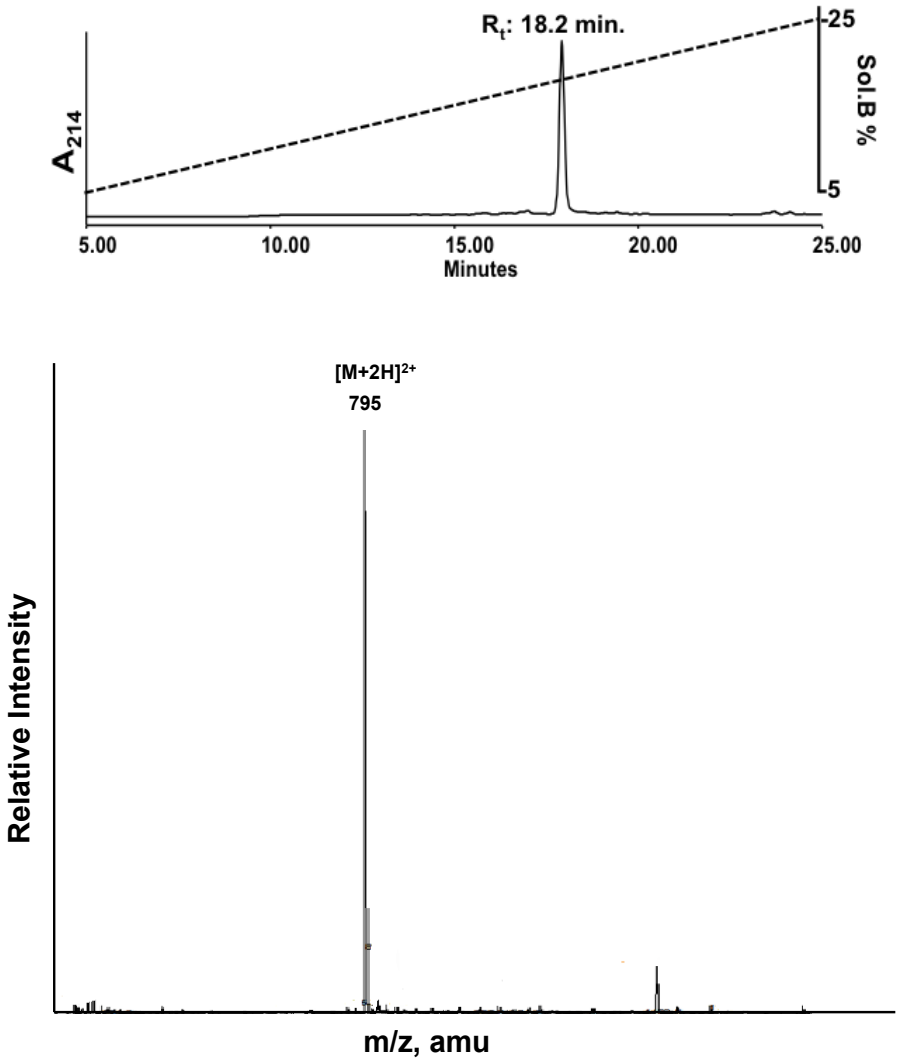

Figure 14: RP-HPLC chromatogram (top) and ESI-MS (bottom) of reduced α-Conotoxin Vi1.1 [DC^{2}C^{3}SNPPC^{8}AHNNPDC^{15}-NH$_2$], the non-PTM version of α-Conotoxin VIl. Reduced Vi1.1 is the starting material for the various oxidation conditions used to study the relation between PTMs and structural isomers. The ESI-MS shows a dominant *m/z of* [M+2H]$^{2+}$ of 795. The theoretical calculated mass of α-Conotoxin VIl is [M+2H]$^{2+}$ of 795.3. α-Conotoxin Vi1.1 eluted at 18.2 minutes when run on a 4.6 mm C_{18} Phenomenex® analytical column using a 1 % minute^{-1} gradient of 90:10 Acetonitrile (MeCN): 0.08 % v/v *aq.* TFA.

When exposed to similar oxidation conditions the non-native α-Conotoxin Vi1.1 generates more peaks than the native α-Conotoxin VIl (Figure 15).

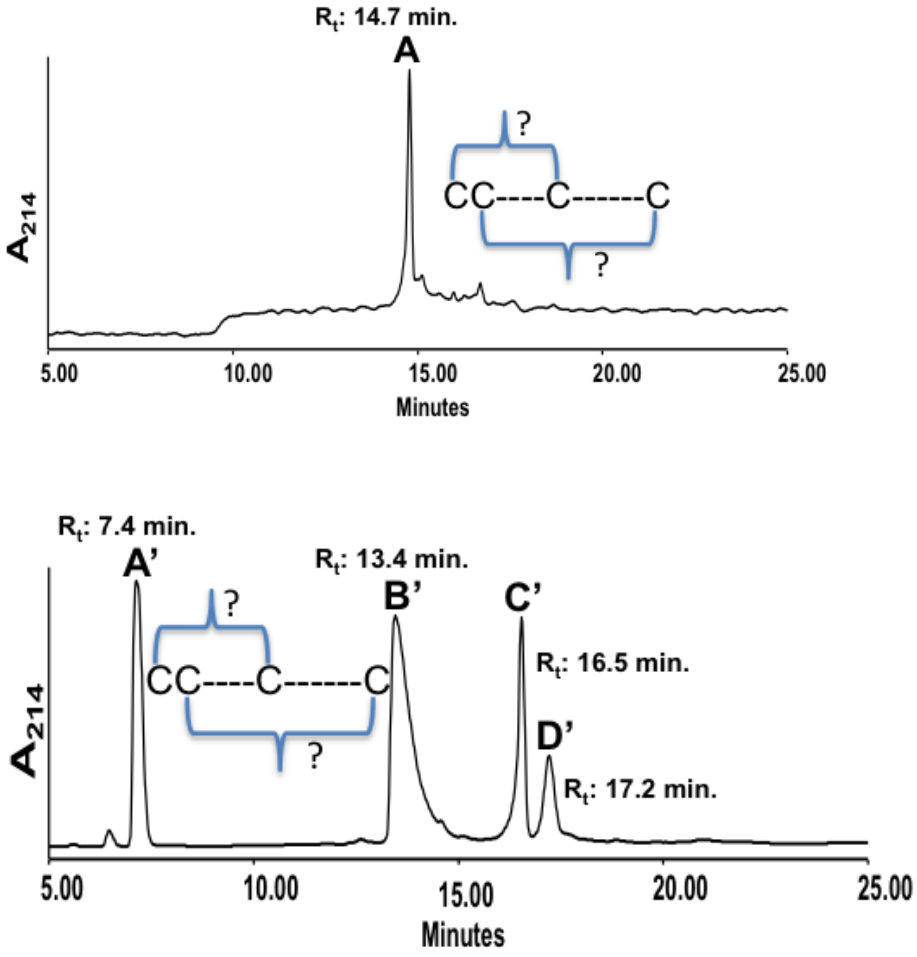

Figure 15: RP-HPLC chromatogram of α-Conotoxin VIl (top) and α-Conotoxin Vi1.1 (bottom) products after a 5-day oxidation in a solution of 0.33M NH_4OAc/ 0.5M GdnHCl at pH 7. Oxidation of α-Conotoxin VIl gave only 1 major product (A= 95 %). Oxidation of α-Conotoxin Vi1.1 gave 4 major products and 1 of the product was more dominant than the other 3 products (A'= 25 %, B'= 42 %, C'= 16% and D'= 8.5 %). Since the oxidation products were generated from random oxidation we do not know the exact disulfide connectivity of the isomers. Both the oxidation products were run on a 4.6 mm C_{18} Phenomenex® analytical column using a 1 % $minute^{-1}$ gradient of 90:10 Acetonitrile (MeCN): 0.08 % v/v *aq.* TFA. The % area of the peaks were obtained by integrating the peaks using Empower® software.

Even when the native peptide generates more than 1 isomer the native isomer is dominant and forms the majority of the oxidation product. Contrary to the native α-Conotoxin VIl the non-native α-Conotoxin Vi1.1 has more oxidation products and the native globular product is not as prominent (Figure 16).

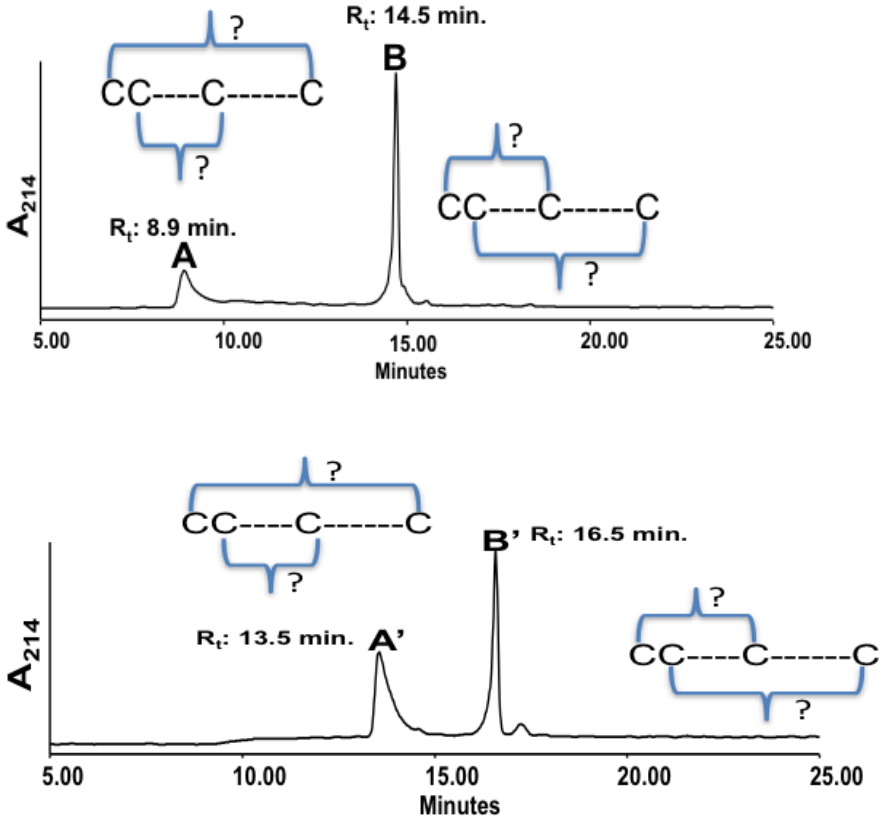

Figure 16: RP-HPLC chromatogram of α-Conotoxin VIl (top) and α-Conotoxin Vi1.1 (bottom) products after a 5-day oxidation in a solution of 0.1M NH_4HCO_3 at pH 8. α-Conotoxin VIl gave 2 products and 1 of the products is more dominant than the other (A=19 % and B=81 %). α-Conotoxin Vi1.1 also gave 2 products but the products were in proportion (A'= 47 % and B'= 48 %). Since the oxidation products were generated from random oxidation we do not know the exact disulfide connectivity of the isomers. Both the oxidation products were run on a 4.6 mm C_{18} Phenomenex® analytical column using a 1 % $minute^{-1}$ gradient of 90:10 Acetonitrile (MeCN): 0.08 % v/v *aq.* TFA. The % area of the peaks were obtained by integrating the peaks using Empower® software. In a separate set of experiment done by a lab mate it was determined that peaks B and B' were native globular isomers and peaks A and A' were non-native ribbon isomer.

This finding indicates that the PTMs help in producing the native isomer and removal of PTMs results in generation of isomers not seen in native venom. The number of isomers generated by α-Conotoxin VIl and α-Conotoxin Vi1.1 vary with different oxidation conditions (Appendix A). Chaotrophic agents like GdnHCl, Urea and NaCl disrupt hydrophobic interactions therefore produce additional isomers, which are not likely to be thermodynamically feasible under physiologic conditions.

After analyzing the various conopeptides we decided on using Tx2005 the non-PTM version of α-Conotoxin TxIC for our cyclization and stability studies. Comprising of 18 amino acids with two disulfide bonds, 44 % of residues display one or more forms of modification, making α-Conotoxin TxIC one of the most highly PTM conopeptides documented to date (Table 6). Since PTMs are essential in determining phyla selectivity and receptor isoform selectivity we could use α-Conotoxin TxIC and Tx2005 as models for either a biodegradable pesticide or an orally available drug. This novel 4/7 conopeptide, as represented by its cysteine framework, shares sequence homology with other α-conotoxins, and demonstrates sequence commonality to other molluscivorous conopeptides, specifically α-Conotoxins Ai1.2 (*C. ammiralis*) and Vc1.1 (*C. victoriae*). This homology is seen explicitly in α-Conotoxin Vc1.1 in its native PTM form: $[Hyp]^{6}[Gla]^{14}$Vc1.1, and more so within the last cysteine loop, with which α-Conotoxin TxIC shares 89 % sequence homology. Craik *et al.* [25] have successfully cyclized Vc1.1 therefore we used their peptide as a guideline when working with ours.

Tx2005 is active on various nAChR isoforms (Table 5). nAChR and its subtypes are known for their physiological involvement in neurotransmission and muscular contraction. Their deregulation has been associated with pathological conditions such as neuropathic pain and tobacco addiction. Additionally, dysfunction in nAChR subtypes has been linked to schizophrenia, Alzheimer's disease and Parkinson's disease [130-134]. A natural product that shows selectivity towards the ion channels that has implication on various medical conditions was determined to be worth pursuing. Furthermore, Tx2005 can be bioengineered as fluorescent probe that will help researchers study disease progression and increase their understanding of regulation and signal transduction in these receptors.

α-Conotoxin TxIC is phyla selective towards mollusks and has the potential to be developed as pesticide against mollusks. Schistosomiasis and Rat-Lung Worm are two major diseases in which snails play the role of vector. Schistosomiasis affects almost 210 million people worldwide, and an estimated 12,000 to 200,000 people die from it every year. According to the World Health Organization around 700 million people live in areas where this disease is common. In terms of damage caused by parasitic diseases Schistosomiasis is second to malaria [135-138]. Rat Lungworm is another parasitic disease that is increasing its incidence in Hawaii. Since 2008 there have been 42 reported cases of Rat lungworm where 38 of those incidents have occurred on the Big Island [139, 140]. Due to its phyla selectivity α-Conotoxin TxIC can be bioengineered to have enhanced selectivity towards pest snails and could be a useful tool for fighting vector snails.

2.4 Conclusion

This investigation demonstrates that PTMs such as *N*-terminal peptide truncation, hydroxylation and γ-carboxylation are employed by *Conus* to increase the chemical and pharmacological diversity of its venom. By diversifying its venom through PTMs, *Conus* can ensure its predatory advantage in the competitive marine ecosystem. Addition and removal of PTMs through chemical synthesis may be a useful strategy for continuing pharmacological exploitation of *Conus* peptides.

Chapter 3: A novel protocol to generate thioester using Trifluoromethanesulfonic Acid

This part of the study was undertaken to explore **Objective 2: To replace hazardous Hydrogen Fluoride (HF) with milder Trifluoromethanesulfonic acid (TFMSA) in generating a *C*-terminal thioester, which is essential to conducting Native Chemical Ligation.**

3.1 Introduction

Linear Solid Phase Peptide Synthesis (SPPS) presents limitations in the production of peptides > 50 amino acids [141]. Convergent synthetic strategies through linking of orthogonally protected peptide fragments have demonstrated advantages in overcoming this constraint [142]. Yet this approach in itself is faced with difficulties regarding their complexity in production and solubility [143-145]. Recently alternative strategies have been investigated incorporating chemoselective ligation techniques [146, 147]. These varying solution phase approaches have already demonstrated their merit and worth in chemical biology with the synthesis of functional proteins, semi-synthetic proteins and its utilization in overcoming difficult synthesis of certain peptides [144, 148, 149].

The strategy of Native Chemical Ligation (NCL), aims to produce a native-like peptide bond at the point of conjugation, using two unprotected peptide fragments [146, 150]. Design and construction of these strategic ligation positions require consideration of kinetic principles regarding chemoselective rates, and their influence on structural activity relationship, not only as it applies to their respective peptide fragments, but its consequences within the ligated product as a whole [151-153].

NCL entails the use of a carboxyl end thioester mediated reaction, which is both highly selective and spontaneous in the formation of a native peptide bond with an opposing α-*N*-amino Cysteine peptide fragment [142, 154]. This cysteine requirement is a potential limitation with some sequences, although in peptide toxins their sequence dispersal, for the maintenance of three-dimensional structure, offers significant incentive for its use [155, 156]. Availability of free cysteine at the *N*-terminus of *C*-terminal

fragment is an important factor considering it's the free thiol participation and subsequent regeneration that results in the native-like peptide bond. Not only has NCL been used to generate longer peptide fragments it has also been successfully adapted to chemically synthesize peptides with cyclic peptide backbone [43].

Fmoc SPPS chemistry has become a dominated synthetic strategy in chemical biology due to its simplified assembly and cleavage procedures. However, this particular approach has presented hurdles in the strategic implementation of NCL as repeated exposure to piperidine during α-*N*-amino deprotection can impact the stability of the thioester resin [157, 158]. Although Fmoc-thiol ester support resins have been reported, these have been mostly outside routine laboratory use [159, 160].

Boc SPPS chemistry has seen greater success in NCL through the incorporation of Hydrogen Fluoride (HF) in cleavage for thioester peptidyl-resins. This poses a limitation, as HF is extremely toxic, volatile and corrosive in nature. Specialized Teflon equipment and handling procedures must be used due to HF's incompatibility with glassware. Since systemic HF poisoning removes Ca^{2+} from soft tissues and bones, whereby creating a disturbance of Ca^{2+} concentrations (hypocalcaemia), HF injuries may be debilitating or even fatal [143, 161]. Thus management and execution of HF cleavage protocols requires high level of experience and represents the principle drawback to the larger incorporation of NCL in chemical biology.

Here we propose a novel technique that replaces HF with Trifluoromethanesulfonic Acid (TFMSA) to generate the required thioester for NCL. TFMSA is a strong acid that is comparatively less hazardous than HF. It also requires less specialized equipment/facilities to handle [162]. Our research aims at replacing HF with TFMSA without compromising with the yield of the reaction. In order to optimize the reaction conditions to achieve target concentration various variables such as time, acid concentration, and different orthogonal protection group scavengers were examined. By replacing HF with TFMSA, which is less toxic and uses conventional lab ware we aim to make the technique of thiol ester ligation safer and accessible Though TFMSA must still be managed with care, its chemistry provides a safer alternative that is readily adaptable to Fmoc laboratories. Here we use a 33 αα test peptide, Huwentoxin-I (HwTx-I) as a candidate to test our novel protocol. HwTx-I contains 6

individual Cysteines (Cys) and has an X—Cys-Cys—X sequence mid-region, which makes it an ideal candidate to test the viability of thioester ligation using TFMSA. We will use our novel TFMSA protocol to generate the 16 αα *N*-terminus fragment with thioester. The *N*-terminus fragment will be ligated to the 17 αα *C*-terminus fragment using NCL to produce the 33 αα HwTx-I.

3.2 Methods

3.2.1 Preparing the MPAL Resin for Thioester Ligation:

Commercially available Methyl benzyl hydryl amine resin (MBHA) does not have thioester functionality that can be used in peptide ligation. The thioester functionality was introduced by modifying the MBHA resin to a MPAL resin by the following procedure. MBHA resin was flow washed with 100 mL of DMF and then swelled overnight with 8 mL-10 mL of DMF plus 650 µL of DIEA. Next morning, the resin was flow washed with ample amount of DMF. After the flow wash activated amino acid mixture containing 2 mmole lyophilized Boc-Leucine amino acid, 4 mL HBTU and 347 µL DIEA was added to the reaction vessel. The activated amino acid was allowed to couple for 40 minutes. If the coupling % is satisfactory we move on to the next amino acid if not we follow the procedure mentioned in section above. When the coupling % is achieved, the Boc protection moiety was removed by washing with TFA in DCM (50 % v/v) twice for 5 minutes each. The reagents and BOC were flow washed with DCM and this was followed by a flow wash with DMF. Next in a scintillation vial 2 mmol of dithiodipropionic acid was activated by dissolving it in 8 mL of 0.5 M HBTU and 1 mL of DIEA. The mixture was added to the reaction vessel and allowed to couple for 40 minutes. Addition of dithiodipropionic acid might introduces esters therefore to counter these esters the system was washed with sufficient DMF and treated with 650 µL of ethanolamine (base) and 200 µL of DIEA in 5 mL of DMF and allowed to react for 40 minutes. Next we treated the system with 2-mercaptoethanol (650 µL) in 5mL of DMF

and 100 µL of DIEA for 60 minutes. 2-mercaptoethnaol was used because it is a reducing agent and introduces a free thiol moiety. The final step is to covalently attach the desired amino acid of choice to the free thiol by using the coupling procedure as mentioned above. We now have a thioester resin with the desired linker and a *C*-terminal amino acid of choice (Figure 17). Upon cleavage this resin will yield a product that can be used in peptide ligation.

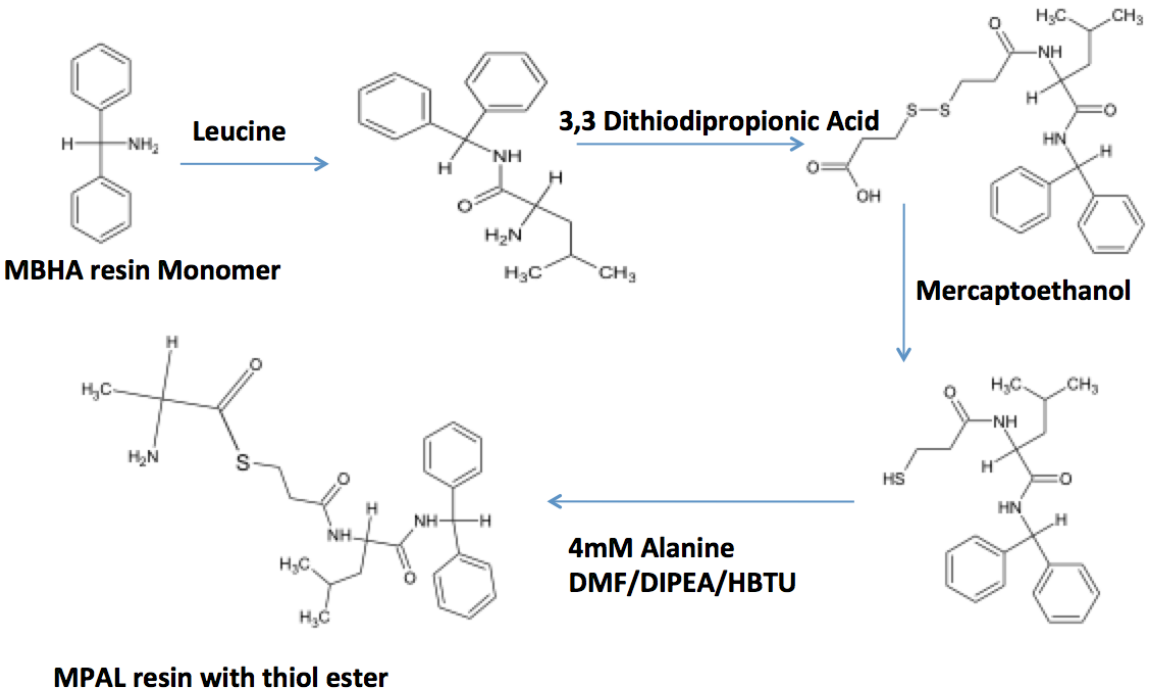

Figure 17: Preparation of the MPAL resin. Upon cleavage the MPAL generates a fragment that has a thioester at the *C*-terminus. MPAL resin is not commercially available therefore the commercially available MBHA resin is modified into a MPAL resin by adding a Leucine, dithiopropionic acid and the first amino acid in the synthesis.

3.2.2 Boc Synthesis of the 16 αα *N*-Terminal Huwentoxin-I Fragment:

Boc synthesis is similar to Fmoc synthesis and requires a similar workflow strategy. However unlike Fmoc, which is base labile Boc, is acid labile therefore we use Trifluoroacetic Acid (TFA) during Boc synthesis. The MPAL resin was flow washed in DMF and swelled overnight with 347 µL of DIEA. Next morning the DMF was flow washed and this is followed by a DCM flow wash. The system was introduced to DCM before Boc removal because TFA reacts with DMF causing the reaction vessel to fume. The removal of the Boc group was accomplished by two 5-minute washes with TFA in DCM (50 % v/v). Boc and residual reagents were flow washed in DMF and the system was reintroduced in a stable DMF environment for coupling. Amino acid activation and coupling are similar to Fmoc chemistry as mentioned in the method section for Chapter 2.

3.2.3 Cleavage of the *N*-Terminal Fragment:

The *N*-terminal fragment was cleaved using Trifluoromethylsulfonic Acid (TFMSA). This cleavage procedure is different from Reagent K cleavage and had to be perfected during the course of dissertation research. Several test runs with differing room temperature incubation, reagents and ice bath incubation were conducted. All the various test runs are mentioned in the results and discussion section. The final perfected procedure is mentioned here.

Cleavage of 50 mg of peptide-bound resin was performed by mixing the resin with 100 µL of thioanisole and 50 µL of EDT in an ice bath for 10 minutes. 1 mL of neat TFA was slowly added to the mixture and allowed to stir in the ice bath for an additional 10 minutes. After the TFA ice bath incubation, 200 µL of (TFMSA) was added dropwise to the mixture and kept in an ice bath to prevent overheating of the reaction. After 10 minutes of mixing the ice bath was taken away and the temperature of the reaction was allowed to increase to room temperature. The slurry was mixed for an additional 120 minutes at room temperatre to remove the peptide from the MPAL resin. The slurry was filtered from the resin and purified in the same manner as the Fmoc SPPS cleavage protocol with special care taken for the presence of TFMSA.

3.3 Results and Discussion

In order to optimize the reaction conditions to achieve target concentration with TFMSA cleavage, a multitude of variables such as incubation time, acid volume, and different orthogonal protection group scavengers were examined. Since past protocols recommended using Triisopropylsilane (TIPS) as a scavenging agent our first cleavage reaction was conducted using TIPS. This reaction was unsuccessful and we were unable to generate any peptide like material (Figure 18).

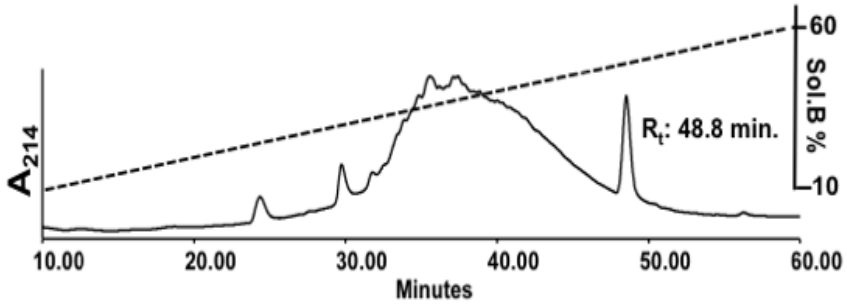

Figure 18: RP-HPLC cleavage profile produced when the *N*-terminal fragment of Huwentoxin-I (HwTx-I) synthesized on the "home-made" MPAL resin was cleaved with Triisopropylsilane (TIPS) as the scavenging agent. When TIPS was used as the scavenging agent no "peptide-like" peaks were seen and the RP-HPLC profile could not be resolved. The resolved peak at 48.8 minutes was mass checked in ESI-MS and was determined to be an adduct of various scavenging agents. The cleavage product was run on a 1 mm C_{18} Phenomenex® narrow bore column using a 1 % $minute^{-1}$ gradient of 90:10 Acetonitrile (MeCN): 0.08 % v/v *aq.* TFA.

We also conducted a second cleavage on a previously cleaved resin but this did not lead to any peptidic material (Appendix B). After experiencing repeated failures with TIPS we switched our scavenging agent to EDT and performed a cleavage reaction. The reaction with EDT gave better results and we were able to generate target peak “A” and multiple other peaks (Figure 19).

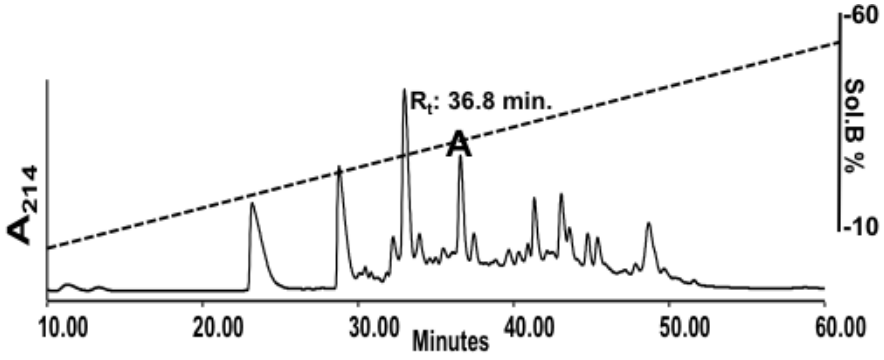

Figure 19: RP-HPLC cleavage profile when the *N*-terminus of HwTx-I synthesized on the MPAL resin was cleaved with 1,2 Ethanedithiol (EDT) as the scavenging agent instead of TIPS. When TIPS was replaced with EDT as the scavenging agent multiple “peptide-like” peaks were seen along with the target peak “A” at 36.8 minutes. The target peak was mass confirmed using ESI-MS. Since an EDT cleavage produced multiple “peptide-like” peaks the remaining cleavages were done with EDT. Our next goal was to optimize the cleavage conditions so that we could maximize the production of target peak “A”. The cleavage product was run on a 1 mm C_{18} Phenomenex® narrow bore column using a 1 % $minute^{-1}$ gradient of 90:10 Acetonitrile (MeCN): 0.08 % v/v *aq.* TFA

Both EDT and TIPS work well with Reagent K cleavage for Fmoc synthesis but EDT proved better for our cleavage strategy. The isopropyl group in TIPS may interact with the methane group in TFMSA, which in turn diminishes the ability of TFMSA to cleave the peptide from the resin. After deciding on the scavenging agent our next aim was to optimize the cleavage reaction.

The initial sets of experiments (A, B, C and D) were conducted to determine the optimum TFMSA volume (Table 7).

Table 7: Percent yield of the target compound *N*-terminal fragment of HwTx-I with thioester at the *C*-terminus (NTN-thioester) under differing volume of TFMSA. Conditions A, B, C and D evaluated product yields at various volumes of TFMSA while keeping the other reagents and incubation time constant for all 4 reaction conditions. The highest product yield was achieved when 100 µL of TFMSA was used for 50 mg of resin.

Cleavage mixture: Thioanisole 100µL; 1,2 EDT 50µL; TFA 1000µL +				
Resin: 50mg	**A**	**B**	**C**	**D**
TFMSA (µL)	**50**	**100**	**150**	**200**
Ice bath 0°C (minutes)	30	30	30	30
Room Temp (minutes)	120	120	120	120
% Area of target[1]	**1.6**	**16.8**	**12.3**	**12.2**

1 As determined by RP-HPLC/UV

As seen in Table 7, during this initial set of conditions other reagents involved in the cleavage reaction were kept constant. TFMSA cleaves the peptide from the solid resin support therefore determining the appropriate TFMSA volume is critical. If TFMSA is used in low volume the acid is not able cleave all the resin bound peptide, which results in low peptide yield. When used in large volume TFMSA being a strong acid is able to degrade the cleaved peptide thereby reducing the final yield of target material. Upon completion of the first set of experiments the desired volume for cleavage was determined to be 100 µL of TFMSA for 50 mg of resin. At volumes less than 100 µL or more than 100 µL the yield of the target compound was lower.

The next sets of experiments (E, F and G) were conducted to determine the optimum incubation at room temperature while keeping the TFMSA constant at 100 μL for all the 3 experiments (Table 8)

Table 8: Percent yield of target compound (NTN-thioester) under various incubation times at room temperature. Conditions E, F, and G assessed optimal incubation time at room temperature while keeping other reagents and incubation time on ice constant for all 3-reaction conditions. The highest peptide yield was obtained when the 50 mg resin was cleaved with 100 μL of TFMSA and incubated at room temperature for 120 minutes.

Cleavage mixture: Thioanisole 100μL; 1,2 EDT 50μL; TFA 1000μL +			
Resin: 50mg	**E**	**F**	**G**
TFMSA (μL)	100	100	100
Ice bath 0°C (minutes)	30	30	30
Room Temp (minutes)	**90**	**120**	**180**
% Area of target[1]	**12.9**	**16.7**	**7.6**

1 As determined by RP-HPLC/UV

As shown in Table 8, when the TFMSA volume and other reagents are kept constant there is an ideal incubation time at room temperature, which results in the highest yield of peptide product. For our peptide when the TFMSA volume was kept at 100 μL the ideal incubation time in room temperature was 2 hours (target peak 16.69 %). When the incubation time was 1.5 hours the target peak was 12.29 %. This reduction in target peak might be due to not all of the resin bound peptide being cleaved at the shorter incubation time. When the incubation time was increased to 3 hours the target peak was determined to be 7.62 %. At increased incubation times it is believed that the acid in the reaction mixture was able to degrade the cleaved peptide, which led to a decrease in peptide yield.

The next sets of experiments (H, I and J) were conducted to determine the optimum incubation time on ice-bath (Table 9).

Table 9: Percent yield of target compound (NTN-thioester) under different incubation times in ice-bath. Conditions H, I, and J evaluated the product yield at increasing ice bath incubation times while keeping the other reagents and incubation time at room temperature constant for all 3 reactions. The highest peptide yield was obtained when the 50 mg resin was cleaved with 100 µL of TFMSA and incubated in an ice bath for 30 minutes.

Cleavage mixture: Thioanisole 100µL; 1,2 EDT 50µL; TFA 1000µL +			
Resin: 50mg	**H**	**I**	**J**
TFMSA (µL)	100	100	100
Ice bath 0°C (minutes)	**30**	**90**	**120**
Room Temp (minutes)	120	120	120
% Area of target[1]	**16.6**	**6.2**	**5.1**

1 As determined by RP-HPLC/UV

TFMSA being a strong acid gives off heat during the cleavage reaction. To minimize the heat generated during this exothermic reaction, the addition of TFMSA to the reaction mixture is done in an ice bath. Keeping all of the other reagents constant, the cleavage was conducted at varying ice incubations of 30 minutes, 60 minutes and 120 minutes. The highest product yield was achieved at 30 minutes of incubation. A decreased yield at longer incubation times in ice bath might be due a decrease in the activity of TFMSA caused by the prolonged exposure to cold temperatures. After conducting the various experiments an optimal cleavage protocol to generate a thioester at the *C*-terminus of the *N*-terminal peptide was developed.

The optimized cleavage reaction for 50 mg of resin is [Thioanisole 100 µL; 1,2 EDT 50 µL; TFA 1000 µL; TFMSA 100 µL; Ice incubation 30 minutes; Room incubation 120 minutes] (Figure 20). The RP-HPLC profile for all the reaction conditions can be seen in Appendix B.

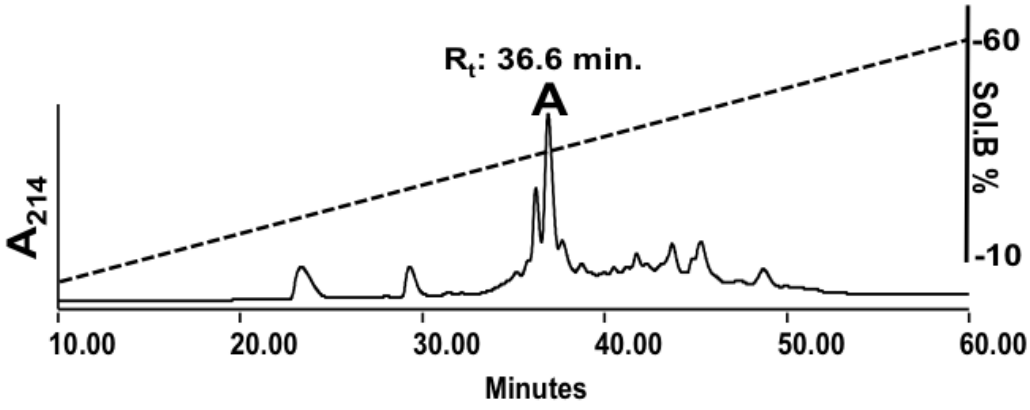

Figure 20: RP-HPLC cleavage profile when the *N*-terminus fragment of HwTx-I synthesized on a MPAL resin was cleaved under Condition B [Thioanisole 100 µL; 1,2 EDT 50 µL; TFA 1000 µL; TFMSA 100 µL; Ice incubation 30 minutes; Room incubation 120 minutes]. The target peak "A" eluted at 36.6 minutes and the mass was confirmed using ESI-MS. When the peaks were integrated using Empower® software the area for the target peak "A" was determined to be 16.8 %. The cleave product was run on a 1 mm C_{18} Phenomenex® narrow bore column using a 1 % $minute^{-1}$ gradient of 90:10 Acetonitrile (MeCN): 0.08 % v/v *aq.* TFA.

3.4 Conclusion

We have successfully devised a novel protocol to generate the thioester, which is required for NCL. Our novel protocol replaces the hazardous HF with milder TFMSA thereby making ligation safer and accessible. HF is extremely toxic, volatile and corrosive in nature. Since the handling of HF requires specialized Teflon equipment and expensive lab facilities, HF usage imposes many limitations. Injuries from HF may be debilitating or even fatal, therefore management and execution of HF cleavage protocols requires a high level of experience. The need for specialized lab equipment (Peptanova™, a commercial company sells Type I and Type II HF cleavage apparatus for €13,275 and € 6950 respectively) and highly trained personnel represents the principle drawbacks to the larger incorporation of NCL in chemical biology. We believe that our novel protocol compliments the existing technology and expands the scope of NCL.

Chapter 4: Huwentoxin-I, A Model Peptide Used to Study the Validity of Our Novel TFMSA Cleavage Protocol for Thioester Generation

This part of the study was undertaken to explore **Objective 3: Use Huwentoxin (HwTx-I) as an example to show the viability of our novel TFMSA cleavage technology in producing thioester containing fragment, which will be utilized in Native Chemical Ligation to produce bioactive peptide.**

4.1 Introduction

Through millions of years of evolution different species have evolved various method of food capture and survival. One of the more fascinating means of prey capture is through incapacitation using poisonous venom. These venomous compounds are generally introduced into the prey through bite or sting. Upon entering the circulatory system, the venom travels to other parts of the body where it targets specific metabolic functions leading to debilitating or fatal consequences for the victim/prey [163]. Most of the venomous organisms found around the world tend to be plants, insects, reptiles, arachnids, and mollusks.

Ornithoctonus huwena is a large Chinese bird spider that belongs to the *Theriphosidae* family, which encompasses a large variety of spiders commonly, referred to as tarantulas. Originally classified under the genus *Selenocosmia* in 1993, it was later reclassified to *Ornithoctonus* in 2001. Nicknamed by the locals as "*Dilaohu"* meaning golden earth tiger, this spider was discovered in the foothills of the Yunnan and Guangxi provinces in China by zoologist Dr. Jiafu Wang. *Ornithoctonus* huwena is a large spider that is approximately 9-12 cm in length and has fangs that can grow up to 9 cm (Figure 21). This nocturnal arthropod incapacitates its prey through a specialized mixture of 13 known different toxins named Huwentoxins (HwTx) and at least 1 lectin. The toxins differ in length and pharmacology as can be seen in Table 10 [164-166].

HwTx-I is a 33 amino acid peptide and is one of the most abundant toxins contained in the venom of *O. huwena*. The 6-cysteine residues in HwTx-I are oxidized

to give 3 disulfide bonds, which provide the toxin with its characteristic cysteine knot motif. This cysteine knot motif is a common feature among cyclotides and conotoxins with 3 disulfide bonds [167]. In addition to providing the peptide with enhanced stability the cysteine knot motif is also responsible for peptide bioactivity.

Originally classified as a N-type Ca^{2+} channel inhibitor, HwTx-I showed activity in the micro-molar range [168]. This finding was contradictory to the belief that toxins should be able to exert its activity in the nano-molar to pico-molar range. Since the production of toxin is energetically taxing on the host organisms it is beneficial to produce toxins that show activity in small concentration. Work done by Bingham and Cummins showed that HwTx-I is a potent inhibitor of the sodium channel, which lead to the reclassification of HwTx I as an inhibitor of the voltage, gated sodium channel [169].

HwTx I was chosen as the model peptide to study Native Chemical Ligation (NCL). Since HwTx-I has a two cysteine residues at the 16^{th} and 17^{th} position making it a prime candidate to study NCL (Refer to the NCL section in chapter 3 for more on the reaction). Another advantage with HwTx-I is that the peptide is well characterized therefore we can compare the bioactivity of the ligated peptide with native peptide and evaluate if ligation has a negative impact on bioactivity. Using this model system novel cleavage technology was developed which was utilized in various stages of this dissertation.

Figure 21: A picture of a female *Ornithoctonus huwena* spider. *Ornithoctonus huwena* is a large spider that is approximately 9-12 cm in length and has fangs that can grow up to 9 cm [162-164] (http://www.pticjipajki.com/galerija/7/Haplopelma_schmidti.jpg).

Table 10: Peptide toxins from the venom of *O. huwena* and their respective sequences and pharmacology. This nocturnal arthropod incapacitates its prey through a specialized mixture of 13 known different toxins named Huwentoxins (HwTx) and at least 1 lectin.

Toxins	Amino Acid Sequence	Pharmacology
HwTx-I	ACKGVFDACTPGKNECCPNRVCSDKHKWCKWKL	Inhibitor of N-type calcium channels at a micromolar (μM) scale), Inhibitor of select Na_v channels at a nanomolar (nM) scale
HwTx-II	LFECSFSCEIEKEGDKPCKKKKCKGGWKCKFNMCVKV	Potentiates the effects of HwTx-I in mammals and has been found to reversibly paralyze insects at a nM scale.
HwTx-III(a)	DCAGYMRECKEKLCCSGYVCSSRWKWCVLPAPW	Enhancement of contractile movements elicited by nerve stimulation in smooth muscle cells. Has also been found to reversibly paralyze insects at a nM scale.
HwTx-IV	ECLEIFKACNPSNDQCCKSSKLVCSRKTRWCKYQI	Inhibitor of TTX-S voltage-gated sodium channels.
(m)HwTx-V	(E)CRWYLGGCSQDGDCCKHLQCHSNYEWCVWDGT	Actively paralyzes and can cause death to insects at nM scale.
HwTx-VI	NCIGEQVPCDENDPRCCSGLVVLKKTLHGIWIKSSYCYKCK	Reversible paralysis in mammals can occur but the specific binding site has yet to be determined.
HwTx-VII	FECSFSCEIEKEGDKPCKKKKCKGGWKCKFNMCVKV	Potentiates the effects of HwTx-I in mammals and has been found to reversibly paralyze insects at a nM scale.
HwTx-VIII	FECSISCEIEKEGESCKPKKCKGGWKCKFNMCVKV	Potentiates the effects of HwTx-I in mammals and has been found to reversibly paralyze insects at a nM scale.
HwTx-IX	IICAPEGGPCVAGIGCCAGLRCSGAKLGLAGSCQ	Can paralyze mammals on the μM scale but has not been investigated any further.
HwTx-X	KCLPPGKPCYGATQKIPCCGVCSHNKCT	Inhibits activity of N-type calcium channels.
HwTx-XI	IDTCRLPSDRGRCKASFERWYFNGRTCAKFIYGGCGGNGNKF-PTQEACMKRCAKA	An inhibitor of serine protease and trypsin also has activity in the CNS at a μM scale.

Information in this table is adapted from Liang *et al.* [162, 167].

4.2 Methods

4.2.1 Fmoc Synthesis of the *C*-Terminal Fragment of Huwentoxin-I:

A manual 0.5 mM scale synthesis of the *C*-terminal fragment, 17 to 33 amino acids was Fmoc assembled on a Rink amide resin (0.44 meq/g). Resin was swelled for 8-10 hours in 25 mL of DMF, with 500 µL of DIEA to increase resin stability. The swollen resin was Fmoc deprotected via flow washing with DMF (1 minute x 2), followed by 50/50% (v/v) piperidine/DMF (1 minute X 2), and then rewashed with DMF (1 minute X 2). 2mM Fmoc-L-amino acids were activated *in-situ* using HBTU (4 mL; 0.5M in DMF; HCTU used for Cys residues), with DIEA added as a proton scavenger (347 µL; 2 mMol). The activated amino acids were then added to the resin and coupled for 20 minutes. Upon completion a Ninhydrin test was performed to ensure coupling yields reached ≥99.5% [124]. On passing yield verification, peptidyl-resin was subjected to repeated deprotection and amino acid activation-coupling cycles as above, ensuring adequate DMF flow washings between consecutive steps. If amino acid coupling yield fell ≤99.5%, the same amino acid was activated and recoupled. Side chain protecting groups included: Cys(Trt), Lys(Boc), Arg(Pbf), Trp(Boc), Asn(Trt), Asp (OBzl). Upon completion of synthesis the peptidyl-resin was washed with DMF (5 mL, x 2) followed by Dichloromethane (DCM; 10 mL) and dried under N_2.

4.2.2 Boc SPPS of the *N*-Terminal Fragment of Huwentoxin-I:

N-terminal segment of Huwentoxin-I, 1 to 16 amino acids, was manually synthesized using Boc chemistry. Boc-Cys-MPAL resin (0.5 mM) was swelled 8-10 hours in 25 mL of DMF. The peptidyl-linker-resin was washed with DMF (20 mL X 3), deprotected twice with 100% TFA (5 mL, 2 X 1 minute), and then re-washed with DMF (40 mL X 2). Boc amino acids, 4 fold excess (2 mMol), were activated *in-situ* using HCTU/DMF (0.4 M, 2 mL) and added to the drained activated resin and then shaken. After 20 min. of coupling Ninhydrin test was performed. If the coupling percentage yield was ≥99.5% the *N*-terminus was deprotected with 100% TFA, DMF washed (5 mL DMF X 2) and the next sequential amino acid activated and coupled, as previously described.

If the coupling was ≤99.5%, the same amino acid was activated and recoupled. Side chain protecting group included: Cys (4MOBzl), Glu(OBzl), Asn (Xan), Lys(Cl-z), Thr(Bzl), Asp(OBzl).

4.2.3 Ligation of the Peptide Fragments Using MPAA:

A stock solution of 6M GdnHCl and phosphate was prepared and stored. On the day of ligation, a ligation buffer solution was prepared by adding 5 mL of 0.42 micron filtered stock solution into a scintillation vial containing 28.7 mg TCEP.HCL (0.1mmmol) and 42.1 mg 4-Mercaptophenylacetic acid (MPAA) (0.26mmmol). MPAA has poor solubility at acidic pH but the solubility is greatly enhanced at pH 7. The GdnHCl allows ligation to occur at high concentration without agglutination of the reactants. TCEP.HCL was used to prevent the free thiols from forming dimer and MPAA helps in ligation by facilitation the thiol-thioester exchange. Minimum amounts of 2 M NaOH and 1 M HCL were used to adjust the pH of ligation buffer to 7.1. In a separate scintillation vial 5 mg of Cys-peptide fragment and 5 mg of Thioester peptide fragment were measured. The ligation buffer was transferred to the peptide scintillation vial to give a peptide concentration of approximately 3 to 5 mM. Since thioester is base labile and the ligation reaction does not proceed at acidic pH it is important to maintain the pH of ligation buffer peptide fragment mixture at pH 7-7.1. The ligation reaction was carried out at room temperature for 240 minutes with minimal shaking using stir bars. After incubation, the reaction was diluted by adding 30 mL of 0.1 % v/v TFA to the ligation mixture. Addition of 0.1 % v/v TFA stops the reaction by lowering the pH. The peptide mixture was loaded into the preparative HPLC to remove the GdnHCl (Figure 22).

4.2.4 Random Disulfide Bond Formation:

Peptide oxidation was achieved with 15 mg of reduced C_{18} RP-HPLC purified peptide, using 0.1 M NH_4HCO_3 pH 8.0 (5 days stirring; 4^{o}C). The oxidized peptide was preparative RP-HPLC/UV isolated and re-purified and the oxidized molecular mass was verified by ESI-MS (Figure 22).

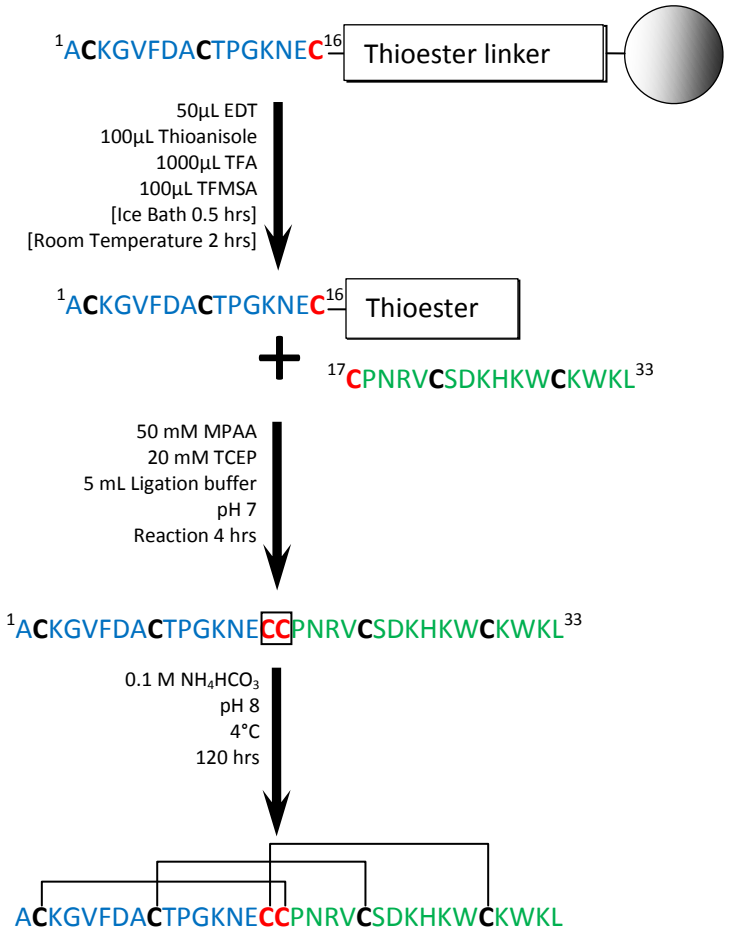

Figure 22: Methodology and optimized reaction conditions for thioester generation through TFMSA cleavage. Once the fragment with thioester (blue) has been produced we can use NCL to join the *N*-terminal (blue) and *C*-terminal (green) fragment at "red" cysteines to form a ligated reduced peptide. Random oxidation of ligated peptide was undertaken to produce a bioactive HwTx-I isomer.

4.2.5 Expression of Voltage-Gated Ion Channels in *Xenopus laevis* Oocytes:

For the expression of Na_v channels ($rNa_v1.2$, $rNa_v1.3$, $rNa_v1.4$, $hNa_v1.5$, the auxiliary subunits rβ1, hβ1) in *Xenopus* oocytes, the linearized plasmids were transcribed using the T7 or SP6 mMESSAGE-mMACHINE transcription kit (Ambion®, Carlsbad, California, USA). The harvesting of stage V-VI oocytes from anaesthetized female *X. laevis* frog was previously described Liman et al [124]. Oocytes were injected with 50 nL of cRNA at a concentration of 1 ng/nL using a micro-injector (Drummond Scientific®, Broomall, Pennsylvania, USA). The oocytes were incubated in a solution containing (in mM): NaCl, 96; KCl, 2; CaCl2, 1.8; MgCl2, 2 and HEPES, 5 (pH 7.4), supplemented with 50 mg/L gentamycin sulfate. Our collaborator Dr. Jan Tytgat (KU Leuven) performed this section.

4.2.6 Electrophysiological Recordings:

Two-electrode voltage-clamp recordings were performed at room temperature (18–22 °C) using a Geneclamp 500 amplifier (Molecular Devices®, Downingtown, Pennsylvania, USA) controlled by a pClamp data acquisition system (Axon Instruments®, Union City, California, USA). Whole cell currents from oocytes were recorded 1–4 days after injection. Bath solution composition was (in mM): NaCl, 96; KCl, 2; CaCl2, 1.8; MgCl2, 2 and HEPES, 5 (pH 7.4). Voltage and current electrodes were filled with 3 M KCl. Resistances of both electrodes were kept between 0.8 and 1.5 MΩ. The elicited currents were filtered at 1 kHz and sampled at 20 kHz using a four-pole low-pass Bessel filter. Leak subtraction was performed using a -P/4 protocol. In order to avoid overestimation of a potential toxin-induced shift in the current–voltage relationships of inadequate voltage control when measuring large sodium currents in oocytes, only data obtained from cells exhibiting currents with peak amplitude below 2 μA were considered for analysis. For the electrophysiological analysis of toxins, a number of protocols were applied from a holding potential of −90 mV with a start-to-start interval of 0.2 Hz. Sodium current traces were evoked by 100 ms depolarizations to Vmax (the voltage corresponding to maximal sodium current in control conditions). To

assess the concentration–response relationships, data were fitted with the Hill equation: $y = 100/[1 + (EC_{50}/[toxin])h]$, where y is the amplitude of the toxin-induced effect, EC_{50} is the toxin concentration at half maximal efficacy [toxin], is the toxin concentration and h is the Hill coefficient. All data are presented as mean ± standard error (S.E.M) of at least 5 independent experiments ($n \geq 5$). All data were tested for normality using a D'Agustino Pearson omnibus normality test. All data were tested for variance using Bonferroni test or Dunn's test. Data following a Gaussian distribution were analyzed for significance using one-way ANOVA. Non-parametric data were analyzed for significance using the Kruskal–Wallis test. Differences were considered significant if the probability that their difference stemmed from chance was 55% ($p < 0.05$). All data was analyzed using pClamp Clampfit 10.4 (Molecular Devices®, Downingtown, Pennsylvania, USA) and Origin 7.5 software (Originlab®, Northampton, Massachusetts, USA). Our collaborator Dr. Jan Tytgat (KU Leuven) performed the electrophysiology experiment.

4.3 Results and Discussion

The novel TFMSA cleavage protocol optimized in Chapter 3 was used to cleave the NTN fragment of HwTx-I. The MS and RP-HPLC profile indicate that TFMSA cleavage resulted in the peptide fragment of the expected mass (Figure 23).

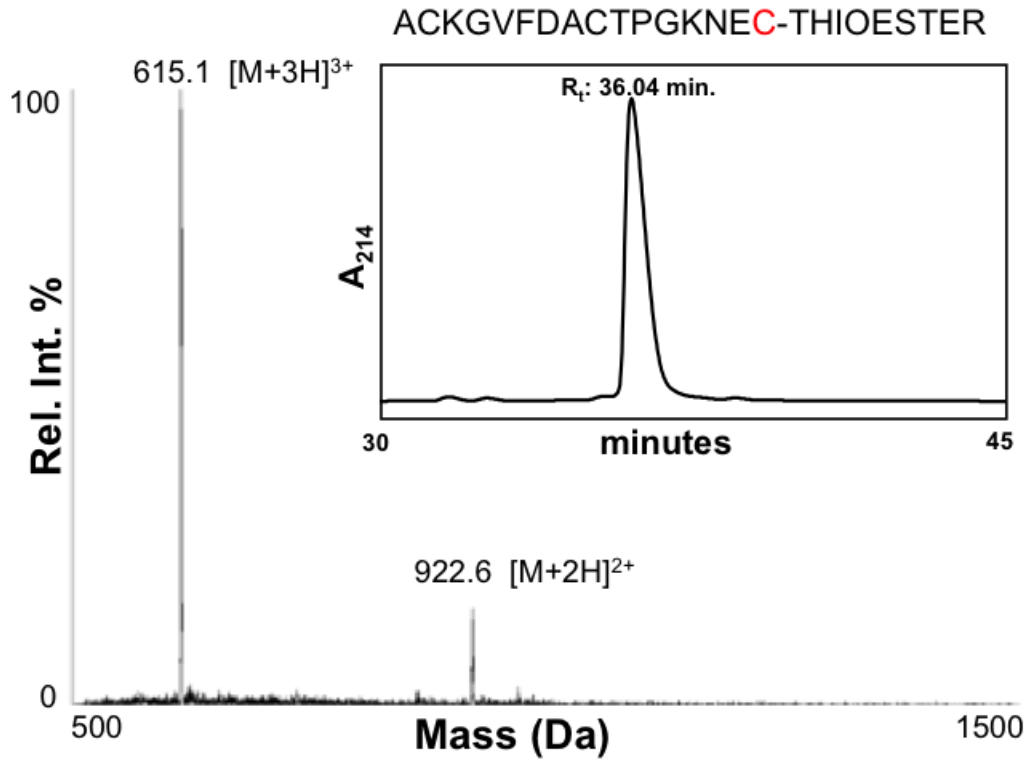

Figure 23: ESI-MS and RP-HPLC Chromatogram of the *N*-terminal fragment of HwTx-I (ACKGVFDACTPGKNEC-Thioester). The ESI-MS shows a dominant *m/z of* $[M+3H]^{3+}$ of 615.1 and a minor *m/z of* $[M+2H]^{2+}$ of 922.6. The theoretical calculated mass of the *N*-terminal fragment is $[M+3H]^{3+}$ of 615.3 and $[M+2H]^{2+}$ of 922.4. The *N*-terminus fragment eluted at 36.04 minutes when run on a 1 mm C_{18} Phenomenex® narrow bore column using a 1 % $minute^{-1}$ gradient of 90:10 Acetonitrile (MeCN): 0.08 % v/v *aq.* TFA. The cysteine residue used in NCL is colored in red. The thioester functionality attached to the cysteine comes off during ligation as a leaving group.

The CTN fragment of HwTx-I was synthesized using Fmoc chemistry and was cleaved using the reagent K protocol (Figure 24).

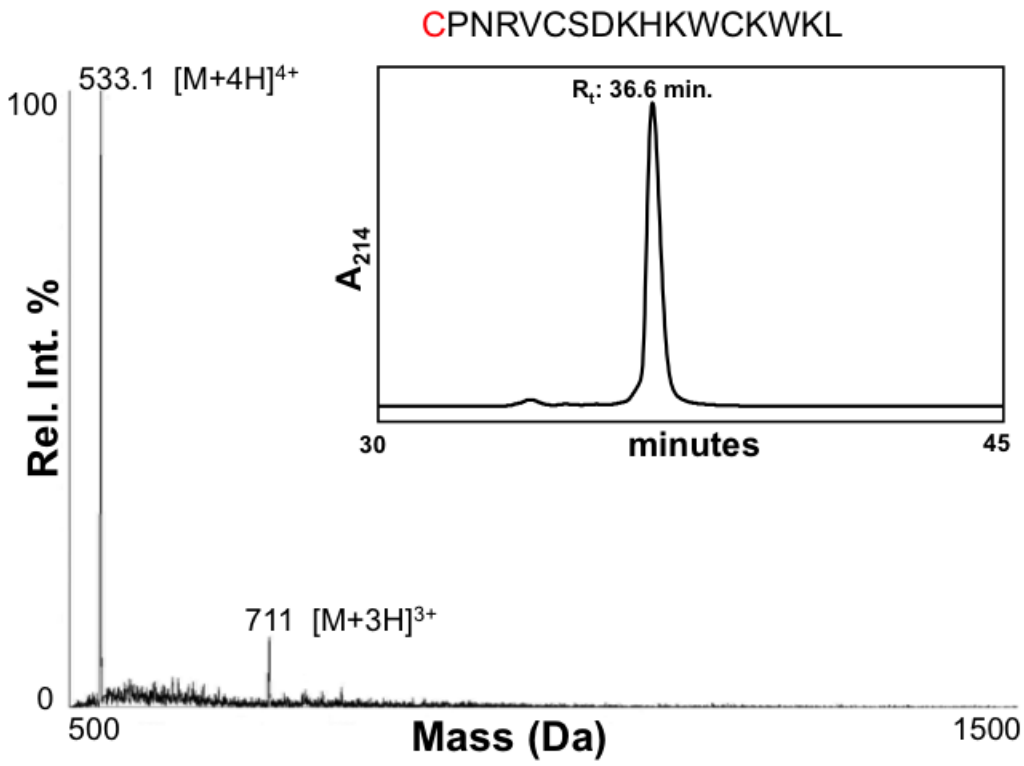

Figure 24: ESI-MS and RP-HPLC Chromatogram of the *C*-terminal fragment of HwTx-I (CPNRVCSDKHKWCKWKL). The ESI-MS shows a dominant *m/z of* $[M+4H]^{4+}$ of 533.1 and a minor *m/z of* $[M+3H]^{3+}$ of 711.0. The theoretical calculated mass of the *C*-terminal fragment is $[M+4H]^{4+}$ of 533.7 and $[M+3H]^{3+}$ of 711.4. The *C*-terminus fragment eluted at 36.6 minutes when run on a 1 mm C_{18} Phenomenex® narrow bore column using a 1 % $minute^{-1}$ gradient of 90:10 Acetonitrile (MeCN): 0.08 % v/v *aq.* TFA. The cysteine residue used in NCL is colored in red.

The NTN fragment has a *C*-terminal thioester and the CTN fragment has a *N*-terminal cysteine. These two functionalities were used to ligate the two peptide fragments using MPAA as the thiol catalyst using the protocol as established by Kent *et al.* [151] . Initially we used benzylmercaptan as the thiol catalyst but we moved to MPAA because MPAA does not have a foul odor and resulted in a cleaner ligation profile (Figure 25).

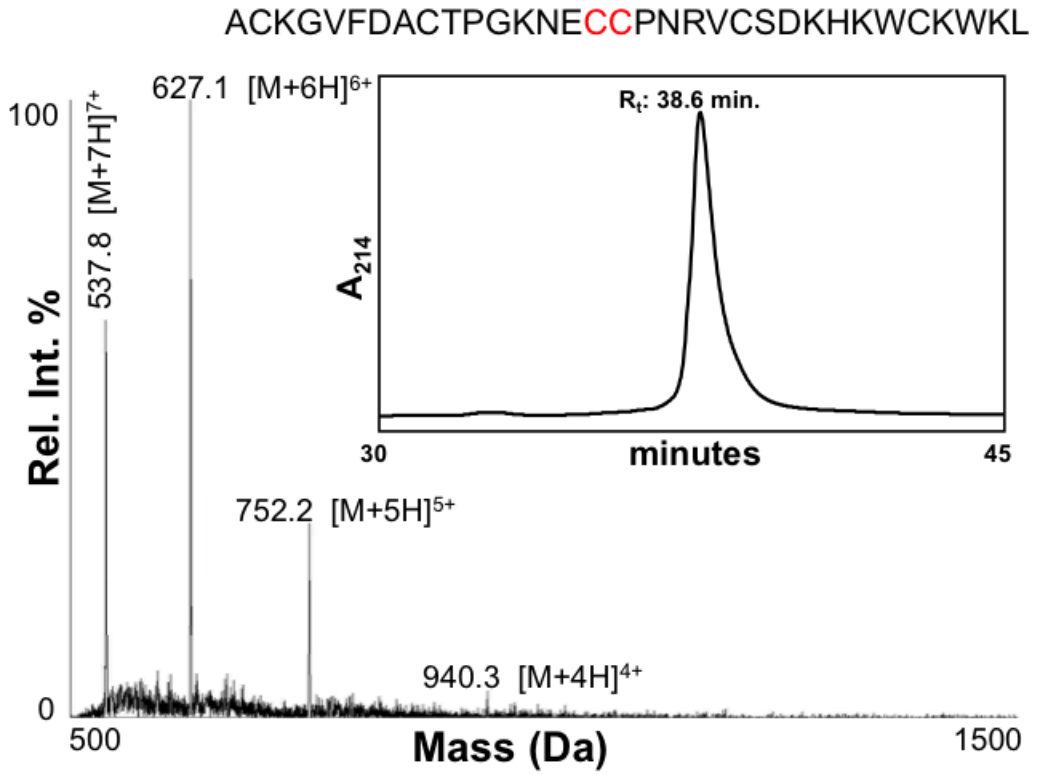

Figure 25: ESI-MS and RP-HPLC Chromatogram of ligated reduced HwTx-I (ACKGVFDACTPGKNECCPNRVCSDKHKWCKWKL). The ESI-MS shows a dominant *m/z of* $[M+6H]^{6+}$ of 627.1 and many minor *m/z of* $[M+7H]^{7+}$ of 537.8, $[M+5H]^{5+}$ of 752.2, $[M+4H]^{4+}$ of 940.3. The theoretical calculated mass of reduced ligated HwTx-I are $[M+6H]^{6+}$ of 627.0, $[M+7H]^{7+}$ of 537.5, $[M+5H]^{5+}$ of 752.2 and $[M+4H]^{4+}$ of 940.0. The ligated reduced fragment eluted at 38.6 minutes when run on a 1 mm C_{18} Phenomenex® narrow bore column using a 1 % $minute^{-1}$ gradient of 90:10 Acetonitrile (MeCN): 0.08 % v/v *aq.* TFA. The cysteine residues used in NCL are colored in red. Since the ligated fragment has more positively ionizable residues it has more charge states that the *N*-terminal fragment or the *C*-terminal fragment.

After ligation we oxidized the peptide using 0.1M NH_4HCO_3 at pH 7.8. The maximum possible combination of disulfide bridges within a peptide may be calculated using the formula $p = \frac{n!}{\left(\frac{n}{2}\right)! \cdot 2^{\frac{n}{2}}}$. Where p is the number of possible disulfide bridges and n is the number of cysteines present within the peptide [15]. HwTx-I has 6 cysteines in its sequence therefore if we use the above-mentioned formula random oxidation of HwTx-I could theoretically yield 15 isomers. Among the many potential isomers only the thermodynamically favored isomers are formed after oxidation. Upon oxidation of the reduced HwTx-I (Figure 25), we were able to produce 10 isomers (Figure 26).

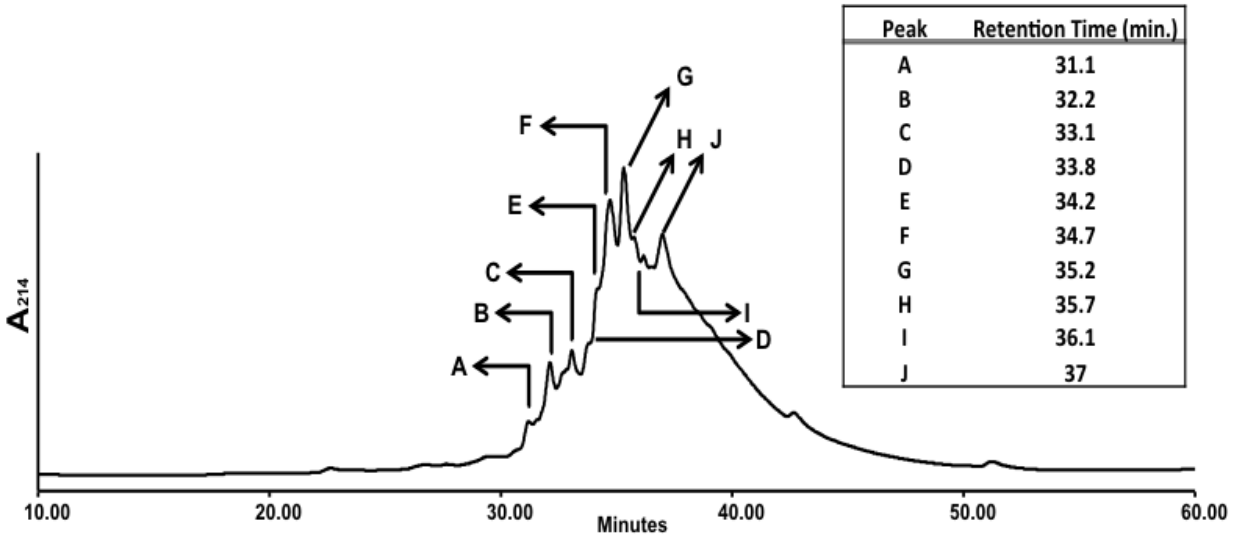

Figure 26: RP-HPLC profile of a random oxidation done on the ligated reduced HwTx-I. The ligated reduced material was oxidized in a solution of 0.1M NH_4HCO_3 at pH 8. HwTx-I has 6 cysteines therefore random oxidation of HwTx-I should theoretically produce 15 isomers. Of the 15 possible isomers we were able to isolate 10 isomers from the random oxidation profile. The retention times of the 10 isomers are as follows Isomer A: 31.1 minutes, Isomer B: 32.2 minutes, Isomer C: 33.1 minutes, Isomer D: 33.8 minutes, Isomer E: 34.2 minutes, Isomer F: 34.7 minutes, Isomer G: 35.2 minutes, Isomer H: 35.7 minutes, Isomer I: 36.1 minutes and Isomer J: 37.0 minutes. All the 10 isomers were mass confirmed using ESI-MS. The isomers from random oxidation had the above-mentioned elution times when run on a 1 mm C_{18} Phenomenex® narrow bore column using a 1 % $minute^{-1}$ gradient of 90:10 Acetonitrile (MeCN): 0.08 % v/v *aq.* TFA.

All the 10 isomers were mass confirmed using ESI-MS. Here we show the RP-HPLC and ESI-MS of Isomer G as a representative example. The RP-HPLC profile of all the isomers can be seen in Appendix C.

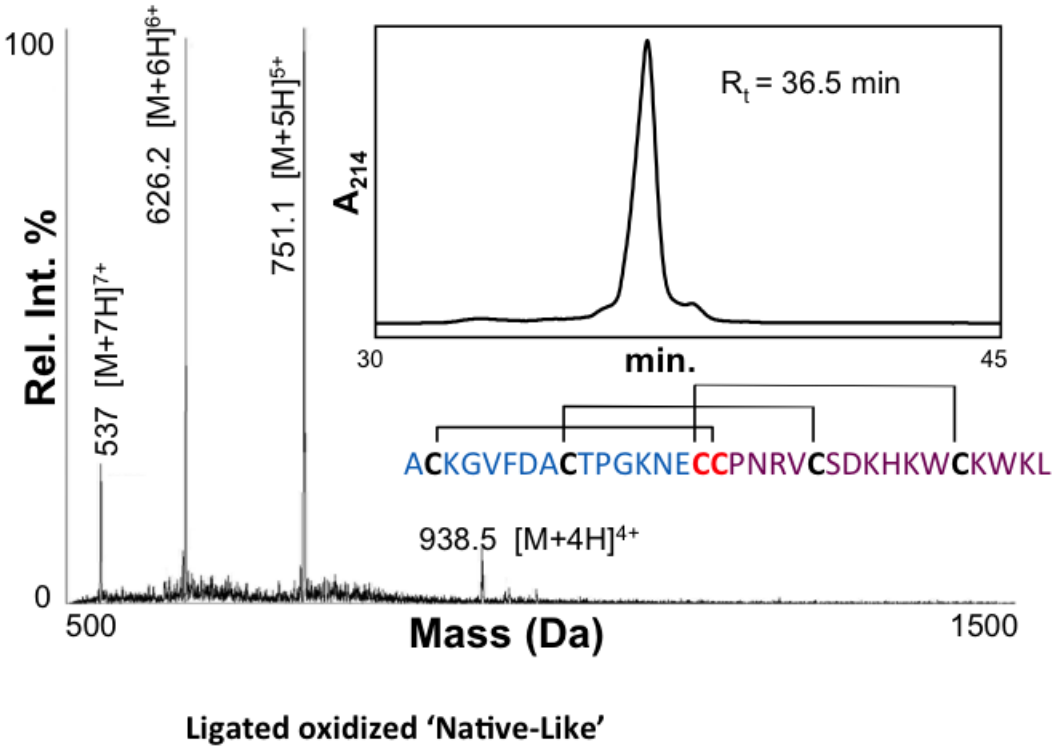

Figure 27: ESI-MS and RP-HPLC Chromatogram of ligated randomly oxidized HwTx-I (ACKGVFDACTPGKNECCPNRVCSDKHKWCKWKL). The ESI-MS shows two dominant *m/z of* $[M+5H]^{5+}$ of 751.1 and $[M+6H]^{6+}$ of 626.2 and two minor *m/z of* $[M+7H]^{7+}$ of 537.0 and $[M+4H]^{4+}$ of 938.5. The theoretical calculated mass of oxidized HwTx-I are $[M+7H]^{7+}$ of 536.2, $[M+6H]^{6+}$ of 625.5, $[M+5H]^{5+}$ of 750.2 and $[M+4H]^{4+}$ of 937.8. The ligated oxidized HwTx-I eluted at 36.5 minutes when run on a 1 mm C_{18} Phenomenex® narrow bore column using a 1 % $minute^{-1}$ gradient of 90:10 Acetonitrile (MeCN): 0.08 % v/v *aq.* TFA. The cysteine residues used in NCL are colored in red. Since the ligated oxidized fragment has more positively ionizable residues it has more charge states that the *N*-terminal fragment or the *C*-terminal fragment. The disulfide bond connectivity of cysteine residues is unknown because the reduced peptide was randomly oxidized.

Of the 10 isomers only the G isomer of HwTx-I (Figure 26) was found to show significant activity against Na_v 1.2, Na_v 1.3, Na_v 1.4 and Na_v 1.5 channel isoforms.

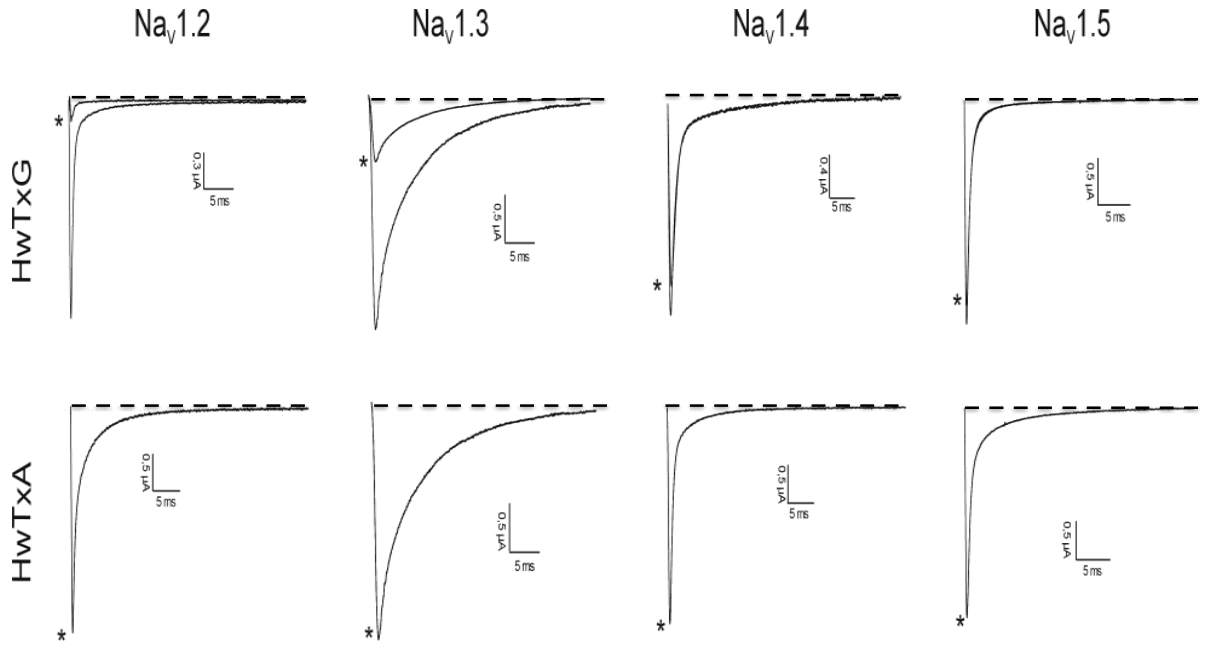

Figure 28: Activity of the G isomer of HwTx-I on various isoforms of Na_v. Using the *Xenopus* oocyte expression system, all isomers were investigated for their activity against Na_v1.2, Na_v1.3, Na_v1.4 and Na_v1.5. Of the 10 isomers only HwTx-G was found to show significant activity against these Na_v channel isoforms. 1 µM HwTx-G inhibited Na_v1.2 channels with 84.4 ± 2.3% while the current through Na_v1.3 channels was reduced with 71.3 ± 3.2%. The same concentration inhibited Na_v1.4 and Na_v1.5 channels with 17.6 ± 1.9% and 15.7 ± 2.8%, respectively. HwTx-A is shown as a representative example for inactive isomers. The asterisk indicates the current trace in the presence of toxin; the dotted line indicates zero current level. Each experiment was performed at least 3 times (n ≥ 3). Data are presented as mean ± S.E.

As seen in Figure 28, 1 µM of HwTx-G inhibited Na_v 1.2 channels with 84.4 ± 2.3% while the current through Na_v1.3 channels was reduced with 71.3 ± 3.2%. The same concentration inhibited Na_v1.4 and Na_v1.5 channels with 17.6 ± 1.9% and 15.7 ± 2.8%, respectively. The synthetic ligated HwTx-I demonstrated isoform selectivity at the voltage gated sodium channels. Na_v channels have specific sites on their transmembrane segments that can be bound to by toxins eliciting a biological response. Since Na_v isoforms are made up of different subunits, our peptide might have different

binding interaction with different subunits of $Na_{v,}$ which might lead to isoform selectivity [170, 171].

In order to assess the concentration dependence of the toxin induced inhibition, concentration-response curves were constructed for $Na_v1.2$ and $Na_v1.3$ channel (Figure 29).

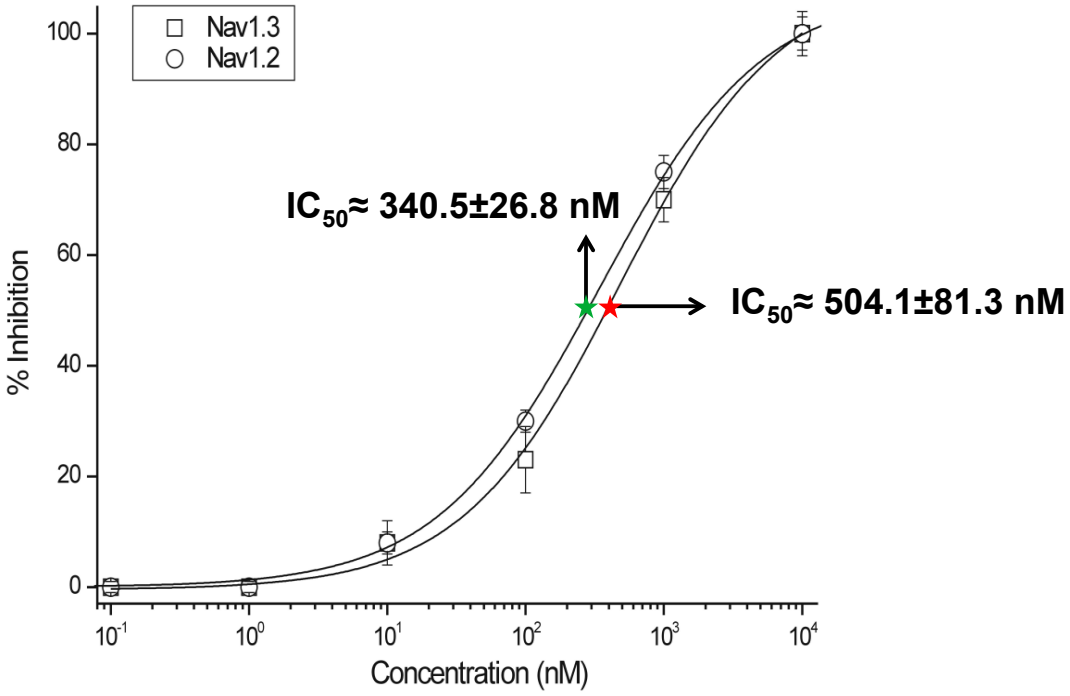

Figure 29: Concentration-response curves for isomer G on $Na_v1.2$ and $Na_v1.3$ channels. Results are indicated as mean ± S.E. from experiments performed in triplicate.

As demonstrated in Figure 29, for $Na_v1.2$, EC_{50} value yielded 340.5 ± 26.8 nM and for $Na_v1.4$, EC_{50} value was determined at 504.1 ± 81.3 nM. Native HwTx-I has an IC_{50} of 640 nM when tested on $Na_v1.7$ [172]. Our collaborators are working on expressing $Na_v1.7$ and will be able to test the synthetic ligated peptide on $Na_v1.7$ in the near future. Since our ligated peptide was able to inhibit the Na_v 1.2 and $Na_v1.3$ in the nM range it gives further evidence that a functional bioactive peptide can be produced through our novel cleavage method.

To further corroborate our methodology we co-eluted the native HwTx venom profile and Isomer G, which was generated through random oxidation of ligated peptide.

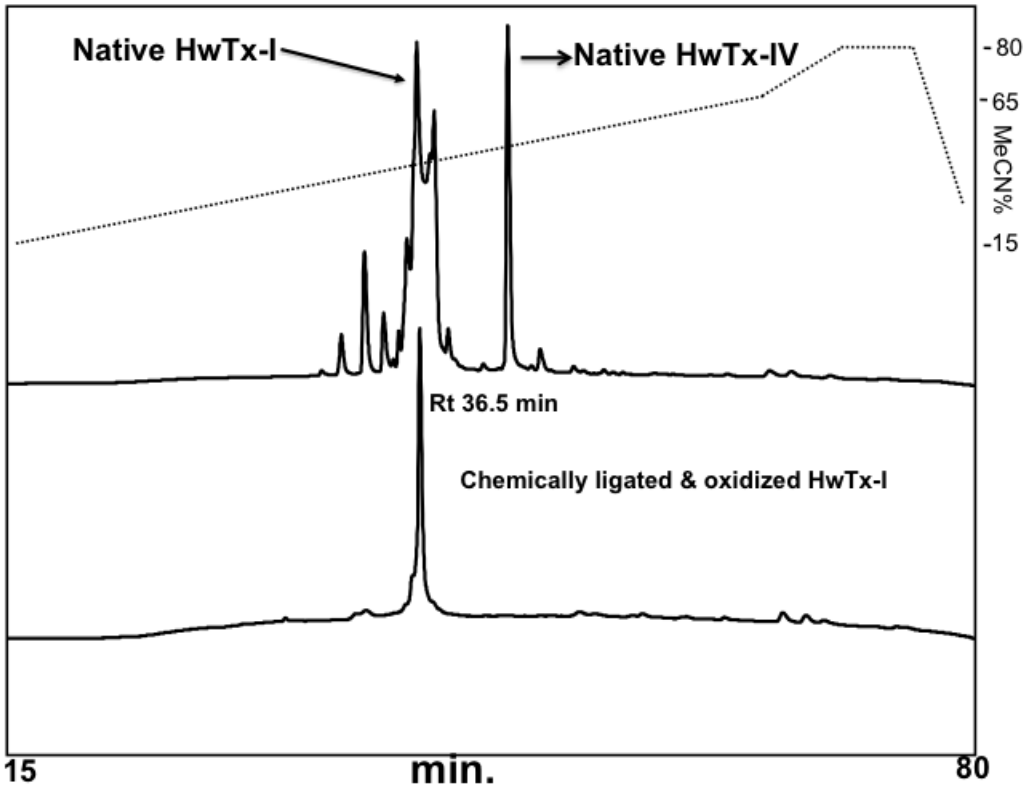

Figure 30: Coelution of native HwTx venom profile with synthetic ligated HwTx-I. *O. huwena* incapacitates its prey through a specialized mixture of 13 known different toxins named Huwentoxins (HwTx) and at least 1 lectin. The other prominent peak in the native venom profile is HwTx-IV. Similar retention time between the native and the synthetic venom indicates that our methodology can produce a “native-like” peptide.

As seen in Figure 30, the native HwTx-I and the active isomer have the same retention time and overlap on the RP-HPLC profile, which provides further evidence that our TFMSA cleavage protocol can be used to produce “native-like” peptide.

In nature we only see some of the potential isomers that are energetically favorable. However through chemical synthesis and preferential oxidation conditions non-native isomers can be generated. Permutations of disulfide bond connectivity can also produce peptide isomers that may possess enhanced pharmacological properties. The number of disulfide isomers possible within a peptide is directly correlated with an increasing number of cysteines within a peptide sequence.

We were able to generate 10 isomers through random oxidation of the native ligated HwTx-I (Figure 26), but only 1 of the 10 isomers showed biological activity. Majority of the isomers might be inactive because HwTx-I has 6 cysteine residues and when oxidized the 6 cysteine residues are arranged in an inhibitory cysteine knot motif. Generation of the cysteine knot motif in chemical oxidation is a well-documented challenge therefore it is not unusual that majority of the isomers did not show bioactivity [173]. One way to circumvent this problem is to oxidize the cysteines through selective oxidation.

HwTx-I asserts its mechanism of action on Na_v channels by binding to an amino acid stretch known as the S3-S4 linker [169]. Typical Na_v channel comprises of four domains with six transmembrane helices. Toxin binding occurs extracellularly near the voltage-sensitive S4 segment, rendering S4 in a ‘close’ position thereby inactivating the flow of ions through the channel [174]. Voltage gated sodium channels play important physiological roles in neuronal signaling and their deregulation is implicated in various pathological states such as epilepsy and seizures [175]. Their control has also been associated with pain management [176]. As such, investigation of HwTx-I and its receptor-ligand interactions is of particular pharmaceutical value. Given the limited nature of venom extractions from *O. huwena*, investigations in HwTx-I are best carried out through synthetic analogues. In order to advance HwTx-I as a drug ‘lead’ or fluorescent marker, it is necessary to understand the contribution of each amino acid within the peptide toxin. Peptide toxins have subtle changes in amino acid sequence that end up having extreme ramifications on their pharmacology. Our future goal is to perform single-point mutations of the amino acid sequence and test each analogue for a change in activity. This task can be performed through 25 separate linear syntheses, with each synthesis comprising of 33 amino acid residues. Alternatively, this task can

also be performed through convergent synthesis using NCL chemistry, which may potentially reduce time and resources. Furthermore, the NCL route could lead to higher quality peptides, both in terms of yield and purity. Our novel cleavage method using TFMSA in association with NCL can be used to perform Alanine walks for future HwTx-I studies.

4.4 Conclusion

We have used our novel TFMSA cleavage protocol to produce a *N*-terminal fragment with thioester. The *N*-terminal fragment was successfully ligated to a *C*-terminal fragment to produce a longer peptide. Our ligated peptide toxin was able to inhibit isoforms of Na_v at nanomolar range. Activity of the ligated toxin was similar to the native toxin thus our hypothesis that TFMSA cleavage protocol can be used for NCL was proven to be correct. Furthermore, the native peptide and ligated peptide eluted at the same time, which further corroborates our hypothesis that the peptide produced through our novel cleavage protocol will be able to retain 'native-like' properties.

Chapter 5: Cyclic Conotoxins

This part of the study was undertaken to explore **Objective 4: Utilize the novel thioester technology to synthesize cyclic α-Conotoxin Tx2005, which is the cyclized non-PTM version of α-Conotoxin TxIC (This objective is the culmination of skills acquired from the previous objectives). Objective 5: Determine the Pharmacodynamics of Cyclic Tx2005 and Objective 6: Examination of bio-stability of Cyclic Tx2005, and Linear Tx2005.**

5.1 Introduction

NCL technology can be implemented to make peptides in which the amino and carboxy termini are attached in a covalent bond to form a cyclic molecule. When the thioester and free cysteine functionalities are present on the same peptide fragment, an intramolecular NCL reaction can be used to generate a cyclic molecule (Figure 31). Recently, naturally occurring cyclic molecules have been discovered in bacteria, plants and animals [54, 177]. NCL reactions can be utilized to synthesize these circular proteins to find potential new drug leads and design scaffolds that aid in drug delivery.

Cyclotides are disulfide rich compounds naturally occurring in plants. They generally have about 30 amino acids and are predominantly found in the Rubiaceae (coffee) and Violaceae (violet) families [66, 178, 179]. Cyclotides fall into two major subfamilies, the bracelet family, which contains two-thirds of cyclotides, and the mobius family, which contains the remaining one-third. There is a third subfamily called trypsin inhibitor family comprised of eight members [180, 181]. Head to tail cyclization and six-conserved cysteine residues arranged in a knotted topology characterizes cyclotides. The cyclic cystine knot morphology provides cyclotides with exceptional stability thereby making them prime candidates for grafting studies and as templates for drug design [68]. These cyclic molecules have shown a vast array of activities ranging from antimicrobial, cytotoxic and anti-HIV. In nature cyclotides function as host defense agents and possess potent insecticidal activity [182, 183].

Craik *et al*. [184], have used NCL to successfully conduct grafting studies on cyclotides. They combined stable cyclotide fragments with bioactive peptide epitopes to

produce chimeric molecules with enhanced biopharmaceutical properties. As a proof of concept they grafted a highly polar region to a cyclotide and showed that the molecule still maintained its structural integrity [182]. Furthermore Gunasekera *et al.*, [185] incorporated an antiangiogenic epitope (RRKRRR) referred to as the poly R sequence into kalata B1. The chimeric molecule possessed antiangiogenic activity and was more stable than the naked epitope. Similarly Thongyoo *et al.* [186] have proposed that the active site in cyclotides loop 1 could be replaced with a sequence to inhibit a protease from the Foot and Mouth Disease virus [184]. Reengineering of cyclotides to produce chimeric molecules has shown promise in therapeutic development, and with further advancement this technology might produce future drugs.

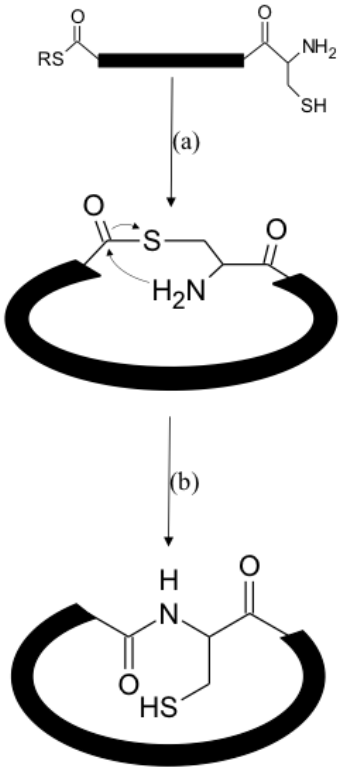

Figure 31: Mechanism showing the cyclization of a linear peptide. The linear peptide, which contains thioester functionality and free cysteine functionality on the same fragment, can undergo intramolecular ligation to form a cyclic peptide. (a) Intramolecular nucleophilic attack results in a cyclic peptide joined by a thioester bond (b) S-N Acyl Shift produces the final cyclic molecule now joined by a native peptide bond.

Like cyclotides, conotoxins are natural products that are rich in cysteine residues thereby providing ample opportunities for NCL. Conotoxins are found in the venom of conesnails and act as potent antagonists of a range of neuronal receptors and ion channels [103, 104]. ω-Conotoxin MVIIA, a potent N-type calcium channel blocker extracted from *Conus magus*, was developed into ziconotide. This “conopeptide” is the first non-opioid IT treatment for the management of chronic refractory pain and is known by its brand name Prialt® [90, 91, 187]. One of the major hurdles in developing conopeptides as therapeutics is overcoming their low oral bioavailability [188]. Peptides and proteins have low oral bioavailability due to degradation caused by digestive enzymes present in the intestinal lumen [21, 23, 189]. Secondly, the inability of peptides to permeate through membranes owing to size and polarity also results in low bioavailability [21,24]. Consequently, any method that improves the stability and bioavailability of peptides and proteins is highly desirable. Work done by Clark *et al.* [118] on cyclic α-Conotoxin MII, Craik *et al*. [19] on cyclic α-Conotoxin Vc1.1 and Lovelace *et al.* [42] on cyclic χ-Conotoxin MrIA has demonstrated that NCL can be used to cyclize conotoxins. Their work shows that when provided with a linker of right size the cyclic molecules can maintain their biological activity and are more stable than native peptides. Cyclization helps with stability by eliminating the free termini of a peptide and makes it less labile to exopeptidases. Additionally cyclization enhances stability by introducing rigidity and reducing the conformational energy of the unfolded state [190]. The added rigidity makes the peptide more resistant to proteases that cleave from the middle of the chain [191]. Conotoxins are a rich source of biological leads that might provide therapies for pain management, seizures, and Parkinson’s [19, 192]. Through cyclization we can improve the therapeutic potential of conotoxins and enhance the number of potential leads in our pharmacological repertoire.

5.2 Methods

5.2.1 Determination of Linker Length:

The number of amino acid residues in the linker between the two termini was determined using the equation developed by Craik *et al.* [43].

$$Number\ of\ Residues\ in\ linker = (Distance\ between\ termini - 5.5)/1.1$$

Structure determination websites such as Quark and Pepfold were used to approximate the 3D structure of the peptide, which allowed us to estimate the distance between the termini. The number of residues calculated from the above equation was compared to linker length in previously published homologous cyclic peptide. Based on all the available information the numbers of residues in the linker was approximated accordingly.

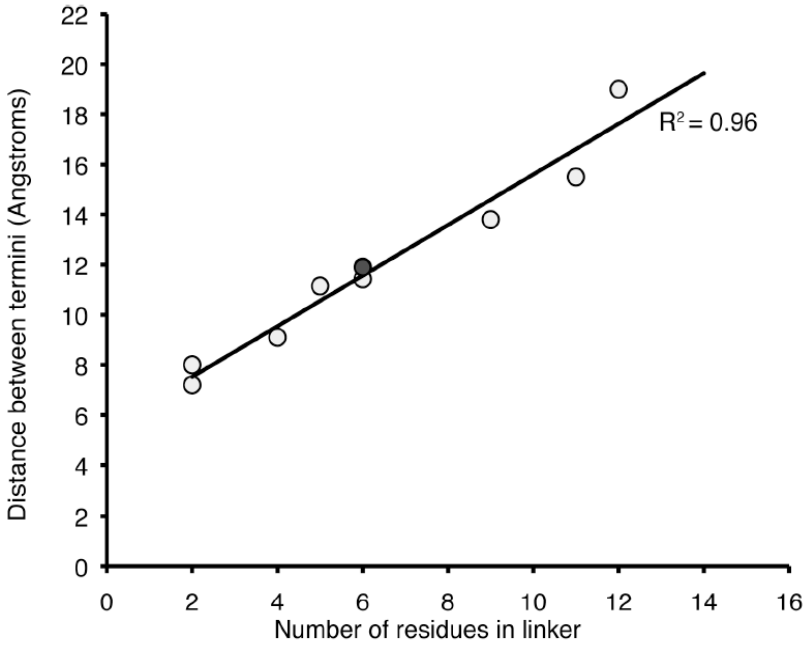

Figure 32: The relationship between *N*- and *C*-termini distance and the approximate number of amino acid residues required in the linker region. Cyclization without a linker region produces an inactive distorted peptide. The presence of a linker region maintains the 3-Dimenisonal conformation of the peptide and allows researchers to engineer a cyclic peptide without changing its native sequence [39].

5.2.2 Synthesis of Cyclic Tx2005 on MPAL Resin:

Boc synthesis of Cyclic Tx2005 ([Pro]^{2,8}[Glu]^{16}α-Conotoxin TxIC [RPQC^{4}CSHPAC^{10}NVDHPEIC-NH_2]), the non PTM variant of α-Conotoxin TxIC [ROQC^{4}CSHOAC^{10}NVDHPγIC-NH_2; γ = γ-carboxyglutamic acid (Gla), O = *4-trans* hydroxyproline (Hyp)], was undertaken on a MPAL resin using a protocol similar to the synthesis of *N*- terminal fragment of HwTx-I.

5.2.3 Synthesis of Cyclic Tx2005 on a 2-Chlorotrityl Resin Using Fmoc Chemistry:

Cyclic peptides were assembled using Fmoc chemistry on a 2-Chlorotrityl resin. 1 mMole of (0.61 SV value) resin was weighed and transferred to a reaction vessel. The resin was swelled overnight in 10-20 mL DCM and 500 µL of DIEA. Procedure for amino acid activation, coupling and drying were similar to the methods described in previous chapters.

5.2.4 Cleavage of Peptide Using TFMSA Cleavage Method:

The cyclic peptide was cleaved using the novel TFMSA cleavage protocol that was developed during the HwTx-I section of the project. The method can be seen in method section for HwTx-I (Chapter 3 and Chapter 4)

5.2.5 Peptide Oxidation:

Peptide oxidation was undertaken by dissolving 10 mg of reduced peptide in 0.1 M NH_4HCO_3 pH 8.0 (5 days stirring; 2^{o}C (cold room). The oxidized peptide was preparative RP-HPLC/UV isolated and re-purified and the oxidized molecular mass was verified by ESI-MS. A second round of rapid iodine oxidation was undertaken to remove the Acm groups.

5.2.6 Method for Cyclization and Removal of Protection Groups Using 2-Chlorotrityl Resins:

Unlike the rink amide resin, 2-Chlorotrityl resin is cleaved in mild acidic conditions. Therefore, a three-step procedure can be undertaken to obtain a cyclic product. Firstly, the resin is cleaved in mild acidic conditions; this is followed by cyclization, which is followed by removal of orthogonal protection group.

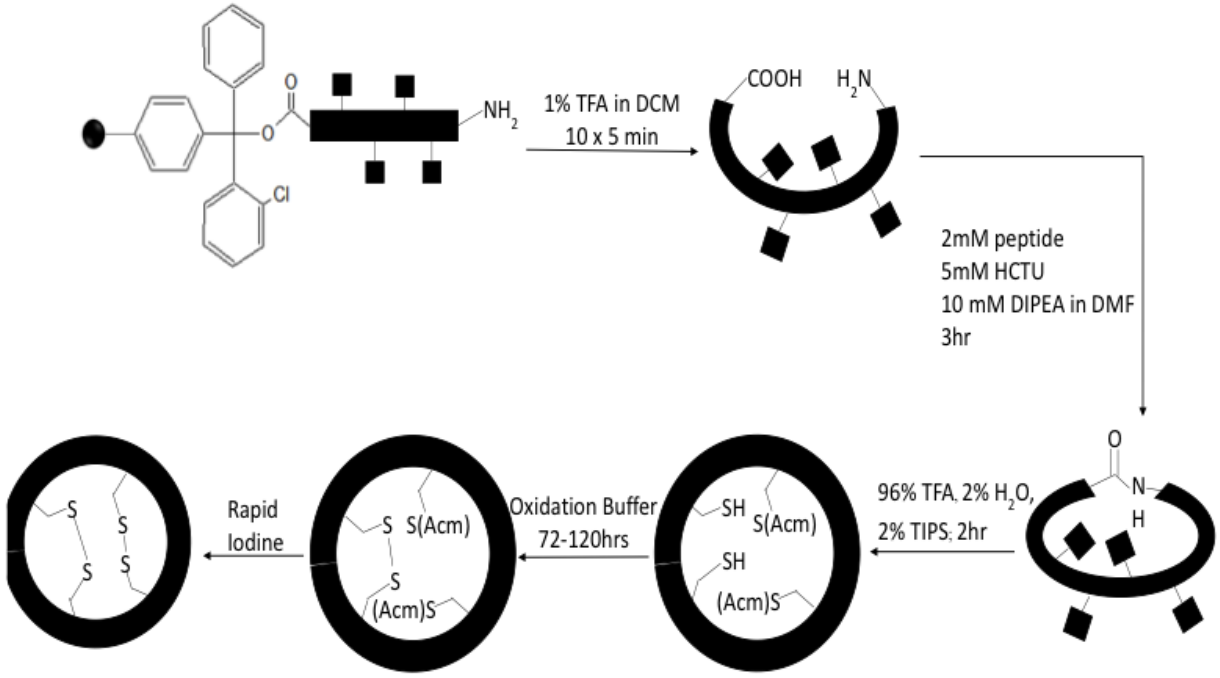

Figure 33: Methodology for Fmoc based cyclization using a 2-Chlorotrityl resin. In this method cleavage of the resin under mild acidic conditions produces a linear peptide that has orthogonal protection groups. The linear peptide is cyclized in a manner that is analogous to amino acid coupling. Following the generation of a cyclic peptide the orthogonal protection groups are removed and the cyclic peptide is oxidized.

5.2.6.1 Cleavage of Peptide Resin:

The first step is to cleave the peptide resin while leaving the orthogonal protection group intact. A 35 mL cleavage solution of 1 % v/v TFA in DCM was prepared and stored in an Erlenmeyer flask. Next 500 mg of resin was placed in a fritted reaction vessel and treated with 3 mL of cleavage solution for 5 minutes. After 5 minutes the cleavage solution was vacuum filtered and collected in a round bottom flask. This procedure was repeated 9 more times and all the elutants were pooled together in the same round bottom flask. A 75 mL solution of 50 % acetonitrile, 0.05 % v/v TFA in water was prepared and added to the round bottom flask. DCM and TFA were removed under vacuum and the resulting solution was lyophilized. The resulting peptide was weighed and stored in scintillation vials for future use.

5.2.6.2 Cyclization of Peptide:

Cleavage of 2-Chlorotrityl resin results in peptide with free *N*- and *C*-termini but all of the orthogonal protection groups are intact. This peptide can form an amide bond between the termini and result in a cyclic product. Cyclization can be treated as an amino acid coupling because both procedures use the same functionality and result in the formation of a covalent peptide bond. Therefore, amino acid coupling and cyclization reaction require similar reagents.

100 mg of the above mentioned peptide was placed in a scintillation vial and dissolved in 19 mL of DMF to give a concentration of 2 mM. 12 mg of HCTU was added to the solution to give a final concentration of 5mM. Next, the solution was shaken for 1 minute and 57 µL of DIEA was added to give the final concentration of 10 mM. The solution was allowed to stir at room temperature for 180 minutes. After the reaction was completed the peptide mixture was transferred to a round bottom flask and diluted with 75 mL of (50 % acetonitrile, 0.05 % v/v TFA in water) and lyophilized overnight. The cyclized product was weighed and collected in a scintillation vial.

5.2.6.3 Removal of Orthogonal Protection Groups:

The orthogonal protection groups are removed using a cleavage cocktail with the following composition: 2 % v/v TIPS: 2 % v/v Water: 96 % v/v TFA. 100 mg of peptide was added to the Erlenmeyer flask, 10 mL of cleavage was cocktail was added to the peptide and allowed to stir for 120 minutes at room temperature. After incubation the cleavage mixture was transferred to a Falcon tube containing 25 mL of liquid nitrogen chilled MTBE. The tube was centrifuged at 3500 rpm for 8 minutes. Supernatant was carefully decanted without disturbing the peptide pellet. The peptide pellet was suspended in 25 mL of cold MTBE and the centrifugation and decantation process was repeated twice. After 3 centrifugations with MTBE a final centrifugation without MTBE was done to remove all scavenging agents from the peptide pellet. A 75 mL solution of (50 % acetonitrile, 0.05 % v/v TFA in water) was used to dissolve the peptide pellet and the solution was transferred to a pear flask. The pear flask was shelled using liquid nitrogen and freeze-dried. The lyophilized peptidic material was removed, massed, and stored in a scintillation vial for future purification.

5.2.6.4 Oxidation of Peptide:

Peptide oxidation was undertaken by dissolving 20 mg of reduced peptide in 0.1 M NH_4HCO_3 pH 8.0 (3 days stirring; 26^{o}C (room temperature). The oxidized peptide was preparative RP-HPLC/UV isolated and re-purified and the oxidized molecular mass was verified by ESI-MS. A second round of rapid iodine oxidation was undertaken to remove the Acm groups.

5.2.6.5 Addition of Fluorophore to Cyclic Tx-2005 with Lys-Azide:

DyLight® 650-phosphine (Thermo Fisher Scientific, Inc.; product No. 88911; molar mass, 1357.37 Da; form, solid; color, blue) was dissolved in the dry water-miscible organic solvent DMF. A 10 mM stock solution of the DyLight® 650 reagent was prepared by dissolving 1 mg in 73.7 µL of DMF. A 0.2 mM stock of the Cyclic Tx2005 (Lys-N3) was prepared by dissolving 2.5 mg in 2.78 mL of 1X phosphate-buffered saline (PBS). The phosphine stock solution was added to the Cyclic Tx2005-LC[azide] solution and diluted to a final concentration final concentration (of DyLight 650-phosphine) at 200 µM. The final reaction solution would have 2 % v/v DMF/*aq* and may be further diluted to 0.5 % v/v DMF/*aq.* after the reaction is completed for effective RP-HPLC (cf. Thermo Fisher Scientific Inc., 2014b). The Dylight® reagent and the Peptide were in a 1:1 mole ratio. The reaction vial was incubated at 22º C for 24 hours. The samples were then prepared for RP-HPLC to remove the PBS buffer and purify out the labeled material

5.2.6.6 Stability Studies for Cyclic Peptide and Linear Peptide:

A 1 mg/mL stock solution of linear and cyclic peptides was prepared in ammonium acetate buffer at pH 7.4. In the same buffer 250 µg/mL stock solution of pancreatin, trypsin and carboxypeptidase were prepared. In an eppendorf equal volume of peptide (100 µL) and enzyme (100 µL) were added to get a mixed final solution with a total volume of 200 µL. The peptide enzyme mixture was incubated at 37^{o}C for the duration of the experiment. At given time points of (0 hours, 3, hours, 6 hours, 24 hours, 26 hours, 28 hours and 48 hours), a 5 µL aliquot of peptide-enzyme mixture is taken and quenched with 95 µL of 5 % v/v formic acid. Samples were stored at 4 ^{o}C and 85 µL was run on HPLC to analyze the stability of peptides. The experiment was performed in triplicate for each peptide and enzyme combination.

5.2.7 Expression of Voltage-Gated Ion Channels in *Xenopus laevis* Oocytes:

For the expression of nAChR (α1, α3, α4, α5; β2, β4; γ; δ; ε) in *Xenopus* oocytes, the linearized plasmids were transcribed using the T7 or SP6 mMESSAGE-mMACHINE transcription kit (Ambion®, Carlsbad, CA, USA). The harvesting of stage V–VI oocytes from anaesthetized female *Xenopus laevis* frog was previously described Liman *et al.* [126]. Oocytes were injected with 50 nL of cRNA at a concentration of 1 ng/nL using a micro-injector (Drummond Scientific®, Broomall, PA, USA). The oocytes were incubated in a solution containing (in mM): NaCl, 96; KCl, 2; $CaCl_2$, 1.8; $MgCl_2$, 2 and HEPES, 5 (pH 7.4), supplemented with 50 mg/L gentamycin sulfate. Our collaborator Dr. Jan Tytgat (KU Leuven) performed this section.

5.2.8 Electrophysiological Recordings:

Two-electrode voltage-clamp recordings were performed at room temperature (18–22°C) using a Geneclamp 500 amplifier (Molecular Devices®, Downingtown, PA, USA) controlled by a pClamp data acquisition system (Axon Instruments®, Union City, CA, USA). Whole cell currents from oocytes were recorded 1–4 days after injection. Bath solution composition was (in mM): NaCl, 96; KCl, 2; $CaCl_2$, 1.8; $MgCl_2$, 2 and HEPES, 5 (pH 7.4). Voltage and current electrodes were filled with 3 M KCl. Resistances of both electrodes were kept between 0.5–1.5 MΩ. During recordings, the oocytes were voltage-clamped at a holding potential of −70 mV and superfused continuously with ND96 buffer via gravity-fed tubes at 0.1–0.2 mL/minute, with 5 minute incubation times for the bath-applied peptides. Acetylcholine (ACh) was applied via gravity-fed tubes until peak current amplitude was obtained (1–3 sec.), with 1–2 minute washout periods between applications. Data were sampled at 500 Hz and filtered at 200 Hz. Peak current amplitude was measured before and following incubation of the peptide. Our collaborator Dr. Jan Tytgat (KU Leuven) performed the electrophysiology experiment.

5.3 Results and Discussion

After we got confirmation through our HwTx-I experiments that our novel TFMSA cleavage protocol could be used to synthesize bioactive peptides we adapted the methodology to synthesize cyclic Tx2005. NCL has been instrumental in the *N*- to *C*-terminal cyclization of χ-Conotoxin MrIa, and α-Conotoxin Vc1.1, some of the first cyclic conotoxins reported [19, 32]. Cyclization of conotoxins thus far has improved their stability as demonstrated with α-Conotoxin MII [118]. In terms of conotoxin drug design, cyclization may help to improve oral bioavailability as it can confer resistance to proteolytic degradation [33]. We used the TFMSA cleavage protocol to produce a linear Tx2005 fragment with a free cysteine at the *C*-terminus and a free thioester at the *N*-terminus (Figure 34).

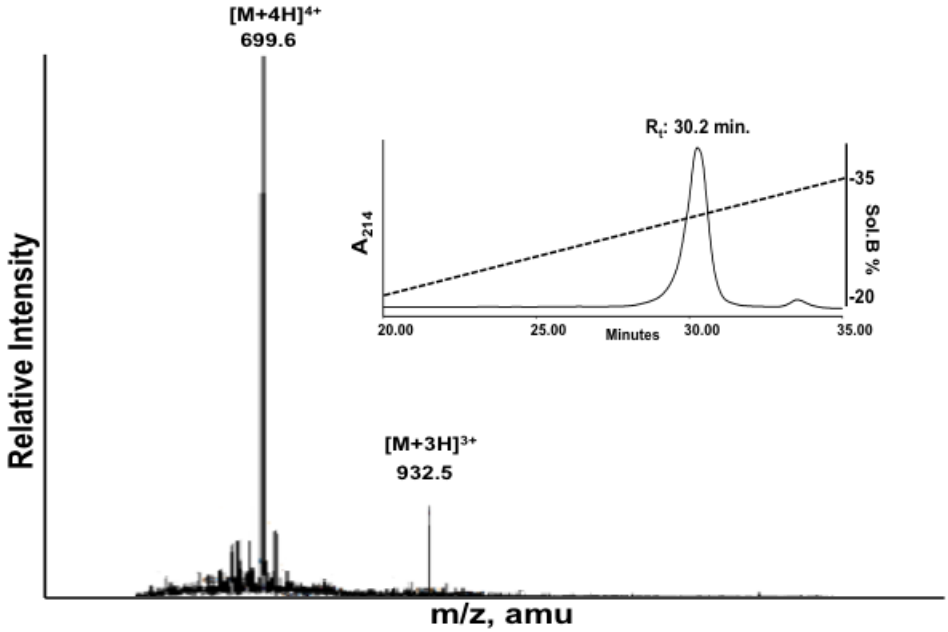

Figure 34: RP-HPLC chromatogram and ESI-MS of linear Tx2005+Linker [RPQC(Acm)CSHPAC(Acm)NVDHPEICGAGAGAG], the starting material for cyclization. Cleaving the MPAL resin with novel optimized TFMSA cleavage protocol produced the linear peptide. The ESI-MS shows a dominant *m/z of* $[M+4H]^{4+}$ of 699.6 and a minor $[M+3H]^{3+}$ of 932.5. The theoretical calculated mass of Tx2005+Linker is $[M+4H]^{4+}$ of 699.0 and $[M+3H]^{3+}$ of 932.6. Tx2005+Linker eluted at 30.2 minutes when run on a 1 mm C_{18} Phenomenex® narrow bore column using a 1 % $minute^{-1}$ gradient of 90:10 Acetonitrile (MeCN): 0.08 % v/v *aq.* TFA.

The two functionalities (*N*-terminus thioester and *C*-terminus free thiol) underwent intramolecular ligation to create a reduced cyclic molecule (Figure 35).

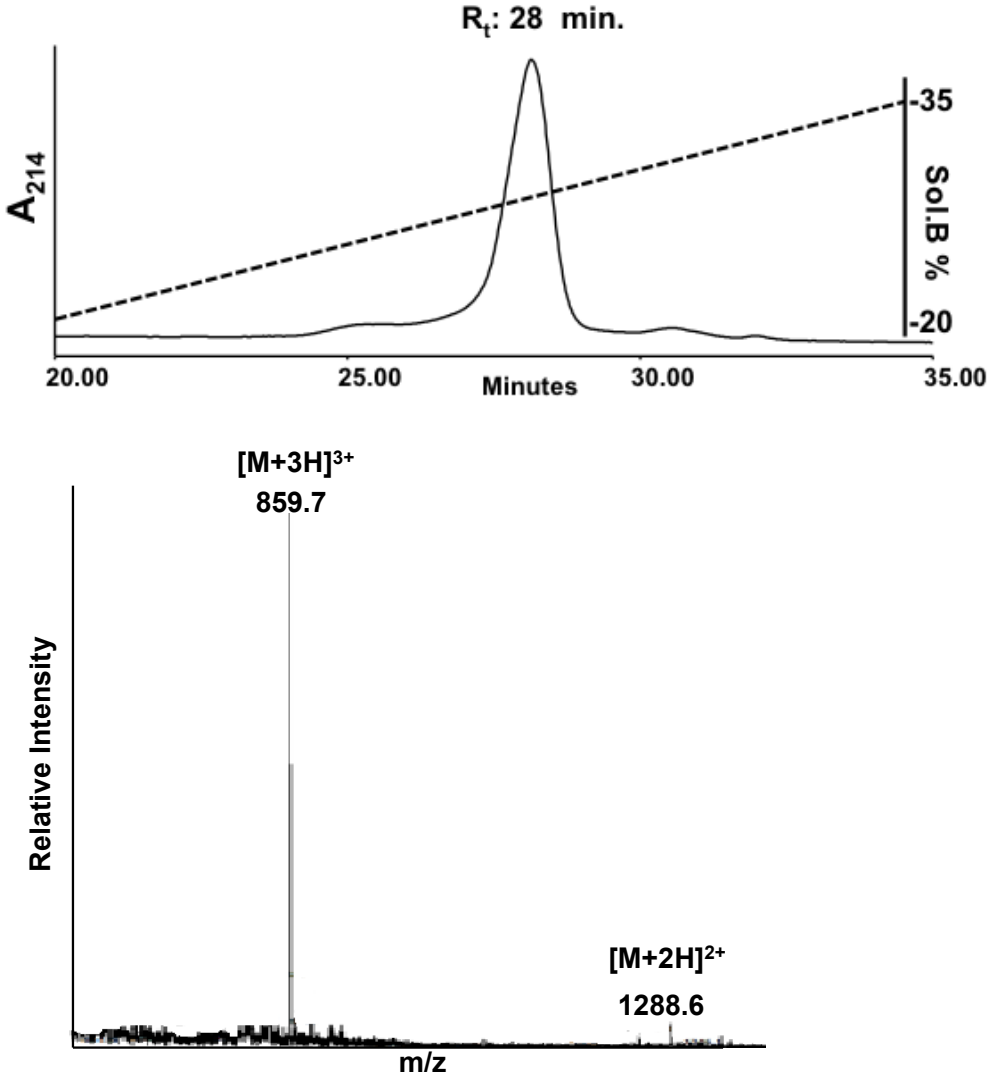

Figure 35: RP-HPLC chromatogram (top) and ESI-MS (bottom) of cyclized reduced Tx2005+Linker. Ligating the linear peptide (Figure 34) in an intramolecular NCL reaction produced the cyclic peptide. The ESI-MS shows a dominant *m/z of* $[M+3H]^{3+}$ of 859.7 and a minor $[M+2H]^{2+}$ of 1288.6. The theoretical calculated mass of cyclized reduced Tx2005+Linker is $[M+3H]^{3+}$ of 859.6 and $[M+2H]^{2+}$ of 1290.0. Cyclic reduced Tx2005+Linker eluted at 28 minutes when run on a 1 mm C_{18} Phenomenex® narrow bore column using a 1 % $minute^{-1}$ gradient of 90:10 Acetonitrile (MeCN): 0.08 % v/v *aq.* TFA. The cyclic reduced material has a one fewer charge state than the linear material (Figure 34) because the ionizable amino group at the *N*-terminus is in a covalent bond with the *C*-terminus, therefore the amino group at the *N*-terminus cannot be protonated.

The reduced peptide was oxidized using a 2-step sequential oxidation strategy to produce a cyclic peptide with disulfide bonds in the right conformation (Figure 36).

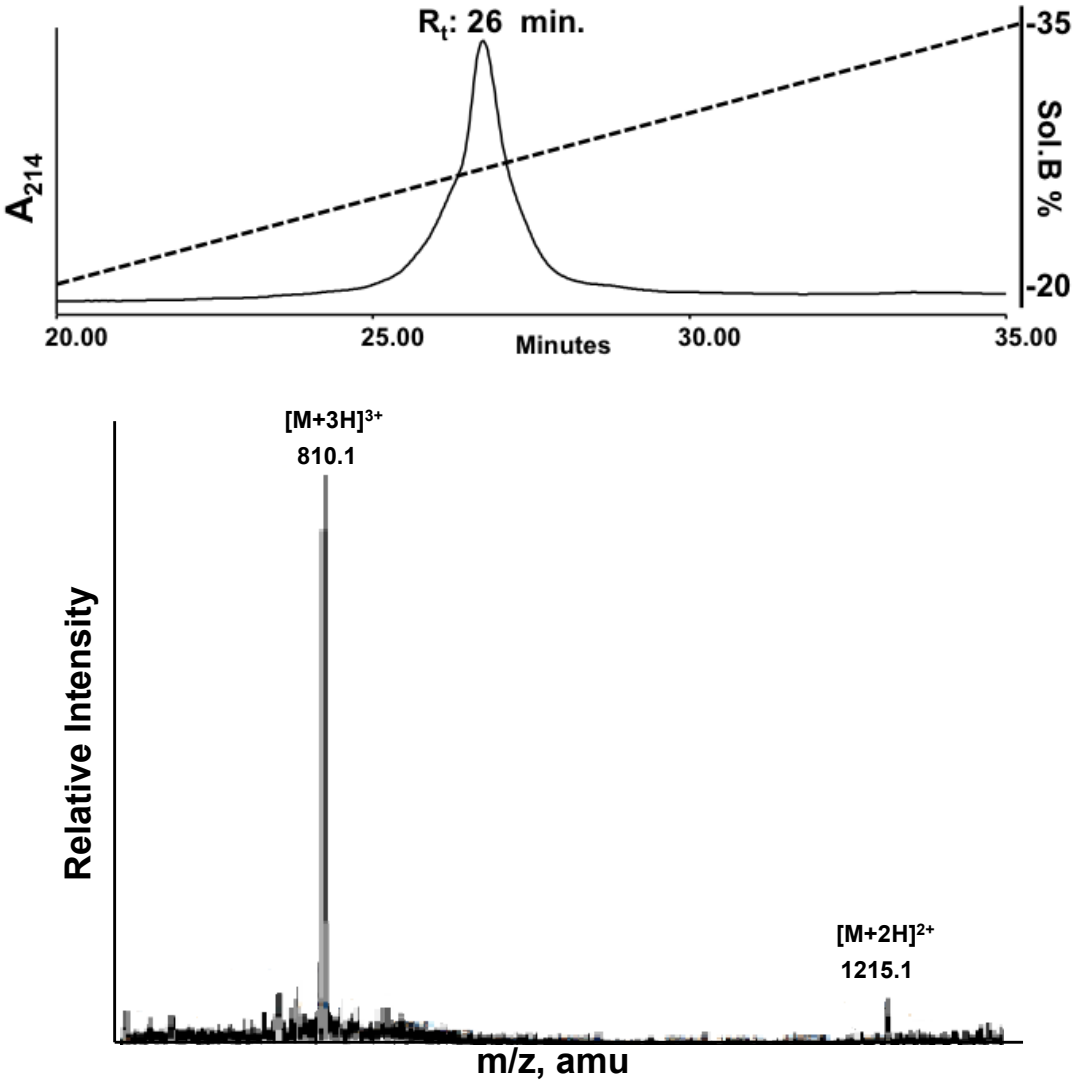

Figure 36: RP-HPLC chromatogram (top) and ESI-MS (bottom) of oxidized Cyclic Tx2005+Linker. The cyclic peptide was produced by oxidizing the reduced peptide (Figure 35) in a 2-step oxidation procedure involving a solution of 0.1M NH_4HCO_3 at pH 8 and rapid iodine oxidation. The ESI-MS shows a dominant *m/z of* $[M+3H]^{3+}$ of 810.1 and a minor $[M+2H]^{2+}$ of 1215.1. The theoretical calculated mass of cyclized reduced Tx2005+Linker is $[M+3H]^{3+}$ of 810.3 and $[M+2H]^{2+}$ of 1215.0. Cyclic oxidized Tx2005+Linker eluted at 26 minutes when run on a 1 mm C_{18} Phenomenex® narrow bore column using a 1 % minute^{-1} gradient of 90:10 Acetonitrile (MeCN): 0.08 % v/v *aq.* TFA. The cyclic oxidized material has a one fewer charge state than the linear material (Figure 56) because the ionizable amino group at the *N*-terminus is in a covalent bond with the *C*-terminus, therefore the amino group at the *N*-terminus cannot be protonated.

In addition, we also produced a cyclic peptide using the 2-Chlorotrityl resin (Figure 37).

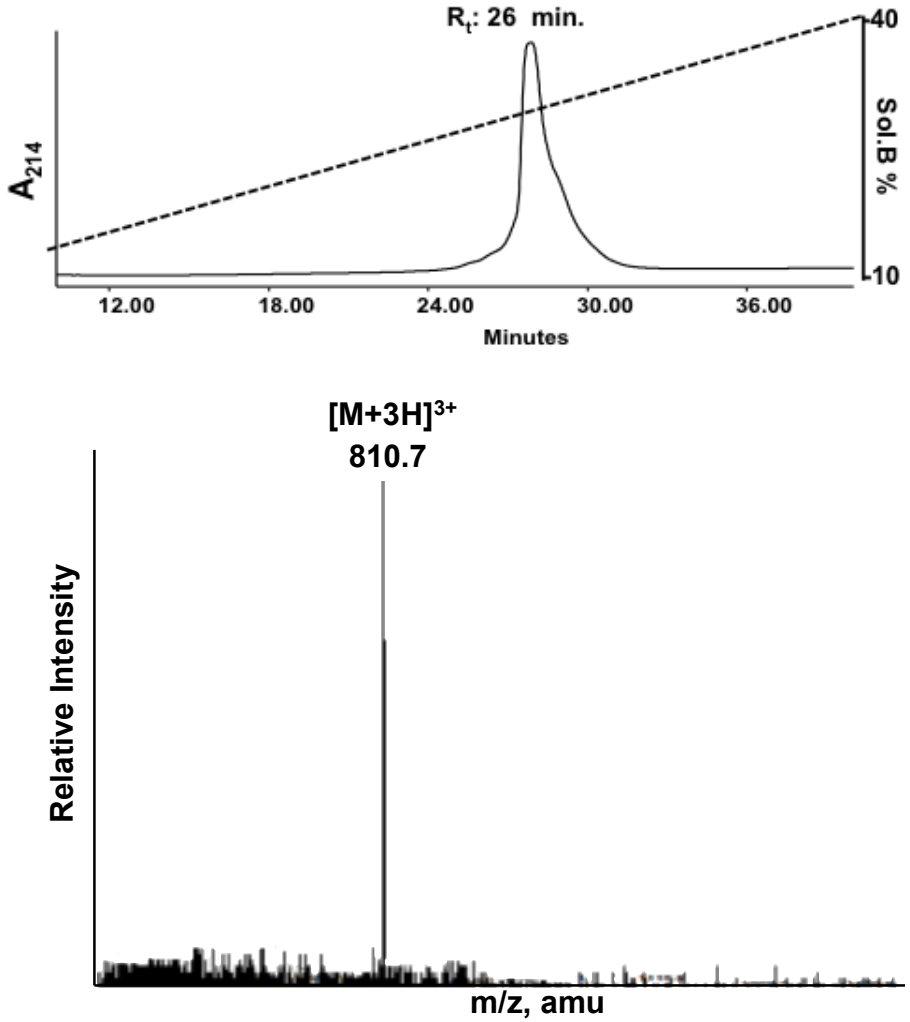

Figure 37: RP-HPLC chromatogram (top) and ESI-MS (bottom) of oxidized Cyclic Tx2005+Linker [RPQCCSHPACNVDHPEICGAGAGAG] synthesized using a 2-Chlorotrityl resin. The oxidized material was obtained by cyclizing the linear product in a reaction that is analogous to amino acid coupling. After cyclization the material was subjected to a 2 step directed oxidation procedure. The ESI-MS shows a dominant *m/z of* $[M+3H]^{3+}$ of 810.7. The theoretical calculated mass of oxidized Cyclic Tx2005+Linker is $[M+3H]^{3+}$ of 810.3. Oxidized Cyclic Tx2005+Linker eluted at 26 minutes when run on a 1 mm C_{18} Phenomenex® narrow bore column using a 1 % minute^{-1} gradient of 90:10 Acetonitrile (MeCN): 0.08 % v/v *aq.* TFA. The cyclic oxidized material has a one fewer charge state than the linear material (Figure 34) because the ionizable amino group at the *N*-terminus is in a covalent bond with the *C*-terminus, therefore the amino group at the *N*-terminus cannot be protonated.

The 2-Chlorotrityl resin allowed us to synthesize a cyclic peptide using Fmoc synthesis, which further expands the available protection strategies that are available for cyclization. Since a 2-Chlorotrityl resin can be cleaved under mild acidic conditions, we produced an orthogonally protected fragment with both a free amino and a free carboxy end. The free fragments were used in an intramolecular amino acid coupling reaction to produce a cyclic peptide (Figure 37). This approach allows flexibility with regards to linker size and provides us the ability to incorporate a lysine azide into the linker sequence. Lysine azide functionality can be used in a Staudinger ligation reaction to result in the production of a cyclic fluorescent probe that can be used to study ligand gated ion channels.

Once the cyclic peptides were synthesized our next goal was to determine the bioactivity and stability of the cyclic peptides. In recent years there has been a paradigm shift in the pharmaceutical industry that has led to an increased effort in finding peptide/protein therapeutics. At the heart of this effort is the desire to synthesize stable peptide drugs that can be administered orally.

Table 11: The pharmacological activity of synthetic α-Conotoxin TxIC and synthetic cyclic Tx2005. The synthetic α-Conotoxin Tx2005, which has no PTMs was not able to elicit a paralytic response in snails but was able to inhibit human nAChR subtypes. Cyclic Tx2005 with 7αα linker was not able to inhibit the α3β2 nAChR as effectively as linear α-Conotoxin TxIC.

Peptide	nAChR subtype [a]	M.I. %
Cyclic Tx2005	α3β2	33
	α3α5β2	N/A
	α3β4, α4β4, α7, α2β2, αβγε	N/A
α-Conotoxin Tx2005	α3β2	96
	α3α5β2	91
	α3β4	77
	α4β4, α7, α2β2, αβγε	<10

[a] Human variants; M.I. = Maximum Inhibition; NA= the assay on nAChR subtype is pending.

As seen in Table 11, our initial results have indicated that Cyclic Tx2005 was able to retain biological activity. Cyclic Tx2005 had a maximal inhibition of 33 % at the α3β2 nAChR subtype. When the linear Tx2005 was tested on the same receptor subtype it was more effective at inhibiting the receptor and had a maximum inhibition of 96% (Table 11). The reduced activity of the cyclic peptide might be due to inappropriate linker length. We approximated our linker length based on modeling software and literature review. The more accurate way of determining linker length is through structures generated from NMR and X-Crystallography. Modeling software is a good alternative when NMR and X-Crystallography is not available but when these technologies are available the data generated from them should take precedence. Ongoing experiments undertaken by lab mates aim to optimize the linker length and produce a cyclic peptide that has activity comparable to linear peptide. We were also able to conduct preliminary stability assays on Cyclic Tx2005 and the results so far are very promising.

Cyclic Tx2005, the Cyclic Tx2005 fluorophore, Linear Tx2005, and Linear Tx2005 containing a linker were subjected to a time course stability assay using Pancreatin, Trypsin and Carboxypeptidase (Figure 38, Figure 39, Figure 40 and Figure 41).

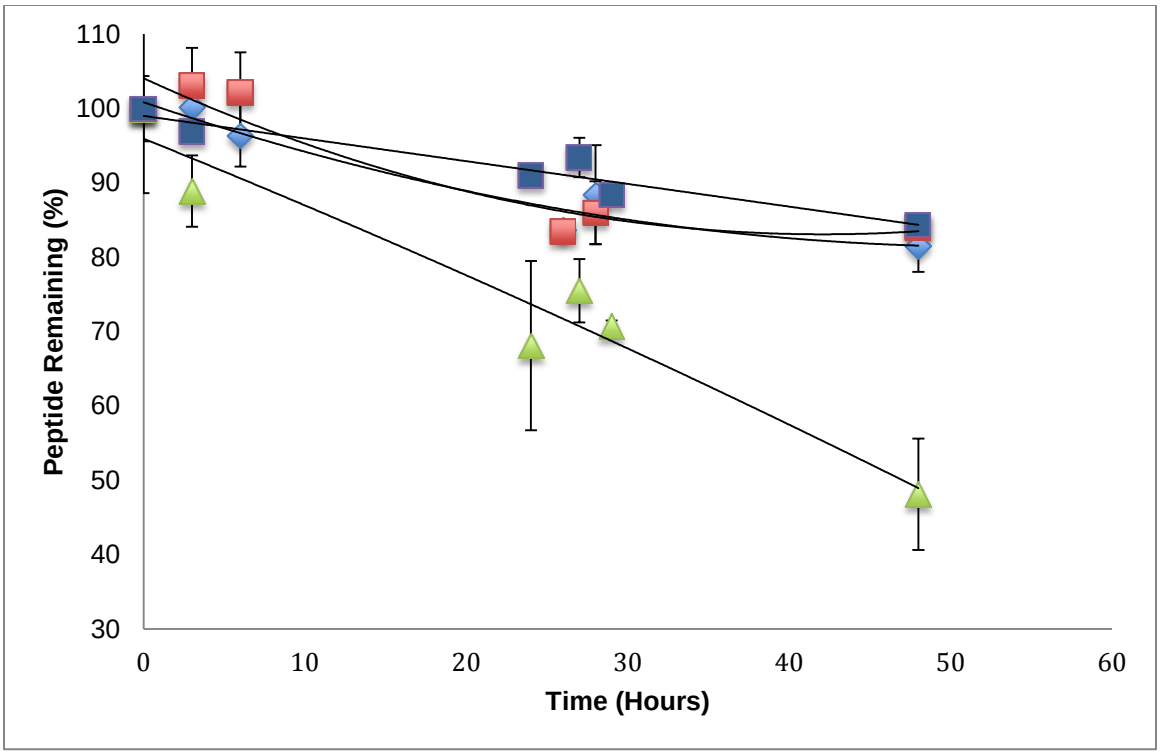

Figure 38: Stability profile of Tx2005 (Blue Diamond), Cyclic Tx2005 (Red Square), Cyclic Tx2005 with fluorophore (Blue Square) and Linear Tx2005 with linker (Green Triangle), when a time course experiment using pancreatin was conducted. The linear Tx2005 shows similar stability to the cyclic peptides but linear peptide with linker is not as stable as the other 3 peptides (n=3).

As seen in Figure 38 all the peptides were relatively stable in pancreatin. After 48 hours the percent of peptide remaining for Cyclic Tx2005, the Cyclic Tx2005 fluorophore, Linear Tx2005 and Linear Tx2005 containing a linker were (81 %, 84 %, 84 % and 48 %) respectively. This can be attributed to pancreatin being a mixture of amylase, lipase and protease. It is hypothesized that more degradation did not occur in this mixture because the other enzymes, might have hindered the protease activity, which may have resulted in unexpected peptide stability. Of the 4 peptides the linear peptide with linker appeared to be the least stable. The relative instability of the linear linker peptide might be due to the 3D structure distortion caused by the addition of extra amino acids to the native peptide sequence.

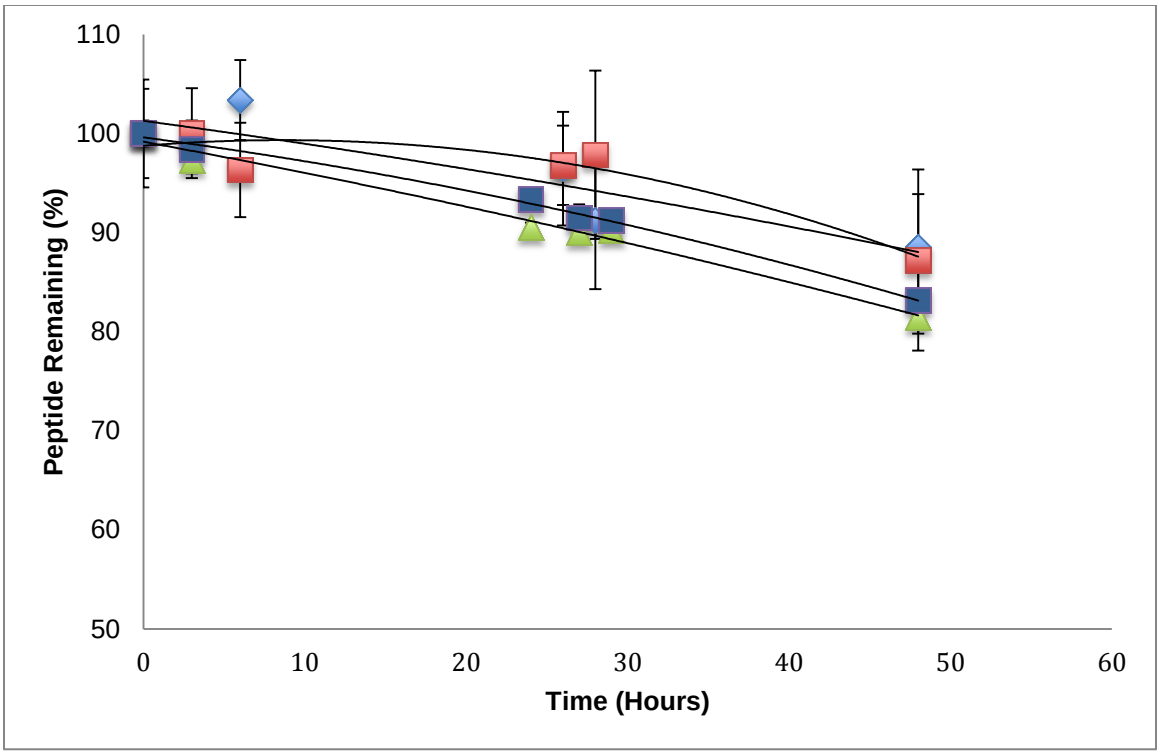

Figure 39: Stability profile of Tx2005 (Blue Diamond), Cyclic Tx2005 (Red Square), Cyclic Tx2005 with fluorophore (Blue Square) and Linear Tx2005 with linker (Green Triangle), when a time course experiment using trypsin was conducted. All 4 peptides show similar stability in trypsin digestion assay (n=3).

As demonstrated in Figure 39 all the 4 peptides had similar stability in trypsin. After 48 hours the percent of peptide remaining for Cyclic Tx2005, Cyclic Tx2005 with fluorophore, Linear Tx2005 and Linear Tx2005 with linker were (87 %, 83 %, 88 % and 81 %) respectively. The stability of the peptides towards trypsin is most likely due to the presence of proline on the *C*-terminus side of arginine, which limits the activity of trypsin.

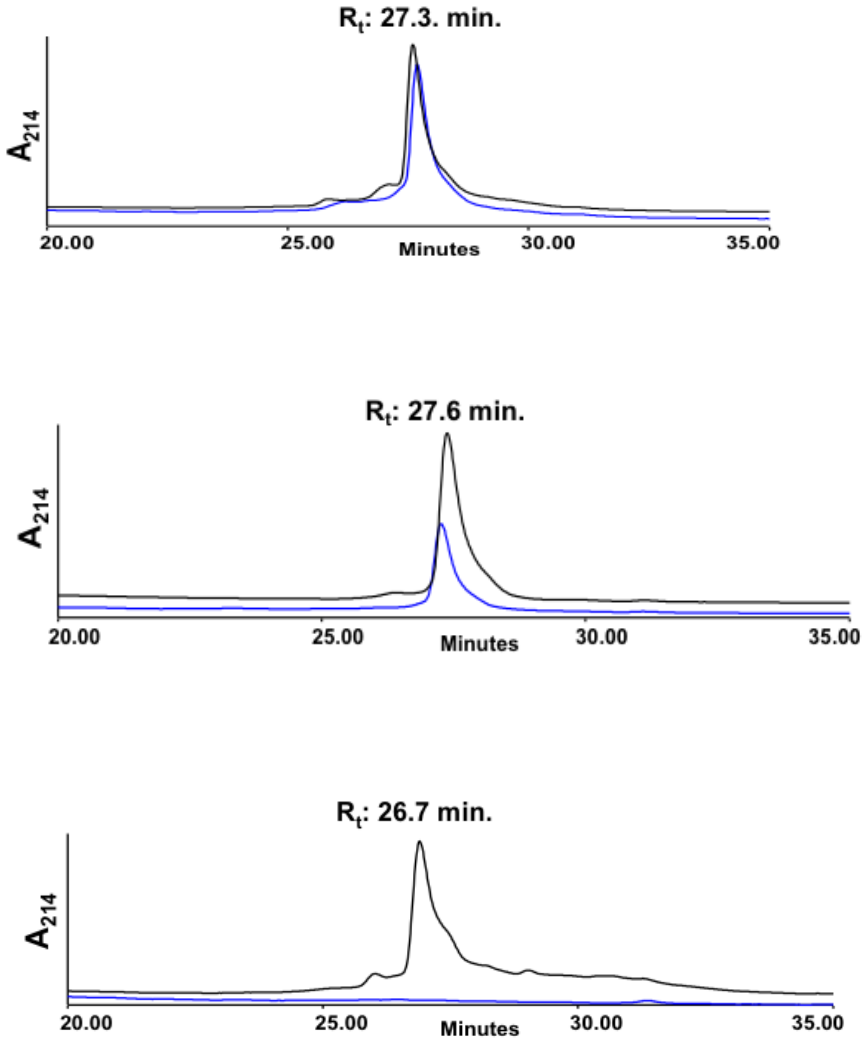

Figure 40: RP-HPLC chromatogram of Cyclic Tx2005 (top), Linear Tx2005 (middle) and Linear Tx2005 with linker (bottom) at 0 and 48 hours of carboxypeptidase treatment. Black line is at 0 hours and blue line is at 48 hours. Cyclic Tx2005 showed the least amount of degradation at 48 hours whereas Linear Tx2005 with linker showed the maximum amount of degradation at 48 hours. All samples were run on a 1 mm C_{18} Phenomenex® narrow bore column using a 1 % minute^{-1} gradient of 90:10 Acetonitrile (MeCN): 0.08 % v/v *aq.* TFA.

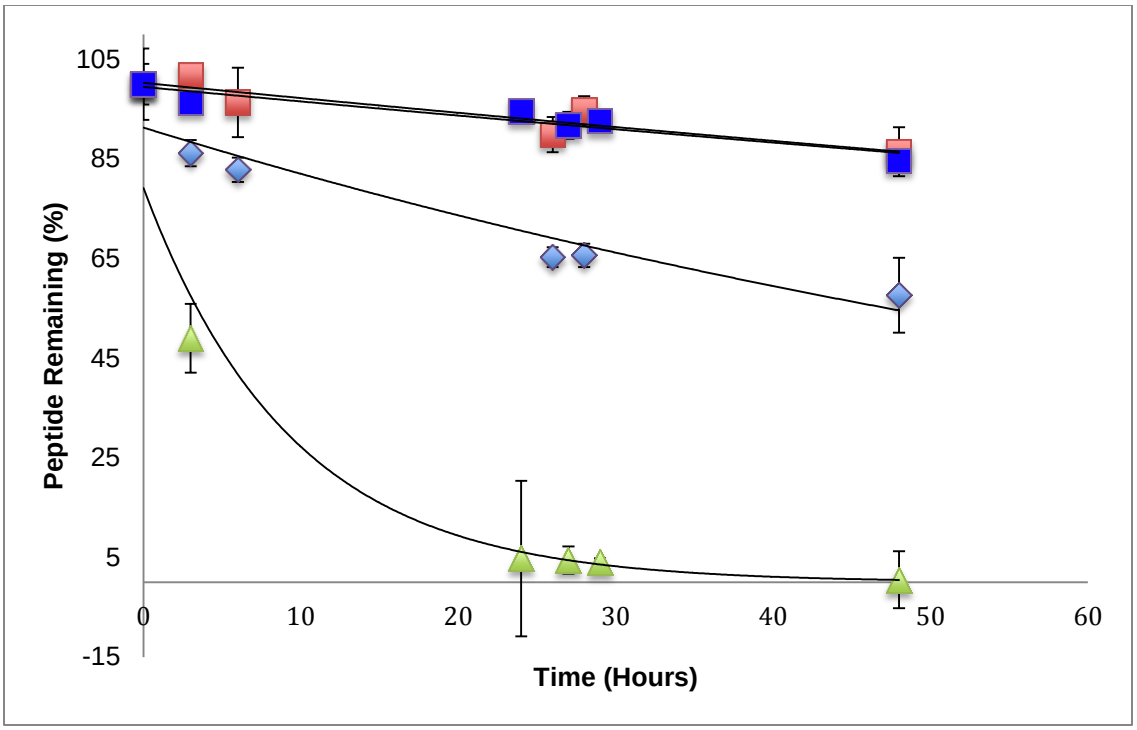

Figure 41: Stability profile of Tx2005 (Blue Diamond), Cyclic Tx2005 (Red Square), Cyclic Tx2005 with fluorophore (Blue Square) and Linear Tx 2005 with linker (Green Triangle), when a time course experiment using carboxypeptidase was conducted. Both the cyclic peptides are stable under carboxypeptidase but the linear peptide with linker is highly unstable in carboxypeptidase. Linear Tx2005 is more stable than the linear peptide with linker but it is less stable than both the cyclic peptides (n=3).

The data from the carboxypeptidase stability assay clearly demonstrated that the cyclic peptides were more resistant towards exopeptidase degradation than linear peptides (Figure 40 and Figure 41). As demonstrated in Figure 41 after 48 hours the percent of peptide remaining for Cyclic Tx2005, Cyclic Tx2005 with fluorophore, Linear Tx2005, and Linear Tx2005 with linker were (86 %, 84 %, 56 % and 0.4 %) respectively. Since the cyclic peptides have their carboxy terminus in a stable covalent bond with the amino terminus the cyclic peptides are resistant to carboxypeptidase degradation. The linear peptides have 2 free termini therefore the carboxy terminus is easily available to degradation from carboxypeptidase. The added instability of linear Tx2005 with linker might be due to the addition of extra amino acids, which aids in the interaction between the substrate and the enzyme through non-covalent interactions. Additionally, the presence of extra amino acids might distort the native structure, hence making the peptide more susceptible to enzyme degradation.

Our experimental setup did not account for the physical force generated in the stomach and the GI tract. Additionally, we conducted the stability assays with individual enzyme, which is not a true reflection of physiologic digestion. In the future the lab is planning on conducting a more comprehensive stability assay, which is more reflective of physiologic conditions. Despite the current limitations the results generated from preliminary digestion studies are very promising and gives us confidence in proceeding with the next phase of digestion assay.

5.4 Conclusion

We have successfully synthesized cyclic peptide Tx2005 and our ESI-MS data confirms that the cyclic peptide is of the right mass. Preliminary bioactivity studies showed that the cyclic peptide was able to retain biological activity. Since our cyclic peptide was less active than linear peptide we plan to optimize the linker length to produce a cyclic peptide that has comparable activity to its linear counterpart. Initial stability studies indicated that cyclic peptide was more resistant to carboxypeptidase than linear peptide. The *in vitro* stability studies are a good starting point but in order to get an accurate representation of physiologic conditions *in vivo* studies are essential. Once we have optimized the linker length we plan on conducting stability studies, which is more reflective of physiologic conditions.

Chapter 6: Future Perspective

Peptides as drugs in general are gaining momentum in commercial drug development due to their high success rate reaching approximately 20-25 % [193] and their abundance in nature. In addition to this, cyclic peptides are bridging the gap between the pharmacokinetic properties of SOMs and biologics, all the while maintaining the superior pharmacodynamic properties of biologics as seen with their high potency and target selectivity. Many of these *N*- to *C*-terminal cyclized peptides have displayed promising therapeutic potential (Table 1). Several approaches have been suggested for the forward movement of cyclic peptides in industry whether they be backbone stabilized with synthetic amino acid linker sequences or stapled through the use of other organic compounds [20, 43]. Koehbach *et al.* [194] have adopted a new screening methodology that applies chemical analysis of extracts in conjugation with bioinformatics analysis of transcript databases. Using mass spectrometry and transcriptome mining they were able to identify novel cyclotide containing species. With new cyclotides being discovered and characterized, the likelihood of finding new therapeutic leads from these biomolecules appears to be increasing.

Considerations for the future development of synthetic cyclic peptides might include the advantages and disadvantages of each approach. Peptide stapling, particularly in the use of a hydrocarbon linker sequence as undertaken by Verdine *et al.* [20] offers the advantage of increased lipophilicity through the introduction of strongly hydrophobic character. In contrast is the use of an amino acid based linker sequence amended by thioester ligation as performed by Clark *et al.*, [188] which provides an avenue for introducing conjugation techniques such as the binding of a fluorescent marker [195] or other synthetic or peptide additions, without modifying the native parent sequence.

Despite advanced techniques such as thioester ligation, SPPS, and recombinant production continually growing prominence in the world of peptide chemistry, scaling up production for cyclic peptides as therapeutics will be an increasingly difficult endeavor. When scaling up peptide production using SPPS from a research laboratory to an industrial level of manufacturing it is essential to conduct a cost-benefit analysis to

optimize the process. Issues such as production cost, security and environmental impact of the synthetic procedure start gaining more prominence when SPPS is conducted on the kilogram to ton scale. The kinetics of a synthetic reaction need to be studied and optimized in order to reduce costs associated with reagents and waste treatment. Another challenge associated with industrial scale SPPS is maintaining a good manufacturing practices (GMP) facility that adheres to all FDA requirements. Reproducible yields of intermediates and final products along with reproducible impurity profiles are essential when converting to an industrial scale. SPPS is a complex, multistep, procedure and maintaining this reproducibility is often a difficult endeavor [196, 197].

Scale-up production of native or synthetic non-cyclized peptides is infamously known for providing roadblocks in large-scale development, whereas cyclic peptides introduce new issues of complex chemistry and proteomic characterization techniques. The adjoining of the *N*- and *C*-termini of peptides through synthetic chemistry generally requires a ligation strategy that must be integrated within the synthesis procedure, further complicating the scale up procedure. Here alternative strategies would be advantageous.

The loss of charges on the *N*- and *C*-termini make quality control and characterization efforts complex by reducing the effectiveness of proteomic sequencing techniques such as mass spectrometry and Edman degradation [33]. Furthermore, *de novo* sequencing of native cyclic peptides for discovery purposes also presents major hurdles due to the aforementioned complications. Currently the only known proteomic sequencing methods for cyclic peptides include a two-step enzymatic digestion coupled with mass spectrometry or Edman process. If digestion sites are not present within the native protein, genetic sequencing may be considered the only option for initial characterization

One promising direction of cyclic peptides is the use of known native scaffolds from cyclotides (plant derived cyclic peptides) as platform for the introduction of active epitope regions of peptides as a method for increasing stability [198]. This scaffolding technique provides potential for the generation of new active regions in an already well-known membrane permeating structure; however limitations with cyclic peptides might

arise due to the potential for increased anaphylactic response, as notoriously seen with biologic based therapies [199].

The development of novel therapeutics can be a precarious venture. Leads continue to fail without fulfilling their potential. Within the last decade, biologics have emerged as a promising source of new leads. Though not without flaws, biologics have faced challenges in drug development. Oral bioavailability remains one of the major roadblocks in the development of biologics as therapeutics. Cyclization holds promise in overcoming this limitation. Engineering of biologics to enhance their therapeutic properties provides medicinal chemists with exciting new avenues for drug development.

References

1. **Espiritu, M.J., A.C. Collier, and J.P. Bingham, *A 21st-century approach to age-old problems: the ascension of biologics in clinical therapeutics.* Drug Discov Today, 2014. 19(8): p. 1109-13.**
2. **Bayer, *Bayer.* 2012.**
3. **Donald L. Pavia, G.S.K., Gary M. Lampman, Randall G. Engel, *A Microscale Approach to Organic Laboratory Techniques*. 5 ed. 2007.**
4. **Sneader, W., *The discovery of aspirin: a reappraisal.* BMJ, 2000. 321(7276): p. 1591-4.**
5. **Angell, M., *Excess in the pharmaceutical industry.* CMAJ, 2004. 171(12): p. 1451-3.**
6. **Parashar Thapa, M.J.E., Chino Cabalteja, Jon-Paul Bingham, *The Emergence of Cyclic Peptides: The potential of Bioengineered Peptide Drugs.* International Journal of Peptide Research and Therapeutics, 2014.**
7. **FDA, *FDA.* 2013.**
8. **Sanger, F., *Determination of nucleotide sequences in DNA.* Biosci Rep, 2004. 24(4-5): p. 237-53.**
9. **Edman, P., *Method for determination of amino acid sequence in peptides. .* Acta Chem. Scand., 1950. 4: p. 34.**
10. **Merrifield, B., *Solid phase synthesis.* Science, 1986. 232(4748): p. 341-7.**
11. **Fenn, J.B., et al., *Electrospray ionization for mass spectrometry of large biomolecules.* Science, 1989. 246(4926): p. 64-71.**
12. **Tanaka, K.e.a., *Protein and polymer analyses up to m/z 100000 by laser ionization time of flight mass spectrometry of large biomolecules.* Rapid Communication Mass Spectrometry, 1988. 2: p. 151-153.**
13. **Jackson, D.A., R.H. Symons, and P. Berg, *Biochemical method for inserting new genetic information into DNA of Simian Virus 40: circular SV40 DNA molecules containing lambda phage genes and the galactose operon of Escherichia coli.* Proc Natl Acad Sci U S A, 1972. 69(10): p. 2904-9.**
14. **Winter, G., *Greg Winter.* Nat Biotechnol, 2011. 29(3): p. 190.**
15. **Espiritu, M.J., et al., *Incorporation of post-translational modified amino acids as an approach to increase both chemical and biological diversity of conotoxins and conopeptides.* Amino Acids, 2014. 46(1): p. 125-51.**
16. **Altelaar, A.F., J. Munoz, and A.J. Heck, *Next-generation proteomics: towards an integrative view of proteome dynamics.* Nat Rev Genet, 2013. 14(1): p. 35-48.**
17. ***The human genome. Science genome map.* Science, 2001. 291(5507): p. 1218.**
18. **Goodfellow, P.N., *The impact of genomics on drug discovery.* Novartis Found Symp, 2000. 229: p. 131-2; discussion 132-5.**
19. **Clark, R.J., et al., *The engineering of an orally active conotoxin for the treatment of neuropathic pain.* Angew Chem Int Ed Engl, 2010. 49(37): p. 6545-8.**
20. **Verdine, G.L. and G.J. Hilinski, *Stapled peptides for intracellular drug targets.* Methods Enzymol, 2012. 503: p. 3-33.**

21. **Lin, J.H., *Pharmacokinetics of biotech drugs: peptides, proteins and monoclonal antibodies.* Curr Drug Metab, 2009. 10(7): p. 661-91.**
22. **Haines, D.J., et al., *Mucosal peptide hydrolase and brush-border marker enzyme activities in three regions of the small intestine of rats with experimental uraemia.* Clin Sci, 1990. 79(6): p. 663-8.**
23. **Woodley, J.F., *Enzymatic barriers for GI peptide and protein delivery.* Crit Rev Ther Drug Carrier Syst, 1994. 11(2-3): p. 61-95.**
24. **Reichert, J.M., *Monoclonal Antibodies as Innovative Therapeutics.* Current Pharmaceutical Biotechnology, 2008. 9(6): p. 423-430.**
25. **Van Itallie, C.M. and J.M. Anderson, *The molecular physiology of tight junction pores.* Physiology (Bethesda), 2004. 19: p. 331-8.**
26. **Pade, V. and S. Stavchansky, *Estimation of the relative contribution of the transcellular and paracellular pathway to the transport of passively absorbed drugs in the Caco-2 cell culture model.* Pharmaceutical Research, 1997. 14(9): p. 1210-1215.**
27. **Lax, R. *The future of peptide development in the pharmaceutical industry*. PharManufacturing, 2010. 10-15.**
28. **Bicker, K.L., et al., *D-amino acid based protein arginine deiminase inhibitors: Synthesis, pharmacokinetics, and in cellulo efficacy.* ACS Med Chem Lett, 2012. 3(12): p. 1081-1085.**
29. **Winkler, D.A., *The role of quantitative structure--activity relationships (QSAR) in biomolecular discovery.* Brief Bioinform, 2002. 3(1): p. 73-86.**
30. **Bockus, A.T., C.M. McEwen, and R.S. Lokey, *Form and function in cyclic peptide natural products: a pharmacokinetic perspective.* Curr Top Med Chem, 2013. 13(7): p. 821-36.**
31. **Jennings, C., et al., *Biosynthesis and insecticidal properties of plant cyclotides: the cyclic knotted proteins from Oldenlandia affinis.* Proc Natl Acad Sci U S A, 2001. 98(19): p. 10614-9.**
32. **Daly, N.L., K.R. Gustafson, and D.J. Craik, *The role of the cyclic peptide backbone in the anti-HIV activity of the cyclotide kalata B1.* FEBS Lett, 2004. 574(1-3): p. 69-72.**
33. **Vila-Farres, X., et al., *In vitro activity of several antimicrobial peptides against colistin-susceptible and colistin-resistant Acinetobacter baumannii.* Clin Microbiol Infect, 2012. 18(4): p. 383-7.**
34. **Cascales, L. and D.J. Craik, *Naturally occurring circular proteins: distribution, biosynthesis and evolution.* Org Biomol Chem, 2010. 8(22): p. 5035-47.**
35. **Felizmenio-Quimio, M.E., N.L. Daly, and D.J. Craik, *Circular proteins in plants: solution structure of a novel macrocyclic trypsin inhibitor from Momordica cochinchinensis.* J Biol Chem, 2001. 276(25): p. 22875-82.**
36. **Korsinczky, M.L., R.J. Clark, and D.J. Craik, *Disulfide bond mutagenesis and the structure and function of the head-to-tail macrocyclic trypsin inhibitor SFTI-1.* Biochemistry, 2005. 44(4): p. 1145-53.**
37. **Sawa, N., et al., *Identification and characterization of lactocyclicin Q, a novel cyclic bacteriocin produced by Lactococcus sp. strain QU 12.* Appl Environ Microbiol, 2009. 75(6): p. 1552-8.**

38. Hallen, H.E., et al., *Gene family encoding the major toxins of lethal Amanita mushrooms.* Proc Natl Acad Sci U S A, 2007. 104(48): p. 19097-101.
39. Tang, Y.Q., et al., *A cyclic antimicrobial peptide produced in primate leukocytes by the ligation of two truncated alpha-defensins.* Science, 1999. 286(5439): p. 498-502.
40. Abuja, P.M., et al., *The cyclic antimicrobial peptide RTD-1 induces stabilized lipid-peptide domains more efficiently than its open-chain analogue.* FEBS Lett, 2004. 566(1-3): p. 301-6.
41. Rohde, H. and O. Seitz, *Ligation-desulfurization: a powerful combination in the synthesis of peptides and glycopeptides.* Biopolymers, 2010. 94(4): p. 551-9.
42. Lovelace, E.S., et al., *Cyclic MrIA: a stable and potent cyclic conotoxin with a novel topological fold that targets the norepinephrine transporter.* J Med Chem, 2006. 49(22): p. 6561-8.
43. Clark, R.J. and D.J. Craik, *Engineering cyclic peptide toxins.* Methods Enzymol, 2012. 503: p. 57-74.
44. Cemazar, M. and D.J. Craik, *Microwave-assisted Boc-solid phase peptide synthesis of cyclic cysteine-rich peptides.* J Pept Sci, 2008. 14(6): p. 683-9.
45. Tavassoli, A. and S.J. Benkovic, *Split-intein mediated circular ligation used in the synthesis of cyclic peptide libraries in E. coli.* Nat Protoc, 2007. 2(5): p. 1126-33.
46. Kohli, R.M., C.T. Walsh, and M.D. Burkart, *Biomimetic synthesis and optimization of cyclic peptide antibiotics.* Nature, 2002. 418(6898): p. 658-61.
47. Marsault, E. and M.L. Peterson, *Macrocycles are great cycles: applications, opportunities, and challenges of synthetic macrocycles in drug discovery.* J Med Chem, 2011. 54(7): p. 1961-2004.
48. Parenty, A., X. Moreau, and J.M. Campagne, *Macrolactonizations in the total synthesis of natural products.* Chem Rev, 2006. 106(3): p. 911-39.
49. Kopp, F. and M.A. Marahiel, *Macrocyclization strategies in polyketide and nonribosomal peptide biosynthesis.* Nat Prod Rep, 2007. 24(4): p. 735-49.
50. Adessi, C. and C. Soto, *Converting a peptide into a drug: strategies to improve stability and bioavailability.* Curr Med Chem, 2002. 9(9): p. 963-78.
51. Gilon, C., et al., *Backbone cyclization: A new method for conferring conformational constraint on peptides.* Biopolymers, 1991. 31(6): p. 745-50.
52. McGeary, R.P. and D.P. Fairlie, *Macrocyclic peptidomimetics: potential for drug development.* Curr Opin Drug Discov Devel, 1998. 1(2): p. 208-17.
53. Walsh, C.T., *Polyketide and nonribosomal peptide antibiotics: modularity and versatility.* Science, 2004. 303(5665): p. 1805-10.
54. Trabi, M. and D.J. Craik, *Circular proteins--no end in sight.* Trends Biochem Sci, 2002. 27(3): p. 132-8.
55. Kaas, Q. and D.J. Craik, *Analysis and classification of circular proteins in CyBase.* Biopolymers, 2010. 94(5): p. 584-91.
56. Hammami, R., et al., *BACTIBASE second release: a database and tool platform for bacteriocin characterization.* BMC Microbiol, 2010. 10: p. 22.
57. Shelburne, C.E., et al., *The spectrum of antimicrobial activity of the bacteriocin subtilosin A.* J Antimicrob Chemother, 2007. 59(2): p. 297-300.

58. **Drider, D., et al., *The continuing story of class IIa bacteriocins.* Microbiol Mol Biol Rev, 2006. 70(2): p. 564-82.**
59. **Gonzalez, C., et al., *Bacteriocin AS-48, a microbial cyclic polypeptide structurally and functionally related to mammalian NK-lysin.* Proc Natl Acad Sci U S A, 2000. 97(21): p. 11221-6.**
60. **Martinez-Bueno, M., et al., *Analysis of the gene cluster involved in production and immunity of the peptide antibiotic AS-48 in Enterococcus faecalis.* Mol Microbiol, 1998. 27(2): p. 347-58.**
61. **Cohen, D.J., et al., *Cyclosporine: a new immunosuppressive agent for organ transplantation.* Ann Intern Med, 1984. 101(5): p. 667-82.**
62. **White, S.H., W.C. Wimley, and M.E. Selsted, *Structure, function, and membrane integration of defensins.* Curr Opin Struct Biol, 1995. 5(4): p. 521-7.**
63. **Tran, D., et al., *Microbicidal properties and cytocidal selectivity of rhesus macaque theta defensins.* Antimicrob Agents Chemother, 2008. 52(3): p. 944-53.**
64. **Cole, A.M., et al., *Retrocyclin: a primate peptide that protects cells from infection by T- and M-tropic strains of HIV-1.* Proc Natl Acad Sci U S A, 2002. 99(4): p. 1813-8.**
65. **Nguyen, T.X., A.M. Cole, and R.I. Lehrer, *Evolution of primate theta-defensins: a serpentine path to a sweet tooth.* Peptides, 2003. 24(11): p. 1647-54.**
66. **Craik, D.J., et al., *Plant cyclotides: A unique family of cyclic and knotted proteins that defines the cyclic cystine knot structural motif.* J Mol Biol, 1999. 294(5): p. 1327-36.**
67. **Craik, D.J. and U. Malik, *Cyclotide biosynthesis.* Curr Opin Chem Biol, 2013. 17(4): p. 546-54.**
68. **Daly, N.L., K.J. Rosengren, and D.J. Craik, *Discovery, structure and biological activities of cyclotides.* Adv Drug Deliv Rev, 2009. 61(11): p. 918-30.**
69. **Gruber, C.W., et al., *Insecticidal plant cyclotides and related cystine knot toxins.* Toxicon, 2007. 49(4): p. 561-75.**
70. **Craik, D.J., *Circling the enemy: cyclic proteins in plant defence.* Trends Plant Sci, 2009. 14(6): p. 328-35.**
71. **Bingham, J.P., et al., *Optimizing the connectivity in disulfide-rich peptides: alpha-conotoxin SII as a case study.* Anal Biochem, 2005. 338(1): p. 48-61.**
72. **Kaas, Q., et al., *ConoServer: updated content, knowledge, and discovery tools in the conopeptide database.* Nucleic Acids Res, 2012. 40(Database issue): p. D325-30.**
73. **Wu, X.C., et al., *Novel conopeptides in a form of disulfide-crosslinked dimer.* Peptides, 2010. 31(6): p. 1001-6.**
74. **Bingham, J.P., et al., *Drugs from slugs. Part II--conopeptide bioengineering.* Chem Biol Interact, 2012. 200(2-3): p. 92-113.**
75. **Olivera, B.M., et al., *Conotoxins.* J Biol Chem, 1991. 266(33): p. 22067-70.**
76. **Luo, S., et al., *Single-residue alteration in alpha-conotoxin PnIA switches its nAChR subtype selectivity.* Biochemistry, 1999. 38(44): p. 14542-8.**
77. **Jin, A.H., et al., *Molecular engineering of conotoxins: the importance of loop size to alpha-conotoxin structure and function.* J Med Chem, 2008. 51(18): p. 5575-84.**

78. Sato, K., et al., *Binding of six chimeric analogs of omega-conotoxin MVIIA and MVIIC to N- and P/Q-type calcium channels.* Biochem Biophys Res Commun, 2000. 269(1): p. 254-6.
79. Drakopoulou, E., et al., *Synthesis and antibody recognition of mucin 1 (MUC1)-alpha-conotoxin chimera.* J Pept Sci, 2000. 6(4): p. 175-85.
80. Mezo, G., et al., *Synthesis and immunological studies of alpha-conotoxin chimera containing an immunodominant epitope from the 268-284 region of HSV gD protein.* J Pept Res, 2000. 55(1): p. 7-17.
81. Galanis, A.S., F. Albericio, and M. Grotli, *Enhanced microwave-assisted method for on-bead disulfide bond formation: synthesis of alpha-conotoxin MII.* Biopolymers, 2009. 92(1): p. 23-34.
82. Jin, A.H., et al., *Structure of alpha-conotoxin BuIA: influences of disulfide connectivity on structural dynamics.* BMC Struct Biol, 2007. 7: p. 28.
83. Hargittai, B. and G. Barany, *Controlled syntheses of natural and disulfide-mispaired regioisomers of alpha-conotoxin SI.* J Pept Res, 1999. 54(6): p. 468-79.
84. MacRaild, C.A., et al., *Structure and activity of (2,8)-dicarba-(3,12)-cystino alpha-ImI, an alpha-conotoxin containing a nonreducible cystine analogue.* J Med Chem, 2009. 52(3): p. 755-62.
85. de Araujo, A.D., et al., *Total synthesis of the analgesic conotoxin MrVIB through selenocysteine-assisted folding.* Angew Chem Int Ed Engl, 2011. 50(29): p. 6527-9.
86. Thapa, P., et al., *Conotoxins and their regulatory considerations.* Regul Toxicol Pharmacol, 2014. 70(1): p. 197-202.
87. Cohen, M.W., O.T. Jones, and K.J. Angelides, *Distribution of Ca2+ channels on frog motor nerve terminals revealed by fluorescent omega-conotoxin.* J Neurosci, 1991. 11(4): p. 1032-9.
88. Durand, J., et al., *Confocal imaging of N-methyl-D-aspartate receptors in living cortical neurons.* Neuroscience, 2000. 97(1): p. 11-23.
89. Saxon, E. and C.R. Bertozzi, *Cell surface engineering by a modified Staudinger reaction.* Science, 2000. 287(5460): p. 2007-10.
90. Lee, S., et al., *Analgesic effect of highly reversible omega-conotoxin FVIA on N type Ca2+ channels.* Mol Pain, 2010. 6: p. 97.
91. Olivera, B.M., et al., *Neuronal calcium channel antagonists. Discrimination between calcium channel subtypes using omega-conotoxin from Conus magus venom.* Biochemistry, 1987. 26(8): p. 2086-90.
92. Safo, P., et al., *Distinction among neuronal subtypes of voltage-activated sodium channels by mu-conotoxin PIIIA.* J Neurosci, 2000. 20(1): p. 76-80.
93. Terlau, H., et al., *mu O-conotoxin MrVIA inhibits mammalian sodium channels, but not through site I.* Journal of Neurophysiology, 1996. 76(3): p. 1423-1429.
94. FDA, *PRIALT(ziconotide intrathecal infusion).* 2006.
95. Essack, M., V.B. Bajic, and J.A. Archer, *Conotoxins that confer therapeutic possibilities.* Mar Drugs, 2012. 10(6): p. 1244-65.
96. Ellison, M., et al., *Alpha-RgIA, a novel conotoxin that blocks the alpha9alpha10 nAChR: structure and identification of key receptor-binding residues.* J Mol Biol, 2008. 377(4): p. 1216-27.

97. **Ellison, M., et al., *Alpha-RgIA: a novel conotoxin that specifically and potently blocks the alpha9alpha10 nAChR.* Biochemistry, 2006. 45(5): p. 1511-7.**
98. **J, K., *From hypertension to angina to Viagara.* Modern Drug Discovery, 1998: p. 31-38.**
99. **Boolell, M., et al., *Sildenafil: an orally active type 5 cyclic GMP-specific phosphodiesterase inhibitor for the treatment of penile erectile dysfunction.* Int J Impot Res, 1996. 8(2): p. 47-52.**
100. **Terrett N.K., D.A.S., Brown D., Ellis P., *Sildenafil (VIAGRATM), a potent and selective inhibitor of type 5 cGMP phosphodiesterase with utility for the treatment of male erectile dysfunction.* Bioorganic and Medicinal Chemistry Letters, 1996. 6(15): p. 1819-1824.**
101. **Muttenthaler, M., K.B. Akondi, and P.F. Alewood, *Structure-activity studies on alpha-conotoxins.* Curr Pharm Des, 2011. 17(38): p. 4226-41.**
102. **Armishaw, C.J. and P.F. Alewood, *Conotoxins as research tools and drug leads.* Curr Protein Pept Sci, 2005. 6(3): p. 221-40.**
103. **Terlau, H. and B.M. Olivera, *Conus venoms: a rich source of novel ion channel-targeted peptides.* Physiol Rev, 2004. 84(1): p. 41-68.**
104. **Terlau, H., et al., *Strategy for rapid immobilization of prey by a fish-hunting marine snail.* Nature, 1996. 381(6578): p. 148-51.**
105. **Olivera, B.M., *Conus peptides: biodiversity-based discovery and exogenomics.* J Biol Chem, 2006. 281(42): p. 31173-7.**
106. **Bingham, J.P., E. Mitsunaga, and Z.L. Bergeron, *Drugs from slugs--past, present and future perspectives of omega-conotoxin research.* Chem Biol Interact, 2010. 183(1): p. 1-18.**
107. **Fainzilber, M., et al., *Mollusc-specific toxins from the venom of Conus textile neovicarius.* Eur J Biochem, 1991. 202(2): p. 589-95.**
108. **Lopez-Vera, E., et al., *Role of hydroxyprolines in the in vitro oxidative folding and biological activity of conotoxins.* Biochemistry, 2008. 47(6): p. 1741-51.**
109. **Ellison, M., et al., *Alpha-conotoxins ImI and ImII target distinct regions of the human alpha7 nicotinic acetylcholine receptor and distinguish human nicotinic receptor subtypes.* Biochemistry, 2004. 43(51): p. 16019-26.**
110. **Bergeron, Z.L., et al., *A 'conovenomic' analysis of the milked venom from the mollusk-hunting cone snail Conus textile--the pharmacological importance of post-translational modifications.* Peptides, 2013. 49: p. 145-58.**
111. **Bruce, C., et al., *Recombinant conotoxin, TxVIA, produced in yeast has insecticidal activity.* Toxicon, 2011. 58(1): p. 93-100.**
112. **Terlau, H., et al., *Strategy for rapid immobilization of prey by a fish-hunting marine snail.* Nature, 1996. 381(6578): p. 148-151.**
113. **Kapono, C.A., et al., *Conotoxin truncation as a post-translational modification to increase the pharmacological diversity within the milked venom of Conus magus.* Toxicon, 2013. 70: p. 170-8.**
114. **Martinez, J.S., et al., *alpha-Conotoxin EI, a new nicotinic acetylcholine receptor antagonist with novel selectivity.* Biochemistry, 1995. 34(44): p. 14519-26.**
115. **EC, J., *Conantokins, from "sleeper" activity to drug development.* Phil. Sci. Lett., 2009. 2: p. 60-66.**

116. **Loughnan, M.L., et al., *Chemical and functional identification and characterization of novel sulfated alpha-conotoxins from the cone snail Conus anemone.* J Med Chem, 2004. 47(5): p. 1234-41.**
117. **McIntosh, J.M., et al., *Gamma-carboxyglutamate in a neuroactive toxin.* J Biol Chem, 1984. 259(23): p. 14343-6.**
118. **Clark, R.J., et al., *Engineering stable peptide toxins by means of backbone cyclization: stabilization of the alpha-conotoxin MII.* Proc Natl Acad Sci U S A, 2005. 102(39): p. 13767-72.**
119. **Dutton, J.L., et al., *A new level of conotoxin diversity, a non-native disulfide bond connectivity in alpha-conotoxin AuIB reduces structural definition but increases biological activity.* J Biol Chem, 2002. 277(50): p. 48849-57.**
120. **Grishin, A.A., et al., *Alpha-conotoxin AuIB isomers exhibit distinct inhibitory mechanisms and differential sensitivity to stoichiometry of alpha3beta4 nicotinic acetylcholine receptors.* J Biol Chem, 2010. 285(29): p. 22254-63.**
121. **Khoo, K.K., et al., *Distinct disulfide isomers of mu-conotoxins KIIIA and KIIIB block voltage-gated sodium channels.* Biochemistry, 2012. 51(49): p. 9826-35.**
122. **Craik, D.J. and D.J. Adams, *Chemical modification of conotoxins to improve stability and activity.* ACS Chem Biol, 2007. 2(7): p. 457-68.**
123. **Hopkins, C., et al., *A new family of Conus peptides targeted to the nicotinic acetylcholine receptor.* J Biol Chem, 1995. 270(38): p. 22361-7.**
124. **Sarin, V.K., et al., *Quantitative monitoring of solid-phase peptide synthesis by the ninhydrin reaction.* Anal Biochem, 1981. 117(1): p. 147-57.**
125. **Meier, J. and R.D. Theakston, *Approximate LD50 determinations of snake venoms using eight to ten experimental animals.* Toxicon, 1986. 24(4): p. 395-401.**
126. **Liman, E.R., J. Tytgat, and P. Hess, *Subunit stoichiometry of a mammalian K+ channel determined by construction of multimeric cDNAs.* Neuron, 1992. 9(5): p. 861-71.**
127. **Stanic, M., *[A simplification of the estimation of the 50 percent endpoints according to the Reed and Muench method].* Pathol Microbiol (Basel), 1963. 26: p. 298-302.**
128. **Asher, O., et al., *Functional characterization of mongoose nicotinic acetylcholine receptor alpha-subunit: resistance to alpha-bungarotoxin and high sensitivity to acetylcholine.* FEBS Lett, 1998. 431(3): p. 411-4.**
129. **Olivera, B.M., *E.E. Just Lecture, 1996. Conus venom peptides, receptor and ion channel targets, and drug design: 50 million years of neuropharmacology.* Mol Biol Cell, 1997. 8(11): p. 2101-9.**
130. **Dineley, K.T., A.A. Pandya, and J.L. Yakel, *Nicotinic ACh receptors as therapeutic targets in CNS disorders.* Trends Pharmacol Sci, 2015. 36(2): p. 96-108.**
131. **Xie, A., et al., *Shared mechanisms of neurodegeneration in Alzheimer's disease and Parkinson's disease.* Biomed Res Int, 2014. 2014: p. 648740.**
132. **Sliwinska-Mosson, M., I. Zielen, and H. Milnerowicz, *New trends in the treatment of nicotine addiction.* Acta Pol Pharm, 2014. 71(4): p. 525-30.**
133. **Ghasemi, M. and A. Hadipour-Niktarash, *Pathologic role of neuronal nicotinic acetylcholine receptors in epileptic disorders: implication for pharmacological interventions.* Rev Neurosci, 2015. 26(2): p. 199-223.**

134. **Picciotto, M.R., et al., *Mood and anxiety regulation by nicotinic acetylcholine receptors: A potential pathway to modulate aggression and related behavioral states.* Neuropharmacology, 2015.**
135. **Fenwick, A., *The global burden of neglected tropical diseases.* Public Health, 2012. 126(3): p. 233-6.**
136. **Lozano, R., et al., *Global and regional mortality from 235 causes of death for 20 age groups in 1990 and 2010: a systematic analysis for the Global Burden of Disease Study 2010.* Lancet, 2012. 380(9859): p. 2095-128.**
137. **Organization, W.H., *Schistosomasis A major public health problem.* 2014.**
138. **Huang, Y.X. and L. Manderson, *The social and economic context and determinants of schistosomiasis japonica.* Acta Trop, 2005. 96(2-3): p. 223-31.**
139. **Now, H.N. *Ratlung worm disease spreads fear acroos the Hawaiian island*. 2015; Available from: http://www.hawaiinewsnow.com/story/28805733/rat-lungworm-disease-spreads-fear-across-hawaii-island.**
140. **Howe, K., *A severe case of rat lungworm disease in Hawa'i.* Hawaii J Med Public Health, 2013. 72(6 Suppl 2): p. 46-8.**
141. **Dawson, P.E. and S.B. Kent, *Synthesis of native proteins by chemical ligation.* Annu Rev Biochem, 2000. 69: p. 923-60.**
142. **Kent, S., *Origin of the chemical ligation concept for the total synthesis of enzymes (proteins).* Biopolymers, 2010. 94(4): p. iv-ix.**
143. **Kent, S.B., *Chemical synthesis of peptides and proteins.* Annu Rev Biochem, 1988. 57: p. 957-89.**
144. **Durek, T., V.Y. Torbeev, and S.B. Kent, *Convergent chemical synthesis and high-resolution x-ray structure of human lysozyme.* Proc Natl Acad Sci U S A, 2007. 104(12): p. 4846-51.**
145. **Goulas, S., D. Gatos, and K. Barlos, *Convergent solid-phase synthesis of hirudin.* J Pept Sci, 2006. 12(2): p. 116-23.**
146. **Dawson, P.E., et al., *Synthesis of proteins by native chemical ligation.* Science, 1994. 266(5186): p. 776-9.**
147. **Dawson, P.E., Churchill, M.J., Ghadiri, M.R. and Kent, S.B.H., *Modulation of Reactivity in Native Chemical Ligation through the Use of Thiol Additives. .* J. Am. Chem. Soc., 1997. 119: p. 4325-4329.**
148. **Torbeev, V.Y. and S.B. Kent, *Convergent chemical synthesis and crystal structure of a 203 amino acid "covalent dimer" HIV-1 protease enzyme molecule.* Angew Chem Int Ed Engl, 2007. 46(10): p. 1667-70.**
149. **Bang, D., N. Chopra, and S.B. Kent, *Total chemical synthesis of crambin.* J Am Chem Soc, 2004. 126(5): p. 1377-83.**
150. **Hackeng, T.M., et al., *Total chemical synthesis of enzymatically active human type II secretory phospholipase A2.* Proc Natl Acad Sci U S A, 1997. 94(15): p. 7845-50.**
151. **Johnson, E.C. and S.B. Kent, *Insights into the mechanism and catalysis of the native chemical ligation reaction.* J Am Chem Soc, 2006. 128(20): p. 6640-6.**
152. **Bang, D., B.L. Pentelute, and S.B. Kent, *Kinetically controlled ligation for the convergent chemical synthesis of proteins.* Angew Chem Int Ed Engl, 2006. 45(24): p. 3985-8.**

153. **Hackeng, T.M., J.H. Griffin, and P.E. Dawson, *Protein synthesis by native chemical ligation: expanded scope by using straightforward methodology.* Proc Natl Acad Sci U S A, 1999. 96(18): p. 10068-73.**
154. **Kent, S., et al., *Through the looking glass--a new world of proteins enabled by chemical synthesis.* J Pept Sci, 2012. 18(7): p. 428-36.**
155. **Lewis, R.J., et al., *Drugs from the peptide venoms of marine cone shells.* Australas Biotechnol, 1994. 4(5): p. 298-300.**
156. **Flinn, J.P., et al., *Role of disulfide bridges in the folding, structure and biological activity of omega-conotoxin GVIA.* Biochim Biophys Acta, 1999. 1434(1): p. 177-90.**
157. **Kent, S.B., *Total chemical synthesis of proteins.* Chem Soc Rev, 2009. 38(2): p. 338-51.**
158. **Kent, S., *Novel forms of chemical protein diversity -- in nature and in the laboratory.* Curr Opin Biotechnol, 2004. 15(6): p. 607-14.**
159. **Tulla-Puche, J. and G. Barany, *On-resin native chemical ligation for cyclic peptide synthesis.* J Org Chem, 2004. 69(12): p. 4101-7.**
160. **Mahto, S.K., et al., *A reversible protection strategy to improve Fmoc-SPPS of peptide thioesters by the N-Acylurea approach.* Chembiochem, 2011. 12(16): p. 2488-94.**
161. **Ozcan, M., A. Allahbeickaraghi, and M. Dundar, *Possible hazardous effects of hydrofluoric acid and recommendations for treatment approach: a review.* Clin Oral Investig, 2012. 16(1): p. 15-23.**
162. **Jubilut, G.N., et al., *Evaluation of the trifluoromethanosulfonic acid/trifluoroacetic acid/thioanisole cleavage procedure for application in solid-phase peptide synthesis.* Chem Pharm Bull (Tokyo), 2001. 49(9): p. 1089-92.**
163. **Del Brutto, O.H., *Neurological effects of venomous bites and stings: snakes, spiders, and scorpions.* Handb Clin Neurol, 2013. 114: p. 349-68.**
164. **Wang, Y.R., et al., *Effect of Huwentoxin-I on the Fas and TNF apoptosis pathway in the hippocampus of rat with global cerebral ischemia.* Toxicon, 2007. 50(8): p. 1085-94.**
165. **Liang, S., *An overview of peptide toxins from the venom of the Chinese bird spider Selenocosmia huwena Wang [=Ornithoctonus huwena (Wang)].* Toxicon, 2004. 43(5): p. 575-85.**
166. **Liang, S.P., et al., *The presynaptic activity of huwentoxin-I, a neurotoxin from the venom of the chinese bird spider Selenocosmia huwena.* Toxicon, 2000. 38(9): p. 1237-46.**
167. **Zhang, D. and S. Liang, *Assignment of the three disulfide bridges of huwentoxin-I, a neurotoxin from the spider selenocosmia huwena.* J Protein Chem, 1993. 12(6): p. 735-40.**
168. **Peng, K., X.D. Chen, and S.P. Liang, *The effect of Huwentoxin-I on Ca(2+) channels in differentiated NG108-15 cells, a patch-clamp study.* Toxicon, 2001. 39(4): p. 491-8.**
169. **Xiao, Y., et al., *Tarantula huwentoxin-IV inhibits neuronal sodium channels by binding to receptor site 4 and trapping the domain ii voltage sensor in the closed configuration.* J Biol Chem, 2008. 283(40): p. 27300-13.**

170. **Goldin, A.L., et al., *Nomenclature of voltage-gated sodium channels.* Neuron, 2000. 28(2): p. 365-8.**
171. **Goldin, A.L., *Diversity of mammalian voltage-gated sodium channels.* Ann N Y Acad Sci, 1999. 868: p. 38-50.**
172. **Meng, E., et al., *Functional expression of spider neurotoxic peptide huwentoxin-I in E. coli.* PLoS One, 2011. 6(6): p. e21608.**
173. **Saez, N.J., et al., *Spider-venom peptides as therapeutics.* Toxins (Basel), 2010. 2(12): p. 2851-71.**
174. **Catterall, W.A., et al., *Voltage-gated ion channels and gating modifier toxins.* Toxicon, 2007. 49(2): p. 124-41.**
175. **Chahine, M., et al., *Voltage-gated sodium channels in neurological disorders.* CNS Neurol Disord Drug Targets, 2008. 7(2): p. 144-58.**
176. **Habib, A.M., J.N. Wood, and J.J. Cox, *Sodium channels and pain.* Handb Exp Pharmacol, 2015. 227: p. 39-56.**
177. **Craik, D.J., *Chemistry. Seamless proteins tie up their loose ends.* Science, 2006. 311(5767): p. 1563-4.**
178. **Svangard, E., et al., *Mechanism of action of cytotoxic cyclotides: cycloviolacin O2 disrupts lipid membranes.* J Nat Prod, 2007. 70(4): p. 643-7.**
179. **Craik, D.J., N.L. Daly, and C. Waine, *The cystine knot motif in toxins and implications for drug design.* Toxicon, 2001. 39(1): p. 43-60.**
180. **Mylne, J.S., et al., *Cyclic peptides arising by evolutionary parallelism via asparaginyl-endopeptidase-mediated biosynthesis.* Plant Cell, 2012. 24(7): p. 2765-78.**
181. **Clark, R.J. and D.J. Craik, *Native chemical ligation applied to the synthesis and bioengineering of circular peptides and proteins.* Biopolymers, 2010. 94(4): p. 414-22.**
182. **Tam, J.P., et al., *An unusual structural motif of antimicrobial peptides containing end-to-end macrocycle and cystine-knot disulfides.* Proc Natl Acad Sci U S A, 1999. 96(16): p. 8913-8.**
183. **Gustafson, K.R., T.C. McKee, and H.R. Bokesch, *Anti-HIV cyclotides.* Curr Protein Pept Sci, 2004. 5(5): p. 331-40.**
184. **Clark, R.J., N.L. Daly, and D.J. Craik, *Structural plasticity of the cyclic-cystine-knot framework: implications for biological activity and drug design.* Biochem J, 2006. 394(Pt 1): p. 85-93.**
185. **Gunasekera, S., et al., *Engineering stabilized vascular endothelial growth factor-A antagonists: synthesis, structural characterization, and bioactivity of grafted analogues of cyclotides.* J Med Chem, 2008. 51(24): p. 7697-704.**
186. **Thongyoo, P., et al., *Chemical and biomimetic total syntheses of natural and engineered MCoTI cyclotides.* Org Biomol Chem, 2008. 6(8): p. 1462-70.**
187. **Miljanich, G.P., *Ziconotide: neuronal calcium channel blocker for treating severe chronic pain.* Curr Med Chem, 2004. 11(23): p. 3029-40.**
188. **Clark, R.J., et al., *Cyclization of conotoxins to improve their biopharmaceutical properties.* Toxicon, 2012. 59(4): p. 446-55.**
189. **Haines, D.J., et al., *Mucosal peptide hydrolase and brush-border marker enzyme activities in three regions of the small intestine of rats with experimental uraemia.* Clin Sci (Lond), 1990. 79(6): p. 663-8.**

190. **Deechongkit, S. and J.W. Kelly, *The effect of backbone cyclization on the thermodynamics of beta-sheet unfolding: stability optimization of the PIN WW domain.* J Am Chem Soc, 2002. 124(18): p. 4980-6.**
191. **Hubbard, S.J., *The structural aspects of limited proteolysis of native proteins.* Biochim Biophys Acta, 1998. 1382(2): p. 191-206.**
192. **Quik, M., et al., *Vulnerability of 125I-alpha-conotoxin MII binding sites to nigrostriatal damage in monkey.* J Neurosci, 2001. 21(15): p. 5494-500.**
193. **Saladin, P.M., B.D. Zhang, and J.M. Reichert, *Current trends in the clinical development of peptide therapeutics.* IDrugs, 2009. 12(12): p. 779-84.**
194. **Koehbach, J., et al., *Cyclotide discovery in Gentianales revisited-identification and characterization of cyclic cystine-knot peptides and their phylogenetic distribution in Rubiaceae plants.* Biopolymers, 2013. 100(5): p. 438-52.**
195. **Bingham, J.P., et al., *Synthesis of an iberiotoxin derivative by chemical ligation: a method for improved yields of cysteine-rich scorpion toxin peptides.* Peptides, 2009. 30(6): p. 1049-57.**
196. **Andersson, L., et al., *Large-scale synthesis of peptides.* Biopolymers, 2000. 55(3): p. 227-50.**
197. **Bruckdorfer, T., O. Marder, and F. Albericio, *From production of peptides in milligram amounts for research to multi-tons quantities for drugs of the future.* Curr Pharm Biotechnol, 2004. 5(1): p. 29-43.**
198. **Daly, N.L. and D.J. Craik, *Design and therapeutic applications of cyclotides.* Future Med Chem, 2009. 1(9): p. 1613-22.**
199. **Purcell, R.T. and R.F. Lockey, *Immunologic responses to therapeutic biologic agents.* J Investig Allergol Clin Immunol, 2008. 18(5): p. 335-42.**

Appendix A: Peptide Isomers and Oxidation Conditions

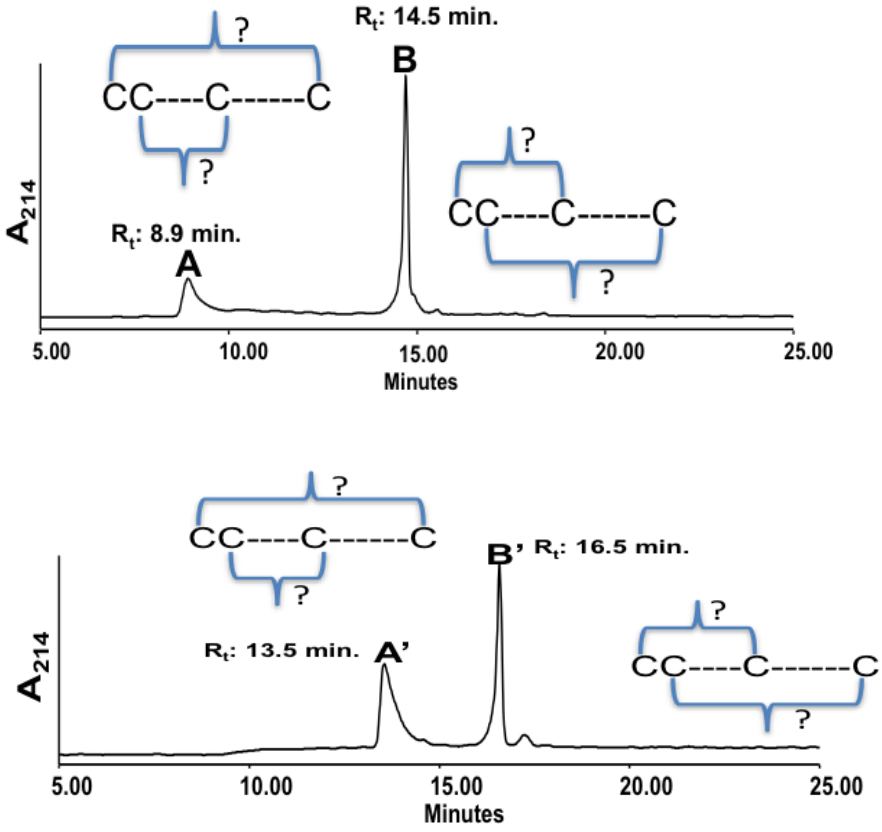

Figure A.1: RP-HPLC chromatogram of α-Conotoxin VIl (top) and α-Conotoxin Vi1.1 (bottom) products after a 5-day oxidation in a solution of 0.1M NH_4HCO_3 at pH 8**.** α-Conotoxin VIl gave 2 products and 1 of the products is more dominant than the other (A=19 % and B=81 %). α-Conotoxin Vi1.1 also gave 2 products but the products were in proportion (A'= 47 % and B'= 48 %). Since the oxidation products were generated from random oxidation we do not know the exact disulfide connectivity of the isomers. Both the oxidation products were run on a 4.6 mm C_{18} Phenomenex® analytical column using a 1 % $minute^{-1}$ gradient of 90:10 Acetonitrile (MeCN): 0.08 % v/v *aq.* TFA. The % area of the peaks were obtained by integrating the peaks using Empower® software. In a separate set of experiment done by a lab mate it was determined that peaks B and B' were native globular isomers and peaks A and A' were non-native ribbon isomer.

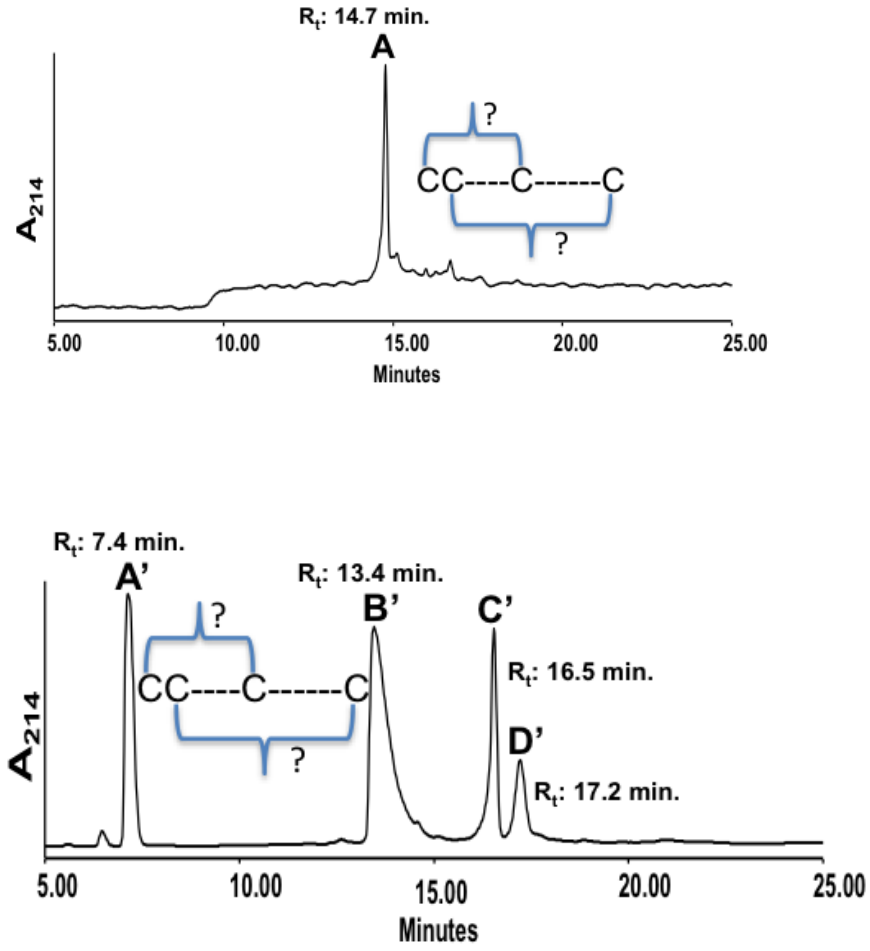

Figure A.2: RP-HPLC chromatogram of α-Conotoxin VIl (top) and α-Conotoxin Vi1.1 (bottom) products after a 5-day oxidation in a solution of 0.33M NH_4OAc/ 0.5M GdnHCl at pH 7. Oxidation of α-Conotoxin VIl gave only 1 major product (A= 95 %). Oxidation of α-Conotoxin Vi1.1 gave 4 major products and 1 of the product was more dominant than the other 3 products (A'= 25 %, B'= 42 %, C'= 16% and D'= 8.5 %). Since the oxidation products were generated from random oxidation we do not know the exact disulfide connectivity of the isomers. Both the oxidation products were run on a 4.6 mm C_{18} Phenomenex® analytical column using a 1 % minute^{-1} gradient of 90:10 Acetonitrile (MeCN): 0.08 % v/v *aq.* TFA. The % area of the peaks were obtained by integrating the peaks using Empower® software.

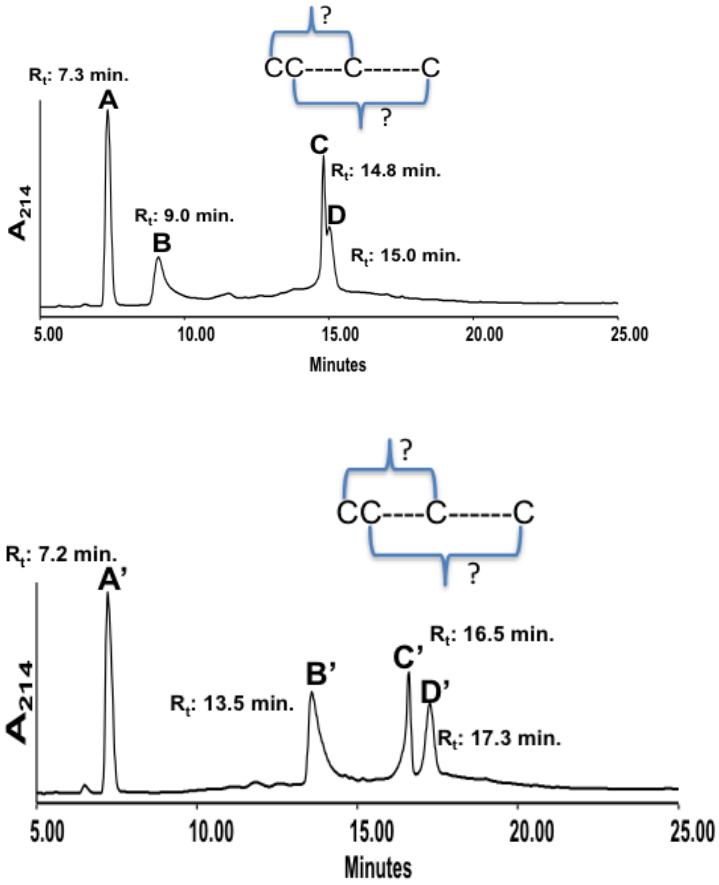

Figure A.3: RP-HPLC chromatogram of α-Conotoxin VIl (top) and α-Conotoxin Vi1.1 (bottom) products after a 5-day oxidation in a solution of 0.33M NH_4OAc/ 0.5M GdnHCl/50 % 2-Propanol at pH 7.5**.** Random oxidation of α-Conotoxin VIl gave 4 products. Of the 4 products 1 of the oxidation product was more dominant than the other 3 products (A= 44 %, B= 17 %, C=21 % and D= 15 %). Oxidation of α-Conotoxin Vi1.1 also gave 4 major products and 1 of the product was more dominant than the other 3 products (A'= 38 %, B'= 21 %, C'=14 % and D'= 17 %). Since the oxidation products were generated from random oxidation we do not know the exact disulfide connectivity of the isomers. Both the oxidation products were run on a 4.6 mm C_{18} Phenomenex® analytical column using a 1 % $minute^{-1}$ gradient of 90:10 Acetonitrile (MeCN): 0.08 % v/v *aq.* TFA. The % area of the peaks were obtained by integrating the peaks using Empower® software.

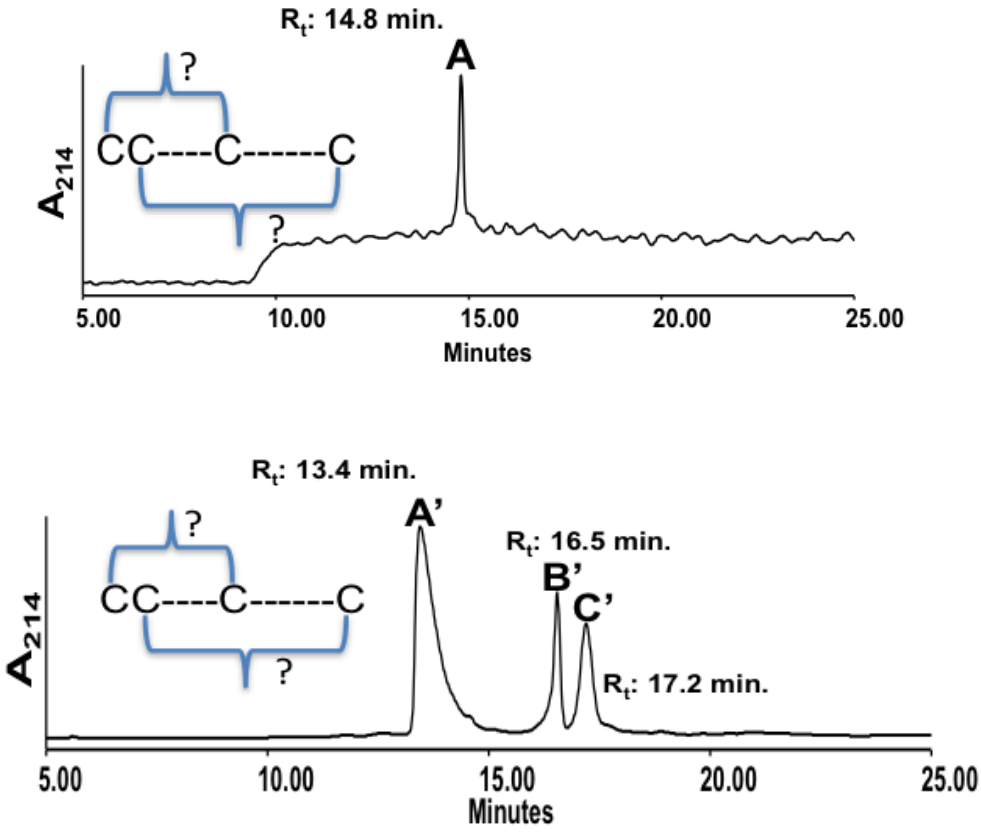

Figure A.4: RP-HPLC chromatogram of α-Conotoxin VIl (top) and α-Conotoxin Vi1.1 (bottom) products after a 5-day oxidation in a solution of 2M urea/0.1 M NaCl/ 0.1M glycine at pH 7.8. Oxidation of α-Conotoxin VIl gave only 1 major product (A= 95 %). Oxidation of α-Conotoxin Vi1.1 gave 3 major products and 1 of the product was more dominant than the other 2 products (A'= 60 %, B'= 15 % and C'=19 %). Since the oxidation products were generated from random oxidation we do not know the exact disulfide connectivity of the isomers. Both the oxidation products were run on a 4.6 mm C_{18} Phenomenex® analytical column using a 1 % minute^{-1} gradient of 90:10 Acetonitrile (MeCN): 0.08 % v/v *aq.* TFA. The % area of the peaks were obtained by integrating the peaks using Empower® software.

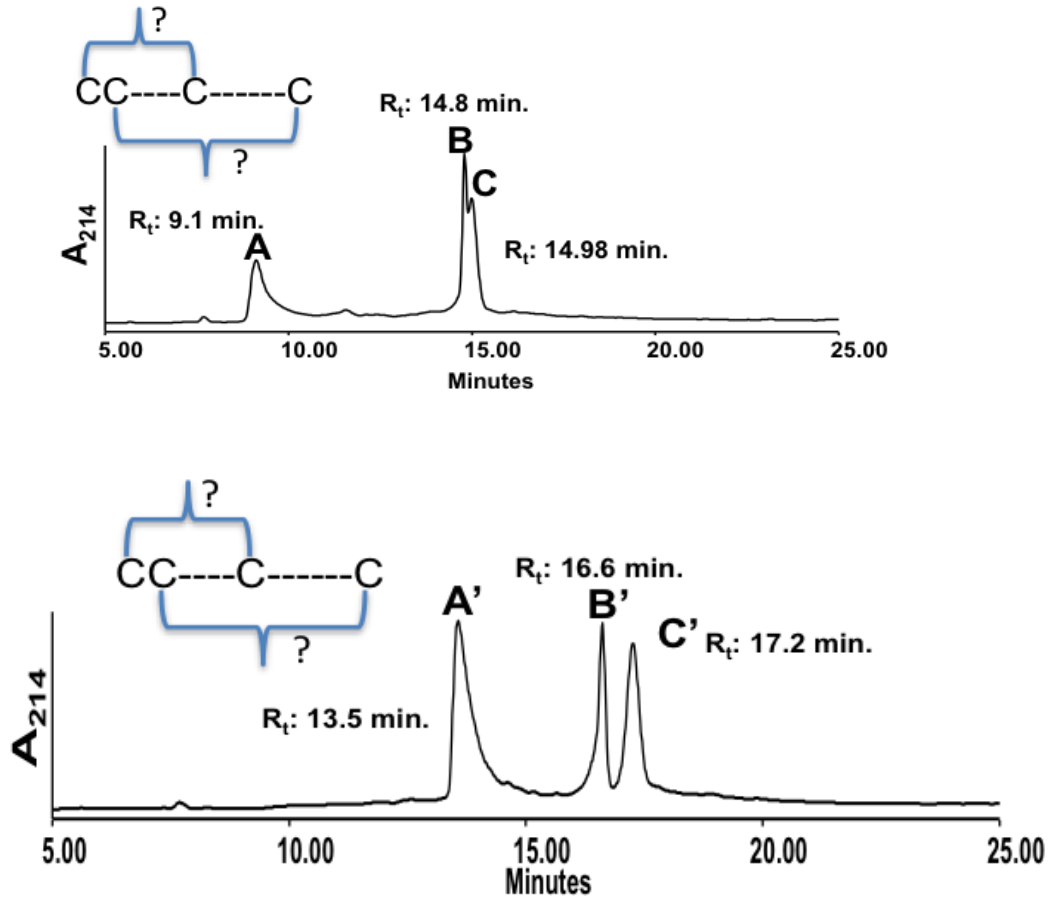

Figure A.5: RP-HPLC chromatogram of α-Conotoxin VIl (top) and α-Conotoxin Vi 1.1 (bottom) products after a 5-day oxidation in a solution of 2M urea/ 0.1M NaCl/ 0.1M glycine/ 50 % 2-Propanol at pH 7.8. Oxidation of α-Conotoxin VIl gave 3 major products and all of the products were in similar proportion (A= 27 %, B= 33 % and C= 38 %). Oxidation of α-Conotoxin Vi1.1 gave 3 major products and 2 of the product were more dominant than the 3rd product (A'= 42 %, B'= 20 % and C'= 36 %). Since the oxidation products were generated from random oxidation we do not know the exact disulfide connectivity of the isomers. Both the oxidation products were run on a 4.6 mm C_{18} Phenomenex® analytical column using a 1 % minute^{-1} gradient of 90:10 Acetonitrile (MeCN): 0.08 % v/v *aq.* TFA. The % area of the peaks were obtained by integrating the peaks using Empower® software.

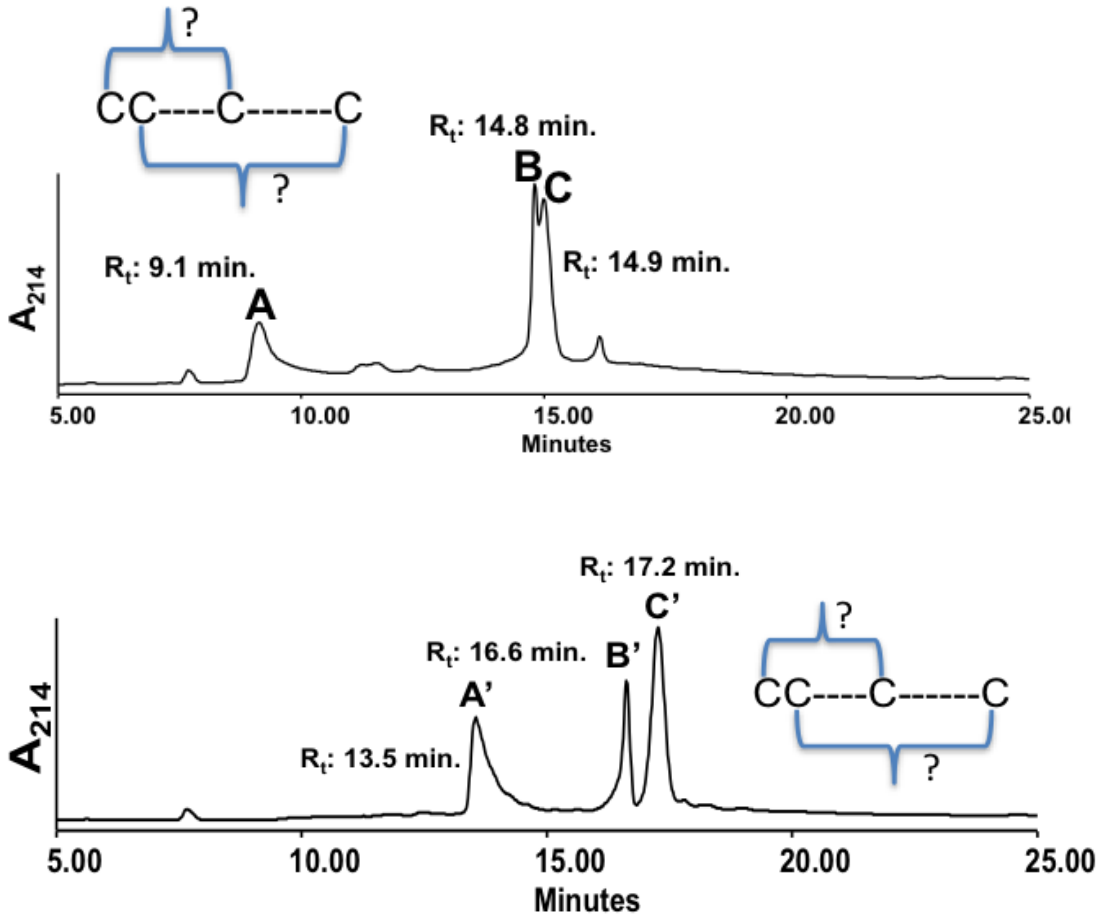

Figure A.6: RP-HPLC chromatogram of α-Conotoxin VIl (top) and α-Conotoxin Vi1.1 (bottom) products after a 5-day oxidation in a solution of 0.1M NH_4HCO_3 /6M urea/ 50 % 2-propanol at pH 7.5. Oxidation of α-Conotoxin VIl gave 3 major products and 1 of the product was more dominant than the other 2 products (A= 20 %, B= 28 % and C= 39 %). Oxidation of α-Conotoxin Vi1.1 gave 3 major products and 1 of the product was more dominant than the other 2 products. The 2 minor oxidation products were proportional to each other (A'= 19 %, B'= 19 % and C'= 60 %). Since the oxidation products were generated from random oxidation we do not know the exact disulfide connectivity of the isomers. Both the oxidation products were run on a 4.6 mm C_{18} Phenomenex® analytical column using a 1 % $minute^{-1}$ gradient of 90:10 Acetonitrile (MeCN): 0.08 % v/v *aq.* TFA. The % area of the peaks were obtained by integrating the peaks using Empower® software.

Appendix B: RP-HPLC of Different Cleavage Conditions

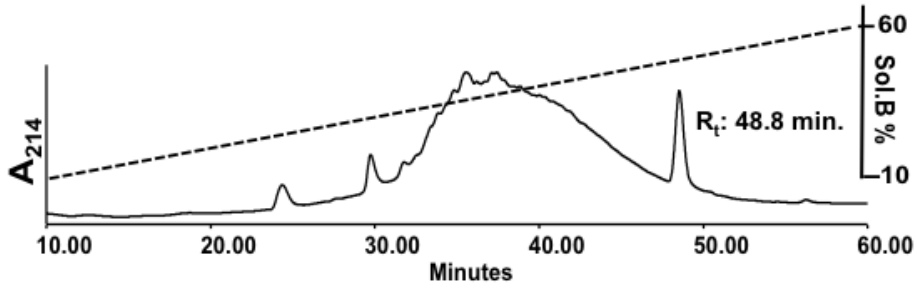

Figure B.1: RP-HPLC cleavage profile produced when the *N*-terminal fragment of Huwentoxin-I (HwTx-I) synthesized on the "home-made" MPAL resin was cleaved with Triisopropylsilane (TIPS) as the scavenging agent. When TIPS was used as the scavenging agent no "peptide-like" peaks were seen and the RP-HPLC profile could not be resolved. The resolved peak at 48.8 minutes was mass checked in ESI-MS and was determined to be an adduct of various scavenging agents. The cleave product was run on a 1 mm C_{18} Phenomenex® narrow bore column using a 1 % $minute^{-1}$ gradient of 90:10 Acetonitrile (MeCN): 0.08 % v/v *aq.* TFA.

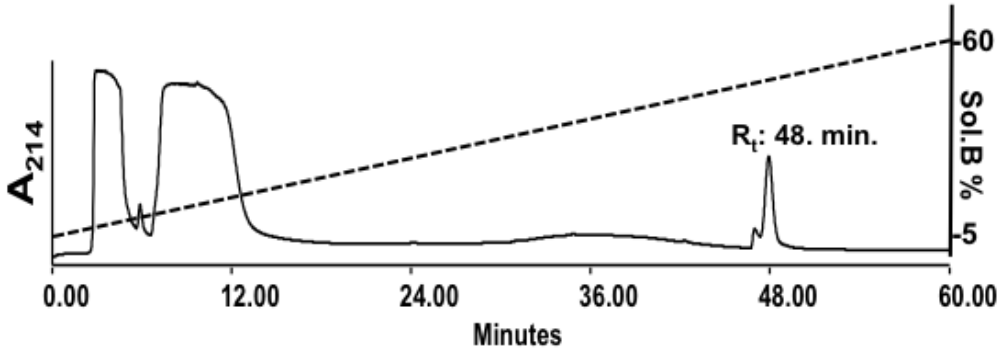

Figure B.2: RP-HPLC profile of a TFA (Reagent K) cleavage conducted on the material obtained from TFMSA cleavage (Figure 2). A second TFA cleavage did not yield any peptide product. The resolved peak at 48.8 minutes was mass checked using ESI-MS and was determined to be an adduct of various scavenging agents. The secondary cleave product was run on a 1 mm C_{18} Phenomenex® narrow bore column using a 1 % $minute^{-1}$ gradient of 90:10 Acetonitrile (MeCN): 0.08% v/v *aq.* TFA.

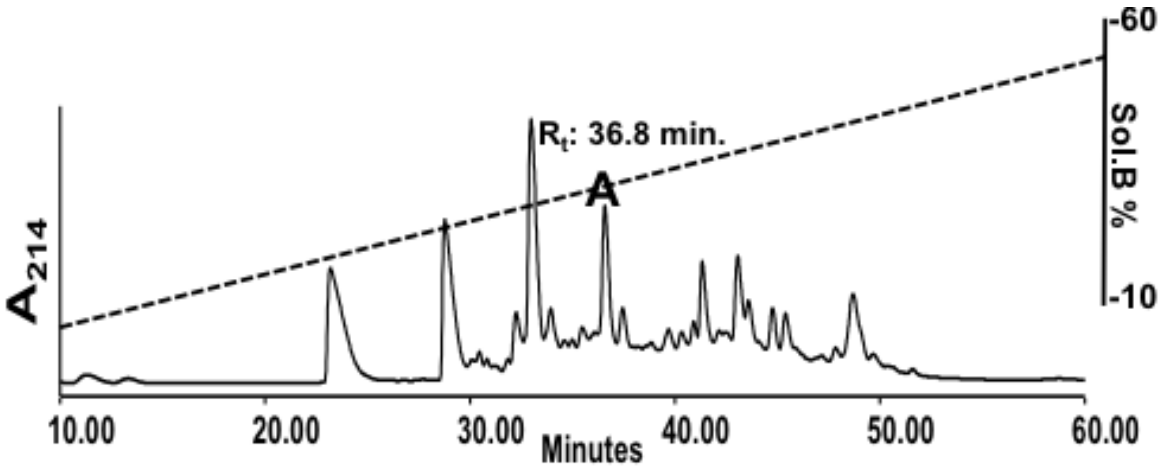

Figure B.3: RP-HPLC cleavage profile when the *N*-terminus of HwTx-I synthesized on the MPAL resin was cleaved with 1,2 Ethanedithiol (EDT) as the scavenging agent instead of TIPS. When TIPS was replaced with EDT as the scavenging agent multiple "peptide-like" peaks were seen along with the target peak "A" at 36.8 minutes. The target peak was mass confirmed using ESI-MS. Since an EDT cleavage produced multiple "peptide-like" peaks the remaining cleavages were done with EDT. Our next goal was to optimize the cleavage conditions so that we could maximize the production of target peak "A". The cleave product was run on a 1 mm C_{18} Phenomenex® narrow bore column using a 1 % minute^{-1} gradient of 90:10 Acetonitrile (MeCN): 0.08 % v/v *aq.*

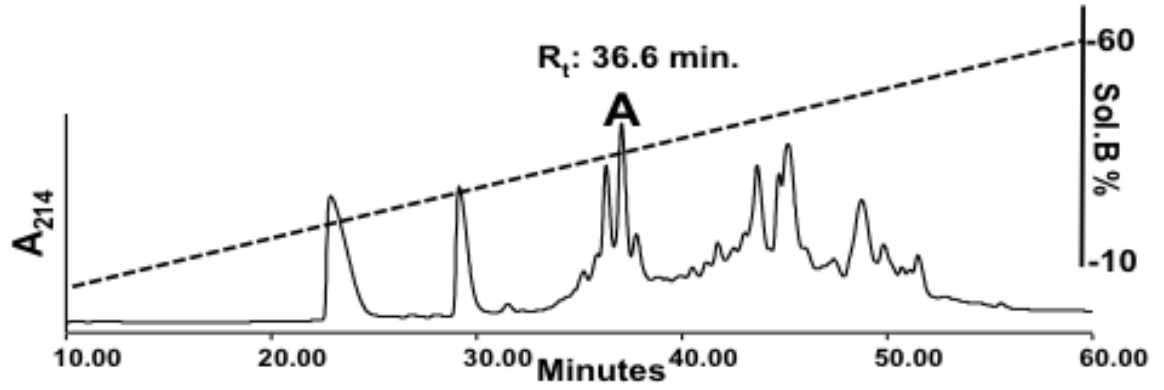

Figure B.4: RP-HPLC cleavage profile when the *N*-terminus fragment of HwTx-I synthesized on a MPAL resin was cleaved under Condition A [Thioanisole 100 µL; 1,2 EDT 50 µL; TFA 1000 µL; TFMSA 50 µL; Ice incubation 30 minutes; Room incubation 120 minutes]. The target peak "A" eluted at 36.6 minutes and the mass was confirmed using ESI-MS. When the peaks were integrated using Empower® software the area for the target peak "A" was determined to be 1.6 %. The cleave product was run on a 1 mm C_{18} Phenomenex® narrow bore column using a 1 % minute^{-1} gradient of 90:10 Acetonitrile (MeCN): 0.08 % v/v *aq.* TFA.

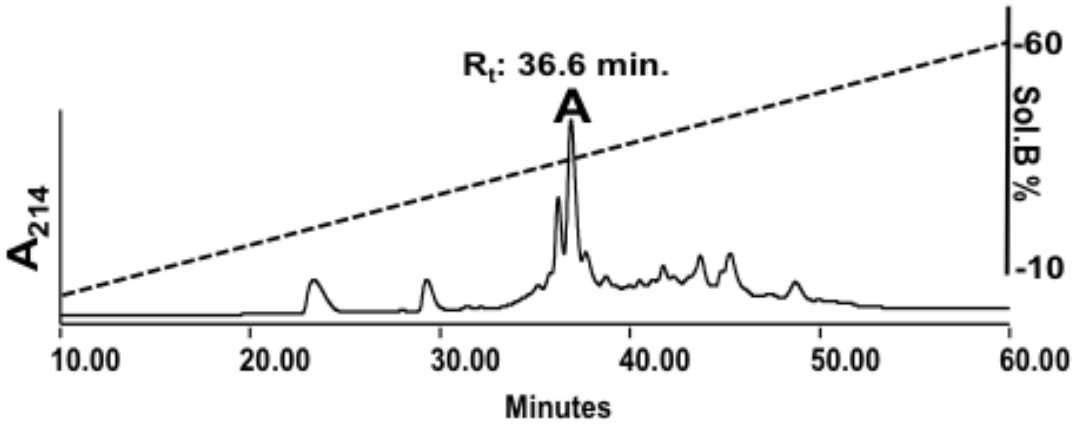

Figure B.5: RP-HPLC cleavage profile when the *N*-terminus fragment of HwTx-I synthesized on a MPAL resin was cleaved under Condition B [Thioanisole 100 µL; 1,2 EDT 50 µL; TFA 1000 µL; TFMSA 100 µL; Ice incubation 30 minutes; Room incubation 120 minutes]. The target peak "A" eluted at 36.6 minutes and the mass was confirmed using ESI-MS. When the peaks were integrated using Empower® software the area for the target peak "A" was determined to be 16.8 %. The cleave product was run on a 1 mm C_{18} Phenomenex® narrow bore column using a 1 % minute^{-1} gradient of 90:10 Acetonitrile (MeCN): 0.08 % v/v *aq.* TFA.

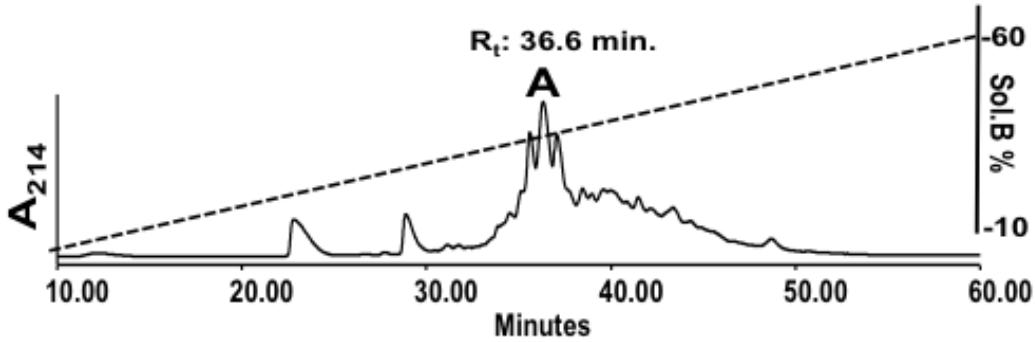

Figure B.6: RP-HPLC cleavage profile when the *N*-terminus fragment of HwTx-I synthesized on a MPAL resin was cleaved under Condition C [Thioanisole 100 µL; 1,2 EDT 50 µL; TFA 1000 µL; TFMSA 150 µL; Ice incubation 30 minutes; Room incubation 120 minutes]. The target peak "A" eluted at 36.6 minutes and the mass was confirmed using ESI-MS. When the peaks were integrated using Empower® software the area for the target peak was determined to be 12.3 %. The cleave product was run on a 1 mm C_{18} Phenomenex® narrow bore column using a 1 % minute^{-1} gradient of 90:10 Acetonitrile (MeCN): 0.08 v/v *aq.* TFA.

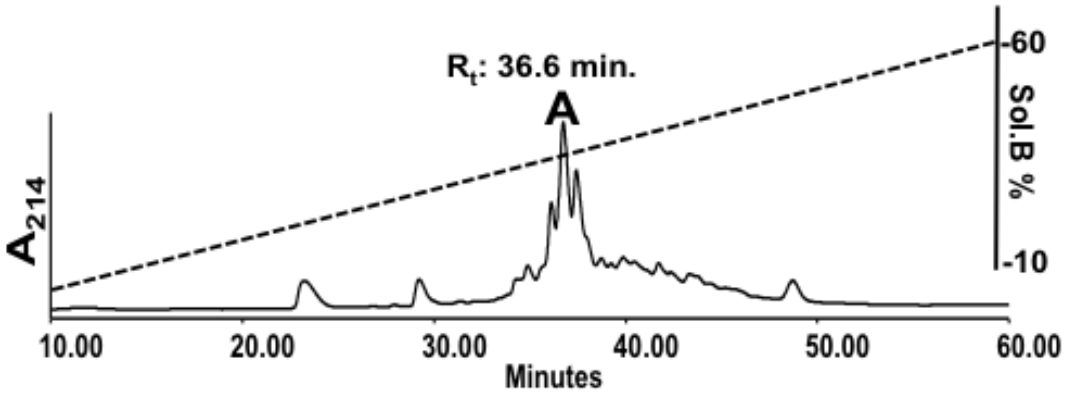

Figure B.7: RP-HPLC cleavage profile when the *N*-terminus fragment of HwTx-I synthesized on a MPAL resin was cleaved under Condition D [Thioanisole 100 µL; 1,2 EDT 50 µL; TFA 1000 µL; TFMSA 150 µL; Ice incubation 30 minutes; Room incubation 120 minutes]. The target peak "A" eluted at 36.6 minutes and the mass was confirmed using ESI-MS. When the peaks were integrated using Empower® software the area for the target peak was determined to be 12.2 %. The cleave product was run on a 1 mm C_{18} Phenomenex® narrow bore column using a 1 % $minute^{-1}$ gradient of 90:10 Acetonitrile (MeCN): 0.08 % v/v *aq.* TFA.

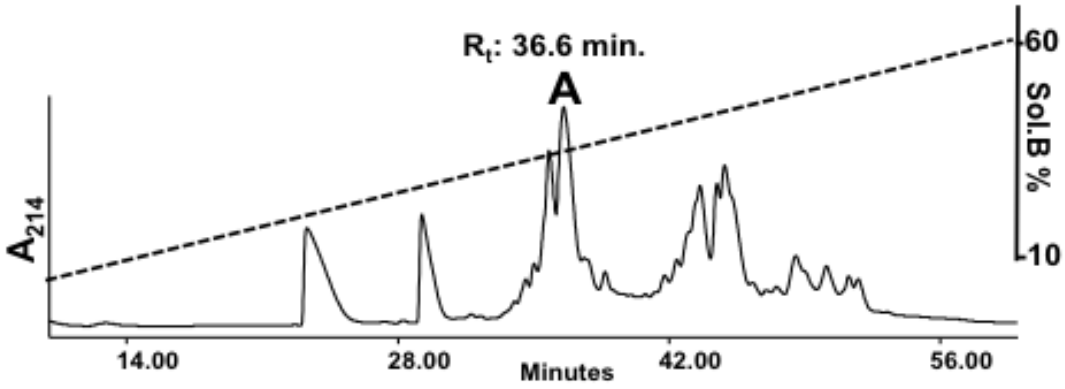

Figure B.8: RP-HPLC cleavage profile when the *N*-terminus fragment of HwTx-I synthesized on a MPAL resin was cleaved under Condition E [Thioanisole 100 µL; 1,2 EDT 50 µL; TFA 1000 µL; TFMSA 100 µL; Ice incubation 30 minutes; Room incubation 90 minutes]. The target peak "A" eluted at 36.6 minutes and the mass was confirmed using ESI-MS. When the peaks were integrated using Empower® software the area for the target peak was determined to be 12.9%. The cleave product was run on a 1 mm C_{18} Phenomenex® narrow bore column using a 1 % $minute^{-1}$ gradient of 90:10 Acetonitrile (MeCN): 0.08% v/v *aq.* TFA.

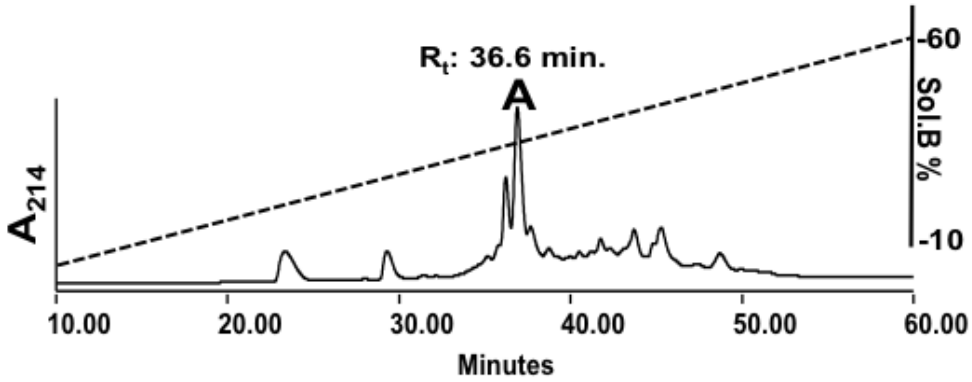

Figure B.9: RP-HPLC cleavage profile when the *N*-terminus fragment of HwTx-I synthesized on a MPAL resin was cleaved under Condition F [Thioanisole 100 µL; 1,2 EDT 50 µL; TFA 1000 µL; TFMSA 100 µL; Ice incubation 30 minutes; Room incubation 120 minutes]. The target peak "A" eluted at 36.6 minutes and the mass was confirmed using ESI-MS. When the peaks were integrated using Empower® software the area for the target peak was determined to be 16.7 %. The cleave product was run on a 1 mm C_{18} Phenomenex® narrow bore column using a 1 % minute^{-1} gradient of 90:10 Acetonitrile (MeCN): 0.08 % v/v *aq.* TFA.

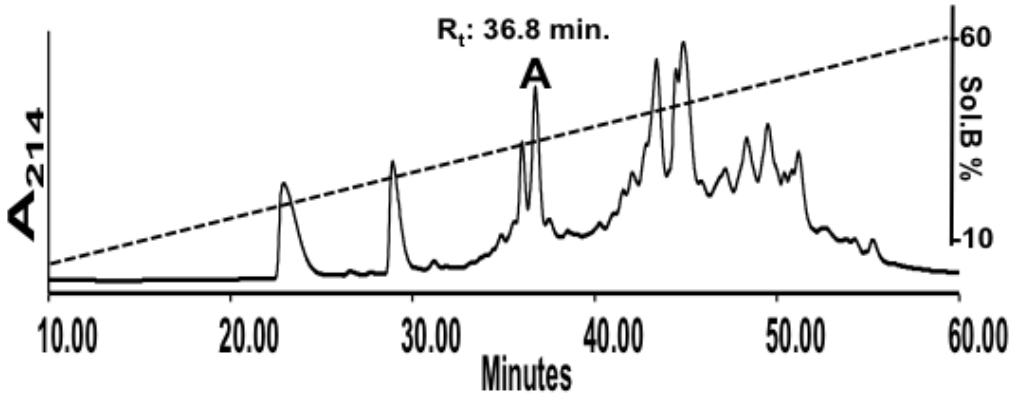

Figure B.10: RP-HPLC cleavage profile when the *N*-terminus fragment of HwTx-I synthesized on a MPAL resin was cleaved under Condition G [Thioanisole 100 µL; 1,2 EDT 50 µL; TFA 1000 µL; TFMSA 100 µL; Ice incubation 30 minutes; Room incubation 180 minutes]. The target peak "A" eluted at 36.8 minutes and the mass was confirmed using ESI-MS. When the peaks were integrated using Empower® software the area for the target peak was determined to be 7.6. The cleave product was run on a 1 mm C_{18} Phenomenex® narrow bore column using a 1 % minute^{-1} gradient of 90:10 Acetonitrile (MeCN): 0.08% v/v *aq.* TFA.

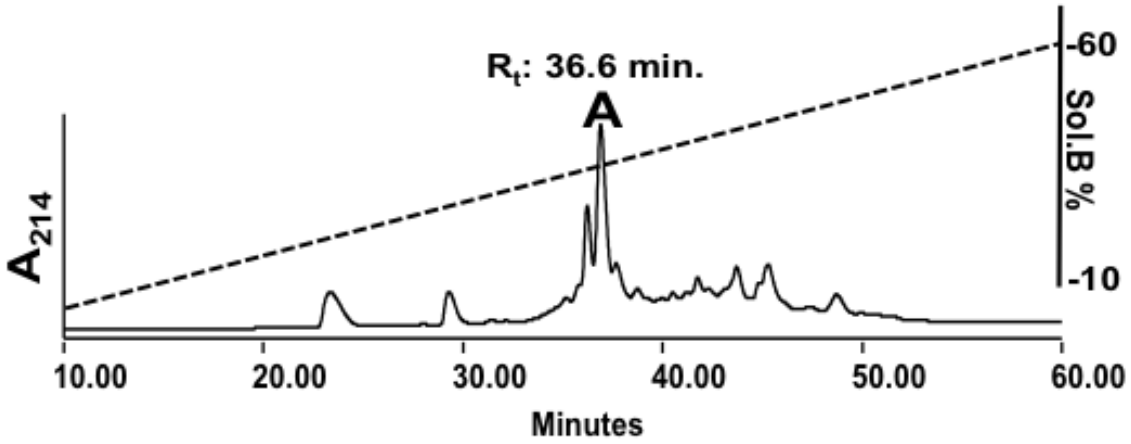

Figure B.11: RP-HPLC cleavage profile when the *N*-terminus fragment of HwTx-I synthesized on a MPAL resin was cleaved under Condition H [Thioanisole 100 µL; 1,2 EDT 50 µL; TFA 1000 µL; TFMSA 100 µL; Ice incubation 30 minutes; Room incubation 120 minutes]. The target peak "A" eluted at 36.6 minutes and the mass was confirmed using ESI-MS. When the peaks were integrated using Empower® software the area for the target peak was determined to be 16.6 %. The cleave product was run on a 1 mm C_{18} Phenomenex® narrow bore column using a 1 % $minute^{-1}$ gradient of 90:10 Acetonitrile (MeCN): 0.08 % v/v *aq.* TFA.

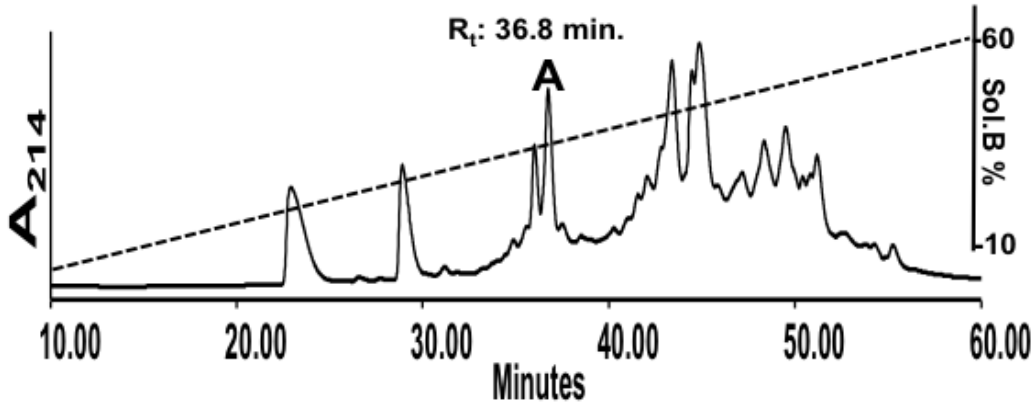

Figure B.12: RP-HPLC cleavage profile when the *N*-terminus fragment of HwTx-I synthesized on a MPAL resin was cleaved under Condition I [Thioanisole 100 µL; 1,2 EDT 50 µL; TFA 1000 µL; TFMSA 100 µL; Ice incubation 90 minutes; Room incubation 120 minutes]. The target peak "A" eluted at 36.6 minutes and the mass was confirmed using ESI-MS. When the peaks were integrated using Empower® software the area for the target peak was determined to be 6.2 %. The cleave product was run on a 1 mm C_{18} Phenomenex® narrow bore column using a 1 % $minute^{-1}$ gradient of 90:10 Acetonitrile (MeCN): 0.08 % v/v *aq.* TFA.

Appendix C: RP-HPLC of Different HwTx-I Isomers

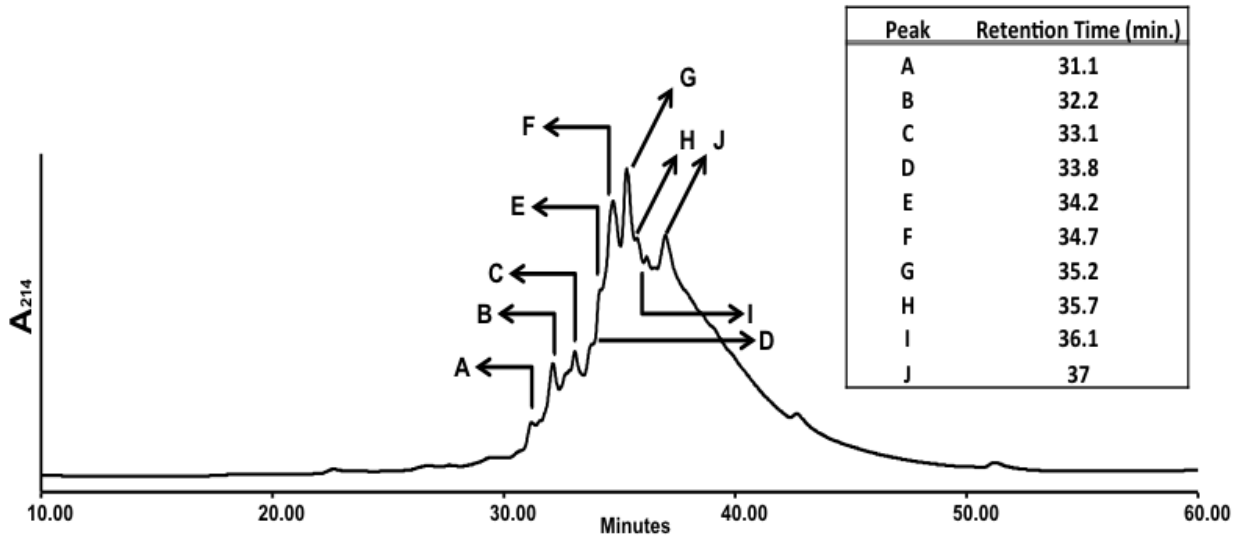

Peak	Retention Time (min.)
A	31.1
B	32.2
C	33.1
D	33.8
E	34.2
F	34.7
G	35.2
H	35.7
I	36.1
J	37

Figure C.1: RP-HPLC profile of a random oxidation done on the ligated reduced HwTx-I. The ligated reduced material was oxidized in a solution of 0.1M NH_4HCO_3 at pH 8. HwTx-I has 6 cysteines therefore random oxidation of HwTx-I should theoretically produce 15 isomers. Of the 15 possible isomers we were able to isolate 10 isomers from the random oxidation profile. The retention times of the 10 isomers are as follows Isomer A: 31.1 minutes, Isomer B: 32.2 minutes, Isomer C: 33.1 minutes, Isomer D: 33.8 minutes, Isomer E: 34.2 minutes, Isomer F: 34.7 minutes, Isomer G: 35.2 minutes, Isomer H: 35.7 minutes, Isomer I: 36.1 minutes and Isomer J: 37.0 minutes. All the 10 isomers were mass confirmed using ESI-MS. The isomers from random oxidation had the above-mentioned elution times when run on a 1 mm C_{18} Phenomenex® narrow bore column using a 1 % $minute^{-1}$ gradient of 90:10 Acetonitrile (MeCN): 0.08 % v/v *aq.* TFA.

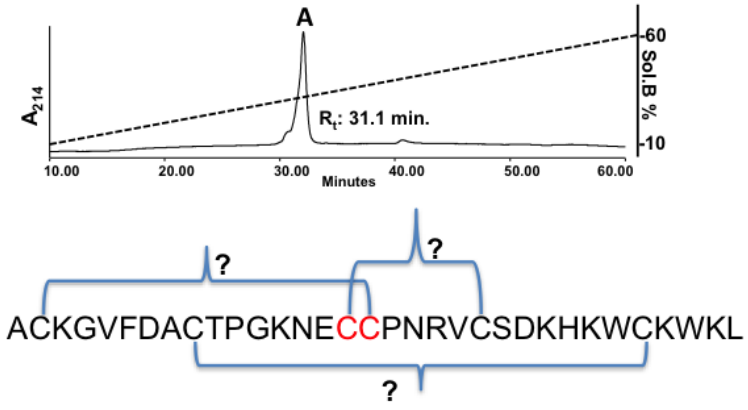

Figure C.2: RP-HPLC profile of Isomer A isolated from a mixture of isomers, which were generated by random oxidation of ligated, reduced HwTx-I in a solution of 0.1M NH_4HCO_3 at pH 8 (Figure 26). The isomer eluted at 31.1 minutes when run on a 1 mm C_{18} Phenomenex® narrow bore column using a 1 % $minute^{-1}$ gradient of 90:10 Acetonitrile (MeCN): 0.08 % v/v *aq.* TFA. Isomer A was mass confirmed using ESI-MS. Since the isomer was generated through random oxidation the disulfide connectivity of the isomer is unknown.

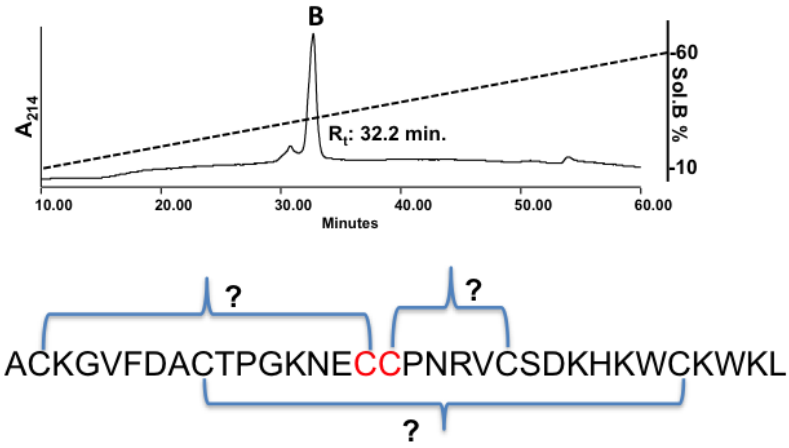

Figure C.3: RP-HPLC profile of Isomer B isolated from a mixture of isomers, which were generated by random oxidation of ligated, reduced HwTx-I in a solution of 0.1M NH_4HCO_3 at pH 8 (Figure 26). The isomer eluted at 32.2 minutes when run on a 1 mm C_{18} Phenomenex® narrow bore column using a 1 % $minute^{-1}$ gradient of 90:10 Acetonitrile (MeCN): 0.08 % v/v *aq.* TFA. Isomer A was mass confirmed using ESI-MS. Since the isomer was generated through random oxidation the disulfide connectivity of the isomer is unknown.

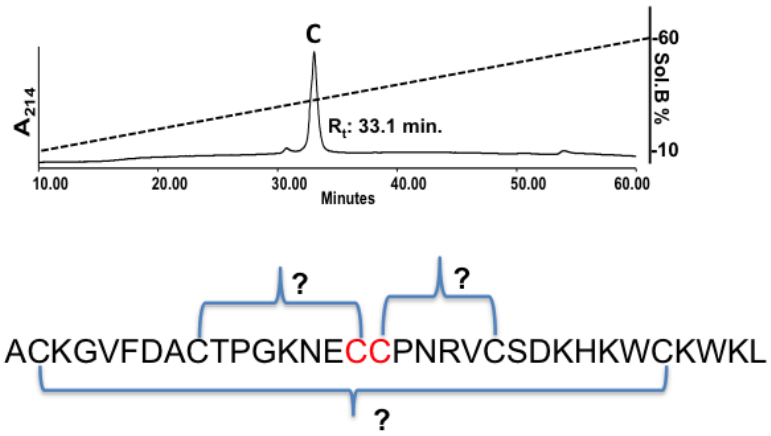

Figure C.4: RP-HPLC profile of Isomer C isolated from a mixture of isomers, which were generated by random oxidation of ligated, reduced HwTx-I in a solution of 0.1M NH_4HCO_3 at pH 8 (Figure 26). The isomer eluted at 33.1 minutes when run on a 1 mm C_{18} Phenomenex® narrow bore column using a 1 % $minute^{-1}$ gradient of 90:10 Acetonitrile (MeCN): 0.08 % v/v *aq.* TFA. Isomer A was mass confirmed using ESI-MS. Since the isomer was generated through random oxidation the disulfide connectivity of the isomer is unknown.

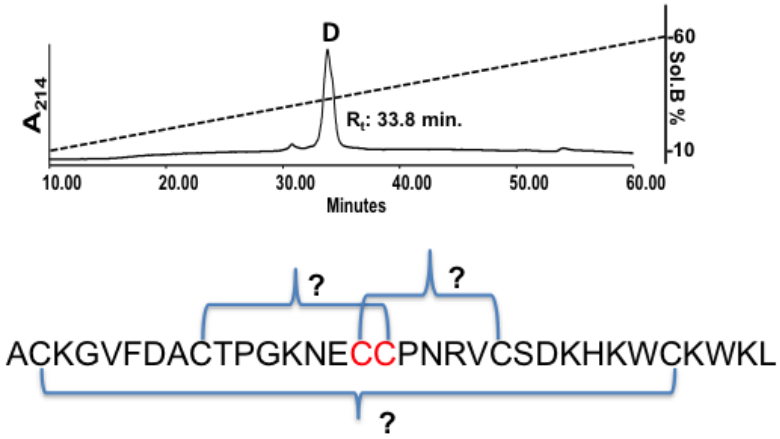

Figure C.5: RP-HPLC profile of Isomer D isolated from a mixture of isomers, which were generated by random oxidation of ligated, reduced HwTx-I in a solution of 0.1M NH_4HCO_3 at pH 8 (Figure 26). The isomer eluted at 33.8 minutes when run on a 1 mm C_{18} Phenomenex® narrow bore column using a 1 % $minute^{-1}$ gradient of 90:10 Acetonitrile (MeCN): 0.08 % v/v *aq.* TFA. Isomer A was mass confirmed using ESI-MS. Since the isomer was generated through random oxidation the disulfide connectivity of the isomer is unknown.

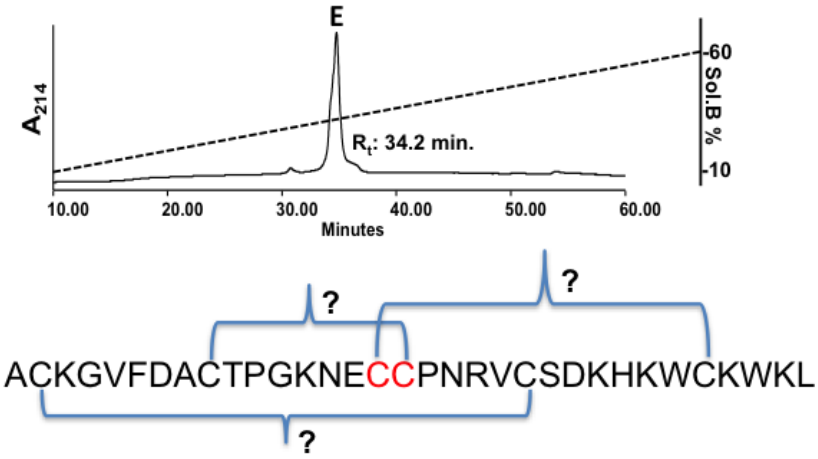

Figure C.6: RP-HPLC profile of Isomer E isolated from a mixture of isomers, which were generated by random oxidation of ligated, reduced HwTx-I in a solution of 0.1M NH_4HCO_3 at pH 8 (Figure 26). The isomer eluted at 34.2 minutes when run on a 1 mm C_{18} Phenomenex® narrow bore column using a 1 % $minute^{-1}$ gradient of 90:10 Acetonitrile (MeCN): 0.08 % v/v *aq.* TFA. Isomer A was mass confirmed using ESI-MS. Since the isomer was generated through random oxidation the disulfide connectivity of the isomer is unknown.

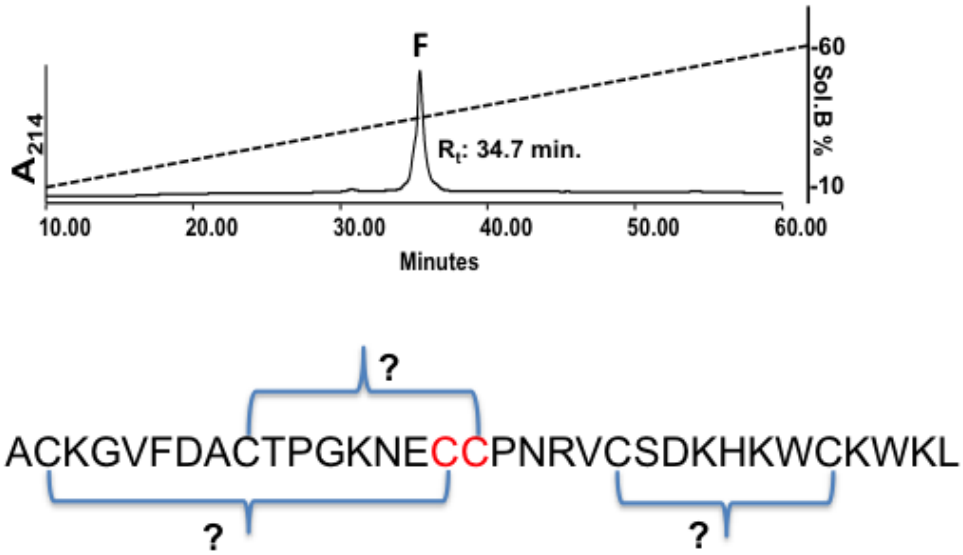

Figure C.7: RP-HPLC profile of Isomer F isolated from a mixture of isomers, which were generated by random oxidation of ligated, reduced HwTx-I in a solution of 0.1M NH_4HCO_3 at pH 8 (Figure 26). The isomer eluted at 34.7 minutes when run on a 1 mm C_{18} Phenomenex® narrow bore column using a 1% $minute^{-1}$ gradient of 90:10 Acetonitrile (MeCN): 0.08 % v/v *aq.* TFA. Isomer A was mass confirmed using ESI-MS. Since the isomer was generated through random oxidation the disulfide connectivity of the isomer is unknown.

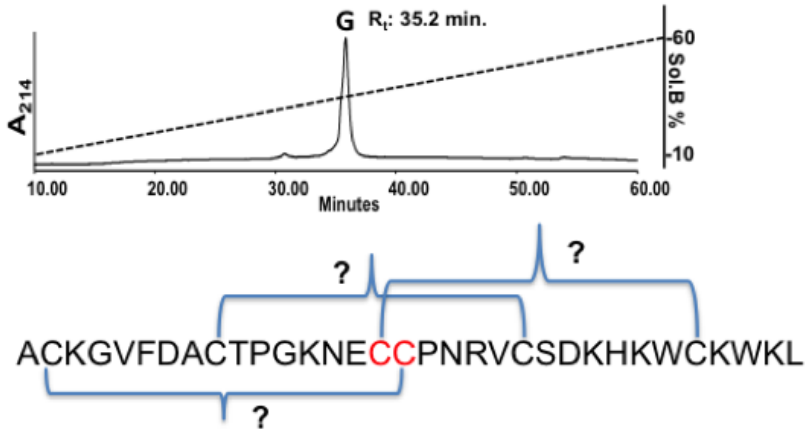

Figure C.8: RP-HPLC profile of Isomer G isolated from a mixture of isomers, which were generated by random oxidation of ligated, reduced HwTx-I in a solution of 0.1M NH_4HCO_3 at pH 8 (Figure 26). The isomer eluted at 35.2 minutes when run on a 1 mm C_{18} Phenomenex® narrow bore column using a 1 % $minute^{-1}$ gradient of 90:10 Acetonitrile (MeCN): 0.08 % v/v *aq.* TFA. Isomer A was mass confirmed using ESI-MS. Since the isomer was generated through random oxidation the disulfide connectivity of the isomer is unknown.

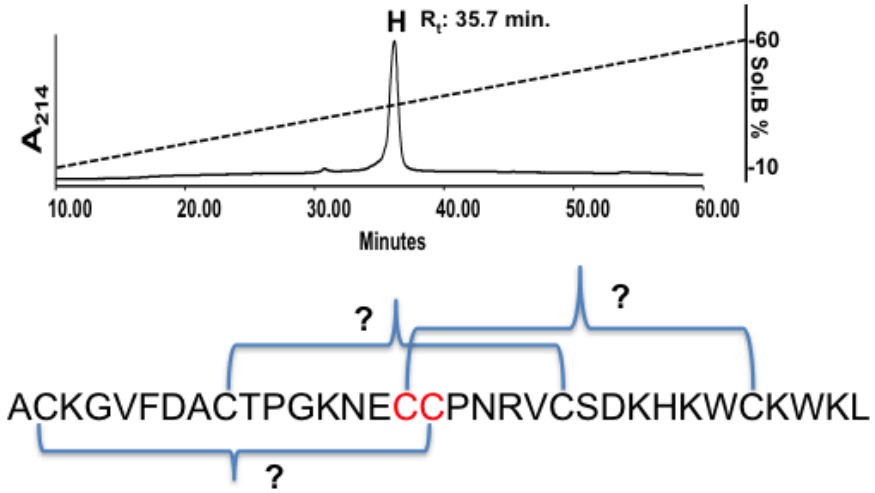

Figure C.9: RP-HPLC profile of Isomer H isolated from a mixture of isomers, which were generated by random oxidation of ligated, reduced HwTx-I in a solution of 0.1M NH_4HCO_3 at pH 8 (Figure 26). The isomer eluted at 35.7 minutes when run on a 1 mm C_{18} Phenomenex® narrow bore column using a 1 % $minute^{-1}$ gradient of 90:10 Acetonitrile (MeCN): 0.08 % v/v *aq.* TFA. Isomer A was mass confirmed using ESI-MS. Since the isomer was generated through random oxidation the disulfide connectivity of the isomer is unknown.

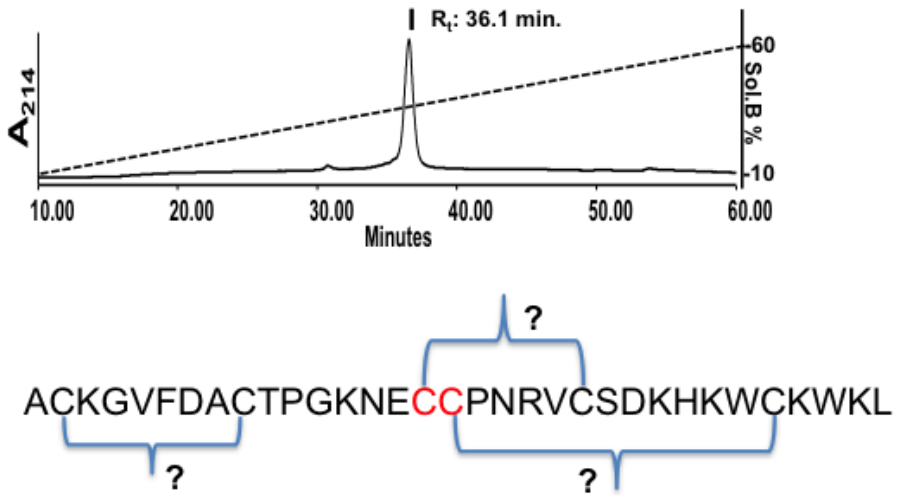

Figure C.10: RP-HPLC profile of Isomer I isolated from a mixture of isomers, which were generated by random oxidation of ligated, reduced HwTx-I in a solution of 0.1M NH_4HCO_3 at pH 8 (Figure 26). The isomer eluted at 36.1 minutes when run on a 1 mm C_{18} Phenomenex® narrow bore column using a 1 % minute^{-1} gradient of 90:10 Acetonitrile (MeCN): 0.08 % v/v *aq.* TFA. Isomer A was mass confirmed using ESI-MS. Since the isomer was generated through random oxidation the disulfide connectivity of the isomer is unknown.

Appendix D: Cyclic Peptides and Stability

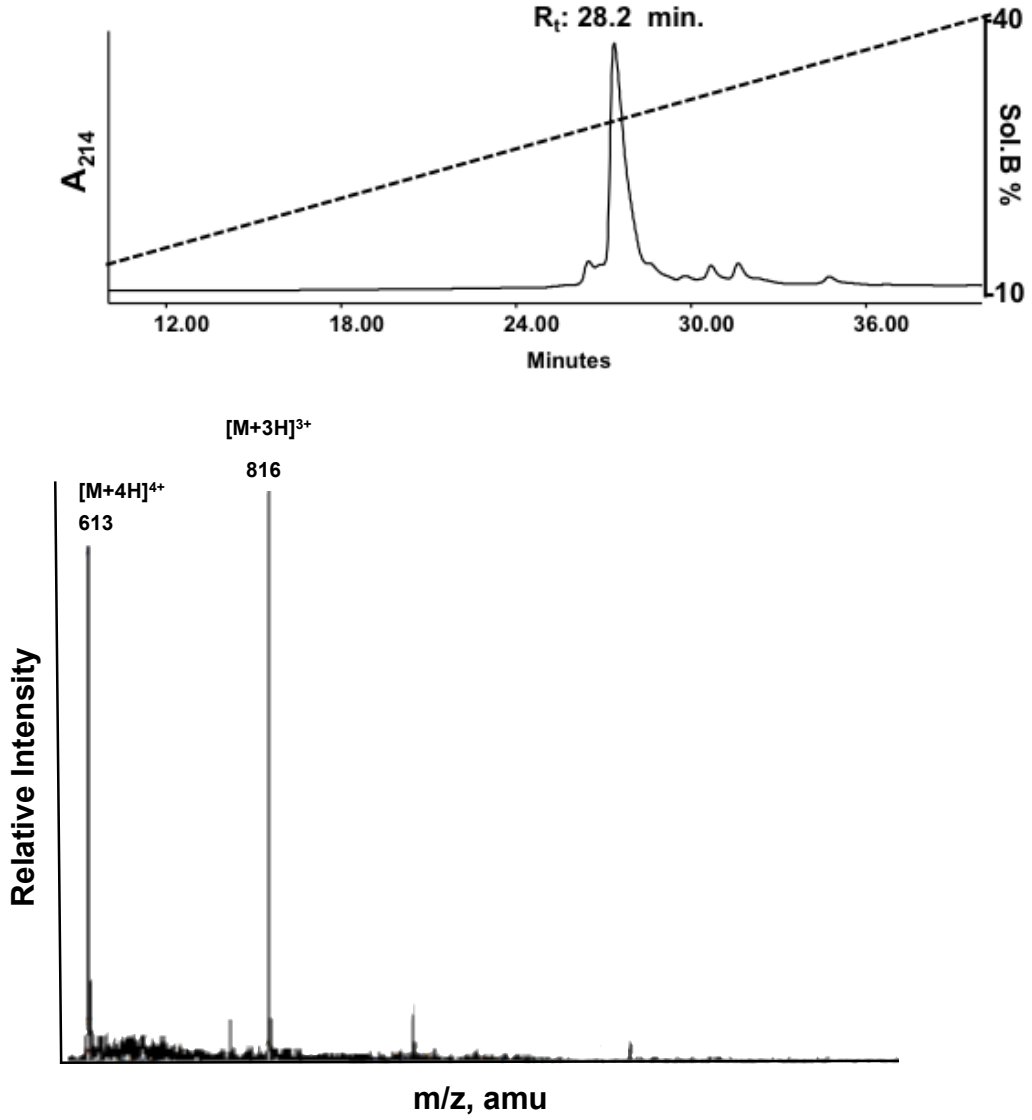

Figure D.1: RP-HPLC chromatogram (top) and ESI-MS (bottom) of linear Tx2005+Linker [RPQCCSHPACNVDHPEICGAGAGAG] the starting material for cyclization, which was synthesized on a 2-Chlorotrityl resin through Fmoc synthesis. The ESI-MS shows 2 dominant *m/z of* $[M+3H]^{3+}$ of 816.6 and $[M+4H]^{4+}$ of 613.0. The theoretical calculated mass of Tx2005+Linker is $[M+4H]^{4+}$ of 613.6 and $[M+3H]^{3+}$ of 817.6. Tx2005+Linker eluted at 28.2 minutes when run on a 1 mm C_{18} Phenomenex® narrow bore column using a 1 % minute^{-1} gradient of 90:10 Acetonitrile (MeCN): 0.08 % v/v *aq.* TFA. The above ESI-MS data for the linear material has the orthogonal protectional groups removed but the linear material used for cyclization had orthogonal protectional groups attached to them. Synthesis through 2-Chlorotrityl resins allows flexibility in linker addition and fluorophore conjugation.

Table D.1: The % degradation of linear Tx 2005 and Cyclic Tx2005 at various time points of 0 hours, 3 hours, 6 hours, 26 hours, 28 hours, and 48 hours when a time course experiment using pancreatin was conducted. All the runs were performed in triplicates.

	% Remaining ± S.E.	
Hours	**Tx2005**	**Cyclic Tx2005**
0	100 ± 4.39	100 ± 4.39
3	100.13 ± 3.84	103.15 ± 5.02
6	96.37 ± 4.17	102.23 ± 5.32
26	83.61 ± 1.12	83.53 ± 1.34
28	88.42 ± 6.65	86.01 ± 4.22
48	81.49 ± 3.44	84.03 ± 1.03

The % Area is determined by integrating the peaks using Empower® software.

Table D.2: The % degradation of linear Tx 2005 with linker and Cyclic Tx2005 with fluorophore at various time points of 0 hours, 3 hours, 6 hours, 26 hours, 28 hours, and 48 hours when a time course experiment using pancreatin was conducted. All the runs were performed in triplicates.

	% Remaining ± S.E.	
Hours	**Tx2005+Linker**	**Cyclic Tx2005+Fluorophore**
0	100 ± 11.37	100 ± 0.93
3	88.90 ± 4.80	96.98 ± 1.40
24	68.12 ± 11.37	91.08 ± 1.12
27	75.51 ± 4.24	93.43 ± 2.65
29	70.75 ± 0.74	88.43 ± 0.14
48	48.14 ± 7.48	84.34 ± 1.34

The % Area is determined by integrating the peaks using Empower® software.

Table D.3: The % degradation of linear Tx 2005 and Cyclic Tx2005 at various time points of 0 hours, 3 hours, 6 hours, 26 hours, 28 hours, and 48 hours when a time course experiment using trypsin was conducted. All the runs were performed in triplicates.

	% Remaining ± S.E.	
Hours	**Tx2005**	**Cyclic Tx2005**
0	100 ± 5.43	100 ± 4.50
3	99.21 ± 2.10	100.03 ± 2.10
6	103.37 ± 4.03	96.32 ± 4.71
26	96.44 ± 5.74	96.78 ± 4.00
28	91.26 ± 6.97	97.84 ± 8.93
48	88.49 ± 5.40	87.22 ± 9.10

The % Area is determined by integrating the peaks using Empower® software.

Table D.412: The % degradation of linear Tx 2005 with linker and Cyclic Tx2005 with fluorophore at various time points of 0 hours, 3 hours, 6 hours, 26 hours, 28 hours, and 48 hours when a time course experiment using trypsin was conducted. All the runs were performed in triplicates.

	% Remaining ± S.E.	
Hours	**Tx2005+Linker**	**Cyclic Tx2005+Fluorophore**
0	100 ± 1.30	100 ± 0.73
3	97.31 ± 1.34	98.43 ± 1.06
24	90.52 ± 0.48	93.34 ± 0.84
27	90.07 ± 0.36	91.47 ± 1.36
29	90.22 ± 1.13	91.23 ± 0.32
48	81.48 ± 1.68	83.13 ± 0.91

The % Area is determined by integrating the peaks using Empower® software.

Table D.5: The % degradation of linear Tx 2005 and Cyclic Tx2005 at various time points of 0 hours, 3 hours, 6 hours, 26 hours, 28 hours, and 48 hours when a time course experiment using carboxypeptidase was conducted.

	% Remaining ± S.E.	
Hours	**Tx2005**	**Cyclic Tx2005**
0	100 ± 7.17	100 ± 4.09
3	86.15 ± 2.63	101.69 ± 0.76
6	82.82 ± 2.45	96.33 ± 6.98
26	65.25 ± 1.96	89.85 ± 3.53
28	65.60 ± 2.34	94.71 ± 2.89
48	57.61 ± 7.49	86.43 ± 4.93

The % Area is determined by integrating the peaks using Empower® software.

Table D.6: The % degradation of linear Tx 2005 with linker and Cyclic Tx2005 with fluorophore at various time points of 0 hours, 3 hours, 6 hours, 26 hours, 28 hours, and 48 hours when a time course experiment using carboxypeptidase was conducted.

	% Remaining ± S.E.	
Hours	**Tx2005+Linker**	**Cyclic Tx2005+Fluorophore**
0	100 ± 0.85	100 ± 0.58
3	48.95 ± 6.90	96.27 ± 0.40
24	4.77 ± 15.60	94.53 ± 0.30
27	4.46 ± 2.74	91.73 ± 2.69
29	3.92 ± 0.89	92.59 ± 1.40
48	0.50 ± 5.72	84.65 ± 1.08

The % Area is determined by integrating the peaks using Empower® software.